

University of Udine

Department of Mathematical, Computer and Physical Sciences

MASTER DEGREE IN MATHEMATICS

Quantum Arithmetical Chaos



Author:
Alberto CAGNETTA

Supervisor:
Giovanni PANTI
Co-supervisor:
Sebastiano SONEGO

Anno Accademico
2021 – 2022

“...*quote...*”

Berry (?)

UNIVERSITY OF UDINE

Department of Mathematical, Computer and Physical Sciences

Master degree in Mathematics

Quantum Arithmetical Chaos

by Alberto CAGNETTA

Abstract

The Thesis Abstract is written here...

PUT IMAGES AND WRITE THE ABSTRACT

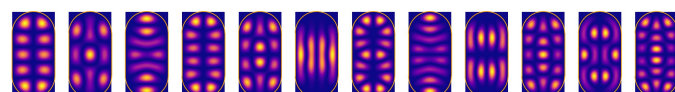
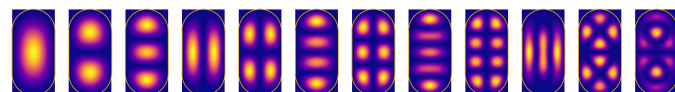


FIGURE 1: First 24 eigenfunctions on Bunimovich Stadium

Acknowledgements

The acknowledgments and the people to thank go here...

Contents

Abstract	iii
Acknowledgements	v
List of Abbreviations	xi
List of Symbols	xiii
Overview	1
Main Section 1	1
0.1 Materials	1
1 Billiards and quantum chaos	3
1.1 Introduction	3
1.1.1 Examples	5
1.2 From classical to quantum billiards	8
1.2.1 Unique ergodicity	8
1.2.2 Quantum regime	8
1.2.3 Some insights about QUE	9
1.3 The classic-quantum correspondence	10
2 Hyperbolic geometry	13
2.1 Iwasawa decomposition	13
2.2 Hyperbolic models: upper-half plane and disk	13
2.2.1 Hyperbolic plane	13
2.2.2 Hyperbolic isometries	17
2.2.3 Hyperbolic surfaces and fuchsian groups	20
2.3 Hyperbolic dynamics	24
2.3.1 Geodesic flow	24
2.3.2 Mixing flow on hyperbolic plane	25
2.3.3 Examples	27
2.4 Spectra of modular surfaces	28
3 Semiclassical analysis	31
3.1 Semiclassical Quantizazion	31
3.1.1 Semiclassical Fourier transform	31
3.1.2 How to quantize	33
3.1.3 Semiclassical Pseudodifferential Operators	36
3.1.4 Symbol Classes	39

3.2	Two main results: Weyl law and Egorov's Theorem	40
3.2.1	Weyl Law in Euclidian space	41
3.2.2	ψ DO on Manifolds	42
3.2.3	Connection between classical and quantum dynamics: Egorov's Theorem	44
4	Quantum ergodicity	47
4.1	Quantum ergodicity	47
4.2	Quantum unique ergodicity	50
4.3	Hassell disproof of QUE	51
5	Selberg trace formula	55
5.1	Trace formula on \mathbb{S}^1	55
5.2	Laplacian operator	57
5.2.1	A brief journey across harmonic analysis on the hyperbolic plane	58
5.3	Periodic geodesics	61
5.4	Pretrace formula	63
5.4.1	Hyperbolic terms	66
5.5	An application: Weyl's law	67
5.6	The case of $\mathrm{PSL}_2 \mathbb{Z}$	69
6	Arithmetic Quantum Unique Ergodicity	71
6.1	Lindenstrauss' result	71
6.1.1	Microlocal lift revised	72
6.2	Hecke recurrence	74
6.2.1	The p -adic extension of $\Gamma \backslash \mathrm{PSL}_2 \mathbb{R}$	74
6.2.2	Hecke operators	77
6.2.3	Hecke invariance	77
6.3	Existence	79
7	Frontiers in <i>Quantum chaology</i>	81
7.1	Numerical simulations	81
7.1.1	Numerical methods	83
7.2	Spectral statistics and Random Matrix Theory	84
7.3	Conclusion	87
7.3.1	Billiard and spectral simulations	87
A	Ergodic notions	89
A.1	Mixing	89
B	Fourier transform	93
B.1	Basic notions	93
B.2	Distributions	94
C	Flows and integrable systems	97
C.1	Ergodic notions	97
C.2	Python codes	99
C.2.1	Billiards	99
C.2.2	Quantum eigenfunctions	107
C.3	FreeFem++	107

List of Figures	109
Bibliography	111

List of Abbreviations

LAH List Abbreviations Here (TO BE DONE)

List of Symbols

c light speed TO BE DONE

Overview

TO BE DONE

- This chapter;
- controllare riferimenti tra le varie sezioni;
- sistemare le appendici;
- attivare link per folder online con video;
- fare l'abstract
- Quantum Cat maps non QUE? Markloff...
- Inserire (alcuni) programmi nell'appendice
- Sistemare APPENDICI A e C
- Accennare meglio agli *scar quantistici*

0.1 Materials

All the materials relevant to this thesis, as well with code of numerical simulations, can be found at ATTIVARE LINK

1 Billiards and quantum chaos

1.1 Introduction

The main “physical” dynamical system we will consider in this thesis is a billiard, which is a model where a (usually dimensionless) particle moves within a bounded domain in the Euclidian space \mathbb{R}^n and bounces off the boundary of the domain elastically. Physically this can be interpreted in several different ways. But we will also consider the same kind of motion but on surfaces, which will have negative curvature, for reasons that we will learn more about later.

The bouncing billiard can be realized, from a physical point of view, by considering, for example, a potential function which zero inside of the considered domain, and equal to infinity otherwise. However, regardless of their physical realization, these kind of system can exhibit a number of interesting properties.

More formally, we will consider the following definition.

Definition 1.1.1 A dynamical metric system is the quadruple (X, χ, μ, R) where (X, χ, μ) is a metric space with σ -algebra χ and R is a μ -measurable map such that μ is R -invariant, i.e. $R_*\mu = \mu$.

Often, R will be more regular than just being measurable. We are now ready to introduce the concept of billiard systems. We will consider essentially, as already mentioned, two main cases:

- **Billiard flows:**

A *billiard* is a bounded, planar domain Ω with a piecewise smooth boundary. The billiard flow is the classical frictionless motion of a particle inside Ω , with angle of incidence to the boundary $\partial\Omega$ equal to angle of reflection off $\partial\Omega$; the total kinetic energy is preserved. In this case, the preserved measure is a multiple of Lebesgue measure, i.e. Liouville measure, given explicitly by $\mu_L = \frac{\mathbb{1}_\Omega}{\lambda(\Omega)}$, where $\lambda(\Omega)$ is the measure of set Ω . If we consider the unit tangent space $T^1\Omega$, then the Liouville measure is given by $\mu_L = \frac{\mathbb{1}_\Omega}{2\pi\lambda(\Omega)}$.

- **Geodesic flows (on manifolds):**

If M is a Riemannian manifold with metric g , then for each point $q \in M$, there is one and only one *geodesic* (i.e. path of minimal length) given a unit direction. So the classical frictionless motion of a particle along local geodesics gives the desired flow. Moreover, it's well defined the unit tangent space T^1M and in this

case the Liouville measure is given by $\mu_L = \frac{1}{2\pi\lambda(M)}$ where $\lambda(M)$ is the “area” of M , with respect to metric g .

In both cases, we will denote the considered flow with Φ_t . Sometimes, it is more convenient to consider only a *discretization* of the flow; for example, in billiard flow case, it can be helpful to consider the map $\Psi = \Phi_T^n$ which gives the position of a point $q \in \Omega$ after time nT .

Billiards systems, even if simple in their definition, can exhibit a certain degree of *chaotical properties*. A good property to look at for this type of features is ergodicity.

Theorem 1.1.2 (Ergodicity, discrete case). *Let (X, χ, μ, R) be a dynamical metric system, with X of finite measure, i.e. a probability space. The followings hold and give a definition of a (discrete) ergodic system:*

- if B is R -invariant, then $\mu(B) = 0$ or $\mu(B^c) = 0$
- if $\mu(A), \mu(B) > 0$ for measurable sets A, B , then it does exist a $k \geq 0$ such that $\mu(A \cap R^{-k}[B]) > 0$.

Roughly speaking, ergodicity requires that a dynamical system cannot be decomposed in smaller and independent dynamical system and every set is taken across all the space X through the action of map R^{-k} , with $k \geq 0$. Moreover, every subset A must be “mixed” with every other subset B , in a certain proportion. In fact, another important feature is the concept of *mixing*.

Definition 1.1.3 (Mixing) *A dynamical metric system (X, χ, μ, R) is called mixing if $\forall A, B \in \chi$ we have*

$$\lim_{n \rightarrow \infty} |\mu(A \cap R^{-n}[B]) - \mu(A)\mu(B)| = 0.$$

Mixing is indeed a stronger property than ergodicity, because it does not only require that the system mixes itself, but every couple of sets A, B should be mixed in *the right proportion*.

We can rewrite these definition for the continuos case.

Definition 1.1.4 (Ergodicity and mixing, continuos case) *Let (X, χ, μ, Φ_t) be a dynamical metric system, with X of finite measure, i.e. a probability space.*

- The flow Φ_t is ergodic if for every measurable set $B \subset X$ which is R_t invariant for every t , then $\mu(B) = 0$ or $\mu(B^c) = 0$;
- The flow Φ_t is mixing if for every measurable sets $A, B \subset X$

$$\mu(A \cap \Phi_t^{-1}[B]) \xrightarrow{t \rightarrow \infty} \mu(A)\mu(B).$$

A more pictorial way to understand ergodicity from a physical point of view is given by the following result, due to Birkhoff.

Theorem 1.1.5 (Birkhoff). *The flow Φ_t is ergodic iff $\forall f \in L^1(X)$,*

$$\lim_{T \rightarrow \infty} \frac{1}{T} \int_0^T f \circ \Phi_t(x) dt = \int_X \varphi d\mu$$

for μ -a.e. $x \in X$.

What theorem 1.1.5 states is that, in an ergodic system, the trajectories are equidistributed in the phase space. There is also a reinterpretation of ergodicity from a “spectral” point of view, considering the precomposing map $R^*f = f \circ R$.

Theorem 1.1.6. Let (X, χ, μ, R) be a metric system e let $p \in [1, +\infty]$. The followings are equivalent:

- the system (X, χ, μ, R) is ergodic;
- the eigenspace of R^* in L_p correspondent to eigenvalue 1 is made up only by a.e. constant functions $\mathbb{C} \mathbf{1}$.

We will go deeper into this “spectral” approach in the following chapters.

1.1.1 Examples

We are now ready to analyze some examples. At first, we will consider some classical billiards.

Billiards:

Example 1.1.1: Biliardo circolare, ellittico

The circular, elliptic billiard is given by the classical “bouncing motion” and a domain $\Omega \subset \mathbb{R}^2$ which is given by a circle or, more generally, an ellipse. In this case, the billiard is not ergodic, as it can be easily seen in the circular case. In fact, if the angle of first bounce is ϑ , then for the symmetry of the circle, this angle is constant through every bounce and so it is a constant quantity over an orbit and depending on the considered orbit. So, for theorem 1.1.6, this system cannot be ergodic. This property has a concrete impact on the aspect of a generic orbit. Seeing figure 1.1, it can be observed that a generic orbit avoids whole parts of the domain.

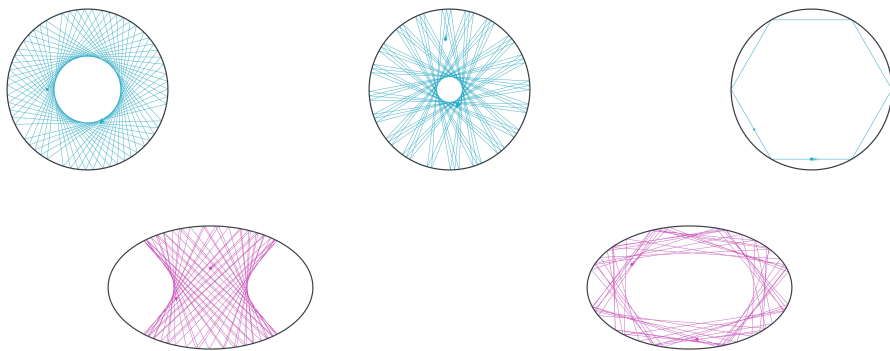


FIGURE 1.1: Billiard trajectories on a circle and an ellipse. The underlying system is conservative, hence the motion is not “everywhere distributed”.

The followings are examples of ergodic billiards.

Example 1.1.2: Bunimovich stadium

This billiard is by far the most famous one and the most studied in details. Albeit it may seem contrived, this billiard is full of remarkable properties and so it is considered the fundamental prototype for a chaotic billiard. The domain Ω is made up by one rectangle and two half-circles on two sides. This billiard is ergodic and mixing. Moreover, it is also “chaotic” in the sense that “near trajectories” have dramatically different time-evolution (see figure 1.2)

We will denote by \mathcal{BS}_l the Bunimovich stadium defined by the rectangle $[-l\frac{\pi}{2}, l\frac{\pi}{2}] \times [-\frac{\pi}{2}, \frac{\pi}{2}]$ and the two semicircle of radius $\pi/2$.

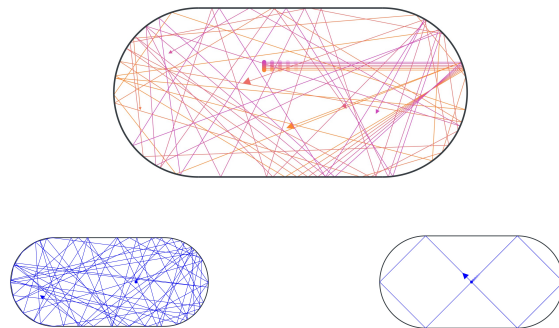


FIGURE 1.2: Billiard trajectories on the Bunimovich stadium.

Example 1.1.3: Barnett’s billiard

This billiard is made up by two circle arcs and two perpendicular segment. The circle arcs must intersect creating an acute angle. Peter Sarnak called this billiard “Barnett’s billiard”, thanks to the latter’s numerical studies on this billiard. We will denote the generic Barnett’s billiard with \mathcal{BNS} . It is mixing and, moreover, Sinai proved that near orbits diverge exponentially.

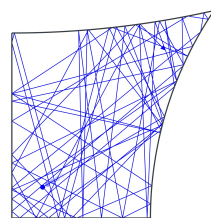


FIGURE 1.3: Barnett’s billiard.

Example 1.1.4: Cassini's billiard and cardioid billiard

Other interesting billiards, which numerically share lots of properties of Bunimovich and Barnett billiards are the Cardioid billiard \mathcal{CS}_r , with domain defined by the cardioid of (polar) equation

$$\rho(\theta) = r(1 - \cos \theta)$$

and the Cassini's oval billiard $\mathcal{COS}_{a,b}$ defined by the equation

$$(x^2 + y^2)^2 - 2 \cdot a^2(x^2 - y^2) + a^4 = b^4, \quad a, b > 0, b > a.$$

In particular, for $b/a \geq \sqrt{2}$ is convex, otherwise for $1 < b/a < \sqrt{2}$ it is peanut-shaped.

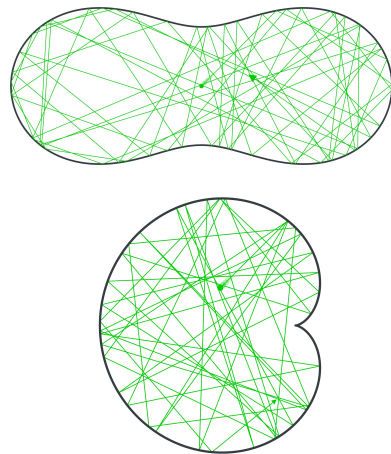


FIGURE 1.4: Billiard trajectories in the Cassini's oval and Cardioid.

As mentioned before, there are also “billiards” induced by geodesic flow on a Riemannian manifold. The flow on the modular surface is a good example of this case (see chapter 2).

Example 1.1.5: Modular surface

It can be shown that on every Riemannian manifold with negative curvature, the geodesic flow Φ_t is ergodic (see Hopf theorem 1.2.4). The geodesic flow on the unit tangent space of the modular surface $\mathrm{PSL}_2 \mathbb{Z} \backslash \mathcal{H}$ (2.2.3) is hence ergodic.



FIGURE 1.5: Ergodic orbit on the modular surface.

1.2 From classical to quantum billiards

1.2.1 Unique ergodicity

Before introducing the “quantum” definition of ergodicity, we recall the definition of unique ergodicity. In general, we give the following definition.

Definition 1.2.1 An ergodic metric system (X, R, μ_L) , where μ_L the standard Liouville measure, is called uniquely ergodic if μ_L is the only finite borel measure, invariant with respect to R .

The definition in the continuos case is essentially the same. The two condition of
 1. finiteness,
 2. uniqueness,
 are very strong. To this, consider a metric space (X, R, μ_L) , and a point $x \in X$ which is periodic. The dirac measure concentrated on points of the finite orbit of x is preserved, but it is not the Liouville measure. We can appreciate the crucial point played by periodic orbits, in this framework.

1.2.2 Quantum regime

In quantum regime, billiards are described by wavefunctions ψ_n whose time-evolution are ruled by the *Schrödinger equation*

$$i\hbar \frac{\partial}{\partial t} \psi_n(x, t) = -\frac{\hbar^2}{2m} \Delta \psi_n(x, t),$$

where Δ depends on the metric considered, with Dirichlet boundary conditions in the planar euclidian case. Moreover $\psi_n \in L^2(\Omega)$, \hbar is Planck’s constant and m is the mass of the particle. From quantum mechanics the generic time dependent solution is the superposition of time dependent solution of the form $\psi_n(x, t) = \exp(-itE_n/\hbar)\varphi_n(x)$, where E_n are quantum energy levels and φ_n are eigenfunctions of the equation

$$-\frac{\hbar^2}{2m} \Delta \varphi = E_n \varphi.$$

So, the “quantum-mechanical” evolution of the billiard is linked to the eigenvalue problem $-\Delta\varphi_n = \lambda_n\varphi_n$, where $\lambda_n = 2mE_n/\hbar^2$. Semiclassical analysis, among other things, deals with find a correspondence between classical motion and the quantum approach. Indeed, the starting question is: how is it possible to translate the concept of ergodicity in this quantum framework, from the classical one?

The feature of ergodicity that it is considered is equidistribution of orbits. We will know pause rigorous mathematical exposition for a brief informal introduction to the subject.

Let’s consider the eigenfunction φ_j correspondent to the eigenvalue λ_j . Considering the absolute square $|\varphi_j|^2$, we get a probability distribution on our billiard Ω or manifold M . There is a *standard* way to lift this probability measure to the unit tangent space, using Wigner measures (see 4.2.1 for further informations). Roughly speaking, for a smooth function $f: T^1\Omega = \Omega \times S^1$ on the unit tangent space, we can define the Wigner measure μ_φ , and hence the integral $\mu_\varphi(f)$, induced by the eigenfunction φ as

$$\mu_\varphi(f) := \langle \text{Op}(f)\varphi, \varphi \rangle_{L^2}$$

where, if $\hat{\psi}$ is the Fourier transform of ψ ,

$$\text{Op}(f)\psi(x) := \int_{\mathbb{R}^2} e^{2\pi i(x \cdot \xi)} \hat{\psi}(\xi) f\left(x, \frac{\xi}{\|\xi\|}\right) d\xi.$$

In particular, Op operator is a *pseudo-differential operator* induced by function f . In 3.1.2 it is explained that this is only one possibilites, as there are other similar way to produce the operator Op, e.g. another one is *Weyl quantization*.

A “natural way” to rewrite the idea “a.e. orbit distributes itself uniformly” in the quantistic case is to formulate the following.

Definition 1.2.2 A dynamical metric system is quantum ergodic if it does exist a subsequence of eigenvalues λ_k for the Laplacian Δ of density one, such that $\mu_k (= \mu_{\varphi_{\lambda_k}})$ converges weakly to the Liouville measure μ .

As will see in section 4.2, any weak limit for measures μ_j is called *quantum limit*. Then, the concept of *unique quantum ergodicity* is translated as follows.

Definition 1.2.3 A quantum system is unique ergodic if the only possible quantum limit is the standard Liouville measure.

A case of particular interest is the one of hyperbolic surfaces X , with the Laplacian operator adapted to the hyperbolic metric 2.2. In this case, the Liouville measure is given by $\mu = \frac{1}{2\pi\lambda(X)}$, where $\lambda(X)$ is the hyperbolic measure of the hyperbolic surface X . The reason behind this interest is the following.

Theorem 1.2.4 (Hopf). Let X be an hyperbolic surface. Then the geodesic flow on T^1X is ergodic.

1.2.3 Some insights about QUE

A main result regarding QE theory is due to Schnirelman, Zelditch and Colin de Verdière, as we will see in chapter 4. Its statement is roughly the following.

Theorem 1.2.5. *If a classical system is ergodic, then the corresponding quantum system is QE.*

In particular, this gives us that Bunimovich stadium billiard \mathcal{BS} and Barnett's billiard \mathcal{BNS} are QE. Moreover, all for all hyperbolic surface, QE holds. So, the following question, made by Colin de Verdière, was:

What are the possible quantum limits?

Driven by theoretical considerations and numerical simulations, Rudnick and Sarnak proposed, in 1993 [RS96], the following conjecture.

Conjecture: *For all hyperbolic surfaces, QUE holds.*

A great achievement, towards this problem, was reached in 2010, thanks to the groundbreaking result due to Lindenstrauss. His work ([LB03],[Lin06]) earned him the Fields Medal.

Theorem 1.2.6 (Lindenstrauss 2006, Soundarajan 2010) *QUE holds for every arithmetic hyperbolic surface.*

Without going in details about what an arithmetic hyperbolic surface is, it is sufficient to know that these surfaces arise from arithmetic methods. So, Lindenstrauss used this information to impose more symmetry on Laplacian eigenfunctions, via *Hecke operators*, which are genuinely arithmetic tools.

On the other hand, another important result about QUE led to the opposite side of the conjecture, in the euclidian case. In fact, in the same year (2010) Hassell proved that QUE doesn't hold for Bunimovich stadium ([Has10a]), as some "bouncing back and forth" eigenstates are still present in the high-energy limit. For more details, see chapter 4.

1.3 The classic-quantum correspondence

We have outlined the main themes of this thesis, so maybe it is a good time to recall what our aim is.

We are interested in understanding how the ergodicity of the geodesic flow does determine the distribution of high-eigenvalue Laplacian eigenfunctions. We recall some informations from appendix A.

On any classical system on a Riemannian manifold (M, g) , the geodesic flow is given by the Hamiltonian vector field X_H generated by the Hamiltonian function $H: M \rightarrow \mathbb{R}$. Integrating the Hamiltonian vector field X_H generates a one parameter family of integral curves. These curves represent the geodesic flow and so we can define $\Phi^t: M \rightarrow M$ which defines the time evolution of a point on the manifold M along this flow. In this context, the manifold M is the configuration space, while the cotangent bundle T^*M of couples (q, p) of position and momentum is the phase space.

We can consider the energy level sets $\Sigma_c := H^{-1}(c)$, which carry a natural flow-invariant measure, called *Liouville measure*. It can be characterized not only by the invariance through the geodesic flow, but also in the following way.

Definition 1.3.1 The Liouville measure μ_L^c is the flow-invariant volume-form on any “energy-shell” Σ_c of a Hamiltonian system. In particular, for $c \in [a, b]$, μ_L^c is characterized by the formula

$$\iint_{H^{-1}[a,b]} f \, dx \, dp = \int_a^b \int_{\Sigma_c} f \, d\mu_L^c \, dc,$$

for a smooth function $f: T^*M \rightarrow \mathbb{R}$.

Now, if (M, g) is a compact manifold with negative curvature, Hopf theorem 1.2.4 assure us that the geodesic flow is ergodic, with respect to Liouville measure. In particular, we will show this in section 2.3, in the case of hyperbolic surfaces generated by Fuchsian groups. The corresponding quantum dynamics is the unitary flow generated by Laplace operator, as a generic time evolution is given by superposition of eigenfunctions $-\Delta \psi = \lambda_n \psi$. At this level, we can “see” that, in some way, the ergodic geodesic flow influences the spectral aspect of the Laplacian, making its eigenfunctions equidistributed.

Having this in mind, in our humble opinion, it seems appropriate to pointing out some important themes for this thesis. These will be useful to keep in mind in chapter 4.

- Intuition behind the semiclassical limit: even if, numerically, we can take the *semiclassical limit* $\hbar \rightarrow 0$, we need the energies to be bounded. So, in semiclassical regime, we expect that the asymptotic behaviour of quantum objects correspond to the classical one;
- The technical aspects of semiclassical analysis: Fourier transform enables us to relate position and momentum variables. So, as semiclassical limit relies on a global rescaling, we will a sort of semiclassical Fourier transform, hence classical Fourier transform theory will be useful.
- Interaction between order and disorder, from simple cases: as it can be seen, lots of the results and problem of this theory is drawn by visualization and numerical simulations; even if starting examples are very simple, the theory behind it isn’t and this framework is a good example of the dichotomy between classical structure and quantum randomness:

The “dichotomy between structure(order) and randomness” seems to apply in circumstances in which one is considering a high-dimensional class of objects... one needs tools such as algebra and geometry to understand the structured component, one needs tools such as analysis and probability to understand the pseudorandom component, and one needs tools such as decompositions, algorithms, and evolution equations to separate the structure from the pseudorandomness.

Terrence Tao, [Tao07]

2 Hyperbolic geometry

2.1 Iwasawa decomposition

Theorem 2.1.1: Iwasawa (real) decomposition

For every matrix $M \in \mathrm{SL}_2 \mathbb{R}$ there exist real matrices K, A, N such that $M = KAN$ and

$$\begin{aligned} K &\in \mathfrak{K} = \mathrm{SO}_2 \mathbb{R} \\ A &\in \mathfrak{A} = \left\{ \begin{pmatrix} a & 0 \\ 0 & a^{-1} \end{pmatrix} : a \in \mathbb{R}_{>0} \right\} \\ N &\in \mathfrak{N} = \left\{ \begin{pmatrix} 1 & b \\ 0 & a1 \end{pmatrix} : b \in \mathbb{R} \right\} \end{aligned}$$

The Iwasawa decomposition of a matrix M ultimately let you see it's action as the composition of three fundamental subgroups of $\mathrm{GL}_2 \mathbb{R}$. This decomposition naturally implies the same decomposition using the projective linear group $\mathrm{PSL}_2 \mathbb{R}$ instead of $\mathrm{SL}_2 \mathbb{R}$. This feature is of particular interest for us because, as we shall see, $\mathrm{PSL}_2 \mathbb{R}$ is the isometry group of the hyperbolic plane.

2.2 Hyperbolic models: upper-half plane and disk

2.2.1 Hyperbolic plane

We will now introduce the hyperbolic plane and some of its fundamental characteristics. A good complete reference for hyperbolic geometry is [Kat92]. As starting point, we will consider the **upper-half plane** model, i.e. the set

$$\mathcal{H} = \mathbb{R} \times \mathbb{R}_{>0} = \{z \in \mathbb{C} : \Im(z) > 0\}$$

with the metric tensor given by

$$g = \frac{1}{y^2} (dx^2 + dy^2).$$

The couple (\mathcal{H}, g) gives us a Riemannian manifold, as the metric tensor g is positive defined. Moreover we can compute the Gaussian curvature κ of this model, using the fact that

$$\kappa = \frac{1}{2} \bar{R}$$

where \bar{R} is the Ricci scalar. The component of the Ricci tensor are obtained by contracting the indices of Riemann tensor R_{abcd} with the inverse metric tensor g^{ac} . Riemann tensor has 16 components, but with easy calculations one ends up with

$$R^1_{212} = -R^1_{221} = R^2_{121} = -R^2_{112} = y^{-2}$$

and all the other components vanish. Hence

$$R_{1212} = R_{2121} = -y^{-4} \text{ and } R_{1221} = R_{2112} = y^{-4}.$$

It can be seen that, using Einstein notation, it holds

$$R_{cadb} = y^{-4}(1 - \delta_{ab} - \delta_{cd})(1 - \delta_{ac}), \quad g^{ab} = y^2 \delta^{ab}$$

Finally,

$$\begin{aligned} R_{ab} &= g^{cd} R_{cadb} = y^2 \delta^{cd} y^{-4} (1 - \delta_{ab} - \delta_{cd})(1 - \delta_{ac}) \\ &= y^{-2} (\delta^{cd} - \delta^{cd} \delta_{ab} - \delta^{cd} \delta_{cd} - \delta^{cd} \delta_{ac} + \delta^{cd} \delta_{ab} \delta_{ac} + \delta^{cd} \delta_{cd} \delta_{ac}) \\ &= y^{-2} (2 - 2\delta_{ab} - 2 - 1 + \delta_{ab} + 1) = -y^{-2} \delta_{ab} \end{aligned}$$

and then

$$R = g^{ab} R_{ab} = -2$$

which yields $\kappa = -1$. This justify the “hyperbolic” adjective, the upper-half plane model is an example of a manifold with constant negative curvature. As we shall see, this greatly modifies the geometrical properties that we are used to.

We will consider the tangent bundle $T\mathcal{H}$ of the hyperbolic plane and the norm of a vector τ in the tangent space T_z is given by

$$\|\tau\|_z = \sqrt{\langle \tau, \tau \rangle_{g,z}} = \frac{|\tau|}{\Im(z)}.$$

The unit tangent bundle is given by

$$T^1\mathcal{H} := \{(z, \tau) \in T\mathcal{H}: |\tau| = \Im(z)\}$$

of tangent vectors with length 1. In this context, the (hyperbolic distance) between two points $z, w \in \mathcal{H}$ can be defined as

$$d: \mathcal{H} \times \mathcal{H} \rightarrow [0, +\infty], \quad d(z, w) = \inf_{\gamma} L(\gamma)$$

where the infimum runs over all curves $\gamma: [0, 1] \rightarrow \mathcal{H}$ such that $\gamma(0) = z, \gamma(1) = w$, and the length of the curve is defined as

$$L(\gamma) := \int_0^1 \|\gamma'(t)\|_z dt = \int_0^1 \|\gamma'(t)\|_z \frac{dt}{\Im(\gamma(t))}.$$

It's interesting to determine and analyze the isometry group of (\mathcal{H}, g) with respect to the hyperbolic metric. More precisely, the set $\text{Isom}(\mathcal{H})$ is the set of smooth maps

$\varphi: \mathcal{H} \rightarrow \mathcal{H}$ that are metric-preserving, i.e.

$$\|\mathrm{D}\varphi(\tau)\|_{\varphi(z)} = \|\tau\|_z, \quad \forall (z, \tau) \in TM$$

The group $\mathrm{PSL}_2 \mathbb{R}$ naturally acts on the extended hyperbolic plane $\hat{\mathcal{H}} = \mathcal{H} \cup \{\infty\}$ via *Möbius transformations*. For any $A = [a b \ c d] \in \mathrm{PSL}_2 \mathbb{R}$, we get

$$A * z = \frac{az + b}{cz + d}$$

if $z \in \mathcal{H}$ and $A * \infty = a/c$, where $a/c = \infty$ if $c = 0$. The action is well defined, as, if $\Im(z) > 0$, than

$$\Im(A * z) = \frac{\Im(z)}{|cz + d|^2} > 0.$$

For the sake of brevity, we will use $A(z)$ instead of $A * z$. This action generalize to an action on the unit tangent bundle $T^1 M$ given by

$$A * (z, \tau) = (A(z), \mathrm{D} A_* \tau).$$

We will denote the action of A on tangent vector τ at point z with $\mathrm{D}_z A \tau$.

The action on $T^1 M$ is faithfully and moreover is transitive. For this, it's sufficient to show that any element (z, τ) is in the $\mathrm{PSL}_2 \mathbb{R}$ -orbit of (i, i) . We have that

$$\begin{bmatrix} 1 & x \\ 0 & 1 \end{bmatrix} \begin{bmatrix} y^{1/2} & 0 \\ 0 & y^{-1/2} \end{bmatrix} i = x + iy = z$$

and so, if $B = \begin{bmatrix} 1 & x \\ 0 & 1 \end{bmatrix} \begin{bmatrix} y^{1/2} & 0 \\ 0 & y^{-1/2} \end{bmatrix} = \begin{bmatrix} y^{1/2} & xy^{-1/2} \\ 0 & y^{-1/2} \end{bmatrix}$, we have that $B^{-1}(z) = i$. In particular, the action of B^{-1} on the tangent vector τ is the identity. Hence $B^{-1} * (z, \tau) = (i, i)$. Via straightforward computation, it can be shown that the subgroup $\mathrm{SO}_2 \mathbb{R}$ is the stabilizer of point i and acts as a rotation on the tangent vector τ . In particular, if $\tau = e^{i\theta}$, let $\alpha = \frac{1}{2}(\frac{\pi}{2} - \theta)$. Then

$$\begin{aligned} \mathrm{D}_i \begin{bmatrix} \cos \alpha & -\sin \alpha \\ \sin \alpha & \cos \alpha \end{bmatrix} i &= \frac{i}{(\cos \alpha + i \sin \alpha)^2} = ie^{-2ia} \\ &= ie^{-i\pi/2} e^{i\theta} = i(i)\tau = \tau \end{aligned}$$

and hence, if

$$A = B \begin{bmatrix} \cos \alpha & -\sin \alpha \\ \sin \alpha & \cos \alpha \end{bmatrix} = \begin{bmatrix} 1 & x \\ 0 & 1 \end{bmatrix} \begin{bmatrix} y^{1/2} & 0 \\ 0 & y^{-1/2} \end{bmatrix} \begin{bmatrix} \cos \alpha & -\sin \alpha \\ \sin \alpha & \cos \alpha \end{bmatrix} \quad (2.1)$$

we get that $A * (i, i) = (z, \tau)$. In particular this is the only matrix $A \in \mathrm{PSL}_2 \mathbb{R}$ such that $A * (i, i) = (z, \tau)$. Hence, we have following.

Lemma 2.2.1. $T^1 \mathcal{H}$ and $\mathrm{PSL}_2 \mathbb{R}$ are homeomorphic.

Proof. The action of matrix (2.1) defines the desired homeomorphism. ■

The group $\mathrm{PSL}_2 \mathbb{R}$ coincides with the group $\mathrm{Isom} \mathcal{H}$, as stated by the following theorem.

Theorem 2.2.2. *The left action of $\mathrm{PSL}_2 \mathbb{R}$ on $T\mathcal{H}$ it's transitive and preserves the area and volume forms*

$$dA = \frac{dx \wedge dy}{y^2}, \quad dV = \frac{dx \wedge dy \wedge d\theta}{y^2}.$$

In particular, the action of $A \in \mathrm{PSL}_2 \mathbb{R}$ is an isometry.

At this point, it's crucial to establish some characterization of the geodesics, i.e. curves of minimal length connecting two given points. It can be shown the following result.

Proposition 2.2.3. *The geodesics are the vertical lines and the semi-circles centred on the real axis.*

Proof. Let $z, w \in \mathcal{H}$. Let's assume first that $z = ai$ and $w = bi$, with $b > a > 0$. Let $\eta(t) = ti$ with $t \in [a, b]$. Then

$$L(\eta) = \int_a^b \|\eta'(t)\|_{\mathcal{H}} dt = \int_a^b \frac{|\mathbf{i}|}{t} dt = \ln(b/a).$$

Moreover, for a generic path

$$\gamma: [a, b] \rightarrow \mathcal{H}, \quad \gamma(t) = x(t) + y(t)\mathbf{i}$$

such that $\gamma(a) = z$ and $\gamma(b) = w$, we have that

$$L(\gamma) = \int_a^b \frac{\sqrt{x'(t)^2 + y'(t)^2}}{y(t)} dt \geq \int_a^b \frac{|y'(t)|}{y(t)} dt \geq \int_a^b \frac{dy}{y} = \ln(b/a)$$

and hence $\ln(b/a)$ is the hyperbolic length of the segment of the y -axis joining ai and bi . As this is valid for any point of the imaginary axis, we deduce that this axis is a geodesic.

Now, for two arbitrary points $z, w \in \mathcal{H}$ it's sufficient to proceed as follows. Let \mathcal{G} the unique vertical line or circle centered on the real axis passing through these two points. If \mathcal{G} is a vertical axis $a + ti$, the matrix $\begin{bmatrix} 1 & -a \\ 0 & 1 \end{bmatrix}$ shifts this line to the imaginary axis; if otherwise \mathcal{G} is a semicircle with endpoints a, b on the real axis, the matrix $\begin{bmatrix} 0 & -1 \\ 1 & -b \end{bmatrix}$ maps \mathcal{G} to the imaginary axis. In both cases, with an element $A \in \mathrm{PSL}_2 \mathbb{R}$ we can map z, w on the imaginary axis and conclude as before. As $\mathrm{PSL}_2 \mathbb{R}$ transformations are isometries, this shows what desired. ■

Having described the hyperbolic geodesics, it would be useful to have a closed formula for the (hyperbolic) distance of two points. This is established by the following lemma.

Lemma 2.2.4. *For $z, w \in \mathcal{H}$, we have*

$$\cosh d_{\mathcal{H}}(z, w) = 1 + \frac{|z - w|^2}{2\Im(z)\Im(w)}.$$

Proof. Let's assume first that $z = ai$ and $w = bi$, with $b > a > 0$. Then

$$\cosh d_{\mathcal{H}}(ai, bi) = \cosh \ln(b/a) = \frac{1}{2} \left(\frac{b}{a} + \frac{a}{b} \right)$$

and

$$1 + \frac{|z-w|^2}{2\Im(z)\Im(w)} = \frac{a^2+b^2}{2ab}.$$

Now, it's sufficient to show that the right hand side of the equality is invariant under the action of $A \in \mathrm{PSL}_2 \mathbb{R}$ to conclude as in the previous result. This is left as exercise. ■

Having the isometry group $\mathrm{PSL}_2 \mathbb{R}$ of the upper-half plane model at hand and a characterization of geodesics, it's now possible to briefly describe the actions of an arbitrarily element $A \in \mathrm{PSL}_2 \mathbb{R}$. In this regard, it's helpful to introduce another model of the hyperbolic plane, namely Poincaré's disk model \mathcal{D} , which is the data of (\mathcal{D}, h)

$$\mathcal{D} = \{z \in \mathbb{C}: |z| < 1\}, \quad h = \frac{4}{(1-|z|^2)^2}(dx^2 + dy^2)$$

This model is totally equivalent with the upper-half plane model \mathcal{H} as they can be isometrically equivalent via the map

$$C: \mathcal{H} \rightarrow \mathcal{D}, \quad C(z) := \frac{iz+1}{z+i}$$

induced, with abuse of notation, by the matrix $C = \frac{1}{\sqrt{2}} \begin{bmatrix} i & 1 \\ 1 & i \end{bmatrix}$.

To see this, if $w = C(z)$ and $z = x + iy$ with $y > 0$, then

$$\begin{aligned} |w|^2 &= \left| \frac{iz+1}{z+i} \right|^2 = \frac{iz+1}{z+i} \frac{\overline{iz+1}}{\overline{z+i}} \\ &= \frac{x^2+y^2+1-2y}{x^2+y^2+1+2y} < 1. \end{aligned}$$

Moreover, if τ_1, τ_2 are tangent vectors at z , then corrispondent tangent vectors $v_i = D C \tau_i$ at w are given by

$$v_i = \frac{\tau_i}{(z-i)^2}$$

and with easy computation one can show that $g(\tau_1, \tau_2) = h(v_1, v_2)$.

This model can be more appropriate to describe some actions, as it's "compact" and more symmetrical. In this model the geodesics are of two kind:

- if $z, w \in \mathcal{D}$ are collinear with the origin 0, then the geodesic is the only diameter passing through z, w ;
- otherwise, the geodesic connecting z, w is the only circle passing through z, w which is perpendicular* to $\partial\mathcal{D}$;

2.2.2 Hyperbolic isometries

As each element $A \in \mathrm{PSL}_2 \mathbb{R}$ has determinat 1, their action is determined by $\mathrm{tr} A$ (WLOG we can assume $\mathrm{tr} A \geq 0$, as A is considered up to multiplication by $\pm I$). There are three cases:

- $\mathrm{tr} A > 2$, hyperbolic matrices;
- $\mathrm{tr} A = 2$, parabolic matrices;

There is a nice geometrical construction for this: let w^ be the point obtained inverting the point w respect to the circle $|z| = 1$; the desired circle is the circle passing through z, w, w^* .

- $\text{tr } A < 2$, elliptic matrices.

Let's see briefly what their action is .

Hyperbolic matrices: $\text{tr } A > 2$

In this case, the eigenvalues are given by

$$\lambda = \lambda_1 = \frac{\text{tr } A + \sqrt{\Delta}}{2} > 1 > \frac{\text{tr } A - \sqrt{\Delta}}{2} = \lambda_2 = \lambda^{-1},$$

and are both real. If v_1, v_2 are the two eigenvectors corresponding respectively to $\lambda_{1,2}$, matrix A can be diagonalized by matrix $E = (v_1 | v_2)$, getting

$$AE = E \begin{bmatrix} \lambda & \\ & \lambda^{-1} \end{bmatrix}.$$

Matrix A acts on the plane $E\mathcal{H}$ “as” the matrix $D = \begin{pmatrix} \lambda & \\ & \lambda^{-1} \end{pmatrix}$ acts on \mathcal{H} . In this case, the action is given explicitly by $D(z) = \lambda^2 z$ and this action is an (euclidian) homotety with center 0 and factor λ^2 . In particular, every points is attract to ∞ or to 0 (depending whatever $\lambda \leq 1$).

For this reason, matrix A it's a (hyperbolic) dilatation, of center $E * 0$, factor λ^2 and direction $E * \infty$.

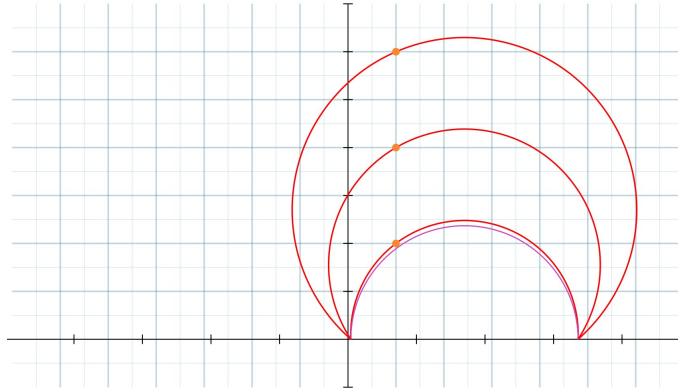


FIGURE 2.1: Action of an hyperbolic matrix on three point. In purple the axis, see the end of this section.

Parabolic matrices: $\text{tr } A = 2$

In this case the two eigenvalues are $\lambda_{1,2} = \lambda = 1$. The matrix A cannot be diagonalized, but it's similar to a matrix $D = \begin{bmatrix} 1 & T \\ 0 & 1 \end{bmatrix}$. In fact, fixed an eigenvector v of A for the eigenvalue 1, this can form a basis for \mathbb{R}^2 with another independent vector v' . Moreover, re-scaling vector v' , we can suppose that $E = (v | v')$ has determinant 1. Hence

$$AE = E \begin{bmatrix} 1 & T \\ 0 & 1 \end{bmatrix}.$$

As before, A acts on the plane $E\mathcal{H}$ “as” the matrix $D = \begin{pmatrix} 1 & T \\ 0 & 1 \end{pmatrix}$ acts on \mathcal{H} . The action of D is $D * z = z + T$, which is a horizontal translation with fixed point ∞ . In particular, the orbits induced by D can be considered as circles of infinity ray with center at ∞ . With this point of view, it's easy to describe the action of A : it's action

will be a hyperbolic translation along circles which are tangents with line $\mathbb{R} \cup \{\infty\}$ at point $E * \infty$.

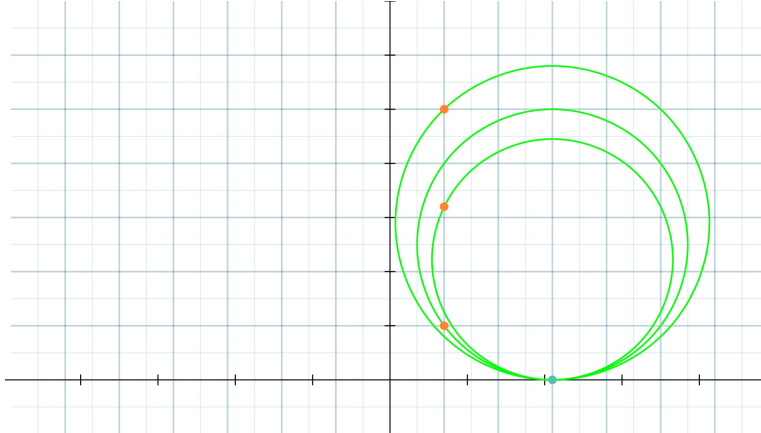


FIGURE 2.2: Action of a parabolic matrix on three point.

Elliptic matrices: $0 < \text{tr } A < 2$

In this case the eigenvalues are complex conjugated $\lambda = \lambda_1 = \bar{\lambda}_2$ of modulus 1 ($\lambda = e^{i\theta}$). Let v the eigenvector corrisponding to the eigenvalue $e^{i\theta}$, so that \bar{v} is the eigenvector for $e^{-i\theta}$. Let $E = (v + \bar{v}, i(v - \bar{v}))$. Scaling E , we can make $|\det T| = 1$.

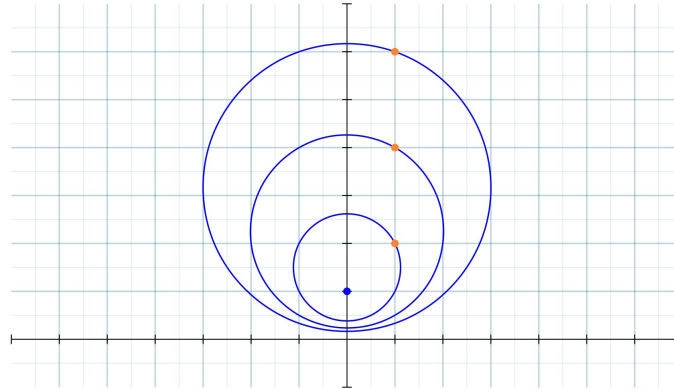


FIGURE 2.3: Action of an elliptic matrix on three point.

Let's assume $\det E = 1$ (the other case is totally analogue). In this case,

$$AE = E \begin{bmatrix} \cos \theta & -\sin \theta \\ \sin \theta & \cos \theta \end{bmatrix} = ER$$

R fixes the point i . The action of R can better visualized in Poincaré's disk model \mathcal{D} : the matrix C sends i in 0 and the corrisponding matrix is given by

$$CRC^{-1} = \begin{bmatrix} e^{-i\theta} & \\ & e^{i\theta} \end{bmatrix}$$

and so the action on \mathcal{D} is given by $z \mapsto e^{-2i\theta} z$, which is exactly a rotation of angle 2θ clockwise. In conclusion, the action of A on $E\mathcal{H}$ is given by hyperbolic rotations around the (unique) fixed point of A in \mathcal{H} .

We could ask ourselves if any action of these matrices could send a geodesic into itself. In this sense, let's recall Iwasawa decomposition 2.1.1: the action of a matrix is decomposed into the product KAN . Hence, given a matrix $KAN = M \in \mathrm{PSL}_2 \mathbb{R}$, it's sufficient to check if there is an invariant geodesic when M is in one of three subgroups of Iwasawa decomposition.

If $M \in \mathrm{PSO}_2 \mathbb{R}$, then M it's a (hyperbolic) rotation around i and then there is no invariant geodesic. In the same way, even if $M = \begin{bmatrix} 1 & x \\ 0 & 1 \end{bmatrix}$ there are no invariant geodesics, as M is an horizontal translation.

Diagonal matrices $A_t = \begin{bmatrix} \exp(t/2) & 0 \\ 0 & \exp(-t/2) \end{bmatrix}$ instead send the $0 - \infty$ geodesic into itself (and $0, \infty$ are fixed points for A_t). In general, an hyperbolic matrix M with $|\mathrm{tr} M| > 2$ is conjugate to a matrix A_t and so the geodesic connecting the two (real) fixed points of M is invariant under the action of M .

It's possible to give an explicit description of this geodesic. Let $M = \begin{bmatrix} a & b \\ c & d \end{bmatrix}$, then the fixed points are given by

$$z_{1,2} = \frac{-(d-a \pm \sqrt{(d-a)^2 + 4cb})}{2c} = -\frac{d-a}{2c} \pm \frac{\sqrt{(d+a)^2 - 4}}{2c}$$

and so the desired geodesic is the semicircle of center $z_C = -(d-a)/2c$ and radius $r = \sqrt{(d+a)^2 - 4}/(2|c|)$. So the equation of the geodesic is

$$|z - z_C|^2 = r^2 \Leftrightarrow c|z|^2 - (d-a)\Re(z) - b = 0 \quad (2.2)$$

If $c = 0$, then the invariant geodesic is vertical, the details are left. In general, such an invariant geodesic is called ***axis*** of hyperbolic matrix M .

2.2.3 Hyperbolic surfaces and fuchsian groups

The starting point to construct hyperbolic surfaces is to consider the analogue of euclidian lattice in this hyperbolic contest, i.e. fuchsian groups. The following result defines a fuchsian group.

Theorem 2.2.5. *Let Γ be a $\mathrm{PSL}_2 \mathbb{R}$ subgroup. The following are equivalent:*

- *The action of Γ on \mathcal{H} is properly discontinuous;*
- *Each Γ -orbit on \mathcal{H} is discrete and each point has finite stabilizer;*
- *Γ is discrete with respect to $\mathrm{PSL}_2 \mathbb{R}$ topology.*

Definition 2.2.6 (Fuchsian group) A subgroup Γ of $\mathrm{PSL}_2 \mathbb{R} = \mathrm{Isom} \mathcal{H}$ that satisfies one of theorem 2.2.5 conditions is called fuchsian group.

We can get an hyperbolic surface by considering the quotient $\Gamma \backslash \mathcal{H}$. In this way, M it's not necessarily a Riemann surface; in fact, if Γ contains some elliptic points then M it's an object called *orbifold*. In general, we will assume that Γ does not have any elliptic elements, with the important exceptions of triangular groups and the modular surface, see METTI SEZIONE più avanti. The following is essential to visualize the action of Γ .

Definition 2.2.7 (Fundamental domain) Let Γ be a fuchsian group and let μ be the hyperbolic area form. Then $D \subset \mathcal{H}$ is a fundamental domain for Γ if

- $\bigcup_{\gamma \in \Gamma} \gamma \bar{D} = \mathcal{H}$;
- $\forall \gamma \neq 1$, we have that $\mu(D \cap \gamma[D]) = 0$; if $D^\circ \cap \gamma[D^\circ] = \emptyset$, the fundamental domain is proper.

It can be shown that, if D_1, D_2 are two fundamental domains of Γ of finite area, then $\mu(D_1) = \mu(D_2)$. A special construction for a fundamental domain is given by Dirichlet.

Definition 2.2.8 (Hyperbolic perpendicular bisector) The perpendicular bisector of a geodesic segment $[z, w]$ is the unique geodesic through the midpoint of $[z, w]$ and orthogonal to $[z, w]$.

The idea of Dirichlet is to consider the set

$$D = D_p(\Gamma) = \{z \in \mathcal{H}: d(z, p) < d(z, \gamma p) \forall \gamma \in \Gamma \setminus \{e\}\}$$

which is the intersection of hyperbolic half-planes

$$H_p(\gamma) = \{z \in \mathcal{H}: d(z, p) \leq d(p, \gamma z)\}$$

delimited by perpendicular bisector. It can be proved ([Kat92]) that a Dirichlet domain is indeed a fundamental domain. Let's now consider some examples.

Example 2.2.6: Triangular groups

Consider an hyperbolic triangle with angles $\pi/a, \pi/b, \pi/c$. In particular it must hold

$$\frac{1}{a} + \frac{1}{b} + \frac{1}{c} < 1$$

If a, b, c are all integers (even ∞), then the group generated by reflections around the three sides of the triangle is a fuchsian group. It's denoted with $\Delta^\pm(a, b, c)$. The group $\Delta(a, b, c)$, instead, is the subgroup of index 2 of $\Delta^\pm(a, b, c)$ with transformations that preserver the orientation. In a more abstract way, a representation of an orientation-preserving triangle group is given by

$$\Delta(a, b, c) = \langle g_a, g_b, g_c : g_a^a = g_b^b = g_c^c = g_a g_b g_c = e \rangle.$$

There is a standard way to construct a triangular group with given integers a, b, c , by Petersson and recently revised by Voight ([VC19], [Pet37]). For $\mathbb{N} \ni t \geq 2$ let

$$\zeta_t = e^{\frac{2\pi i}{t}}, \quad \lambda_t = 2\Re(\zeta_t), \quad \mu_t = 2\Im(\zeta_t).$$

If $t = \infty$, then $\zeta_\infty = 1$. Then, an immersion of $\Delta^\pm(a, b, c)$ in PSL_2 is given by $g_a \mapsto M_a, g_b \mapsto M_b$ and $g_c \mapsto M_c = -M_b^{-1}M_a^{-1}$ where

$$M_a = \frac{1}{2} \begin{bmatrix} \lambda_{2a} & \mu_{2a} \\ -\mu_{2a} & \lambda_{2a} \end{bmatrix}, \quad M_b = \frac{1}{2} \begin{bmatrix} \lambda_{2b} & t\mu_{2c} \\ -\mu_{2c}/t & \lambda_{2b} \end{bmatrix},$$

with $t = c + \sqrt{c^2 - 1}$, $c = \frac{\lambda_{2a}\lambda_{2b}+2\lambda_{2c}}{\mu_{2a}\mu_{2b}}$. In particular, we have

$$M_a^a = M_b^b = M_c^c = I.$$

TO BE ADDED SOME FIGURES

Example 2.2.7: Modular surface

The *modular surface* is the quotient $\Gamma \backslash \mathcal{H}$ where $\Gamma = \text{PSL}_2 \mathbb{Z}$. The group $\text{PSL}_2 \mathbb{Z}$ is generated by the two matrices

$$J = \begin{bmatrix} & -1 \\ 1 & 0 \end{bmatrix}, \quad S = \begin{bmatrix} 1 & 1 \\ & 1 \end{bmatrix}$$

The modular surface can be seen as the triangular group $\Delta(2, 3, \infty)$ and the above construction gives the two matrices

$$M_2 = \begin{bmatrix} & -1 \\ 1 & 0 \end{bmatrix}, \quad M_3 = \begin{bmatrix} 1/2 & 3/2 \\ -1/2 & 1/2 \end{bmatrix}.$$

The third one is hence $M_\infty = \begin{bmatrix} 3/2 & 1/2 \\ -1/2 & 1/2 \end{bmatrix}$. These could appear as different generators (and actually they are different from the above ones) but the two groups of generators are conjugated by the matrix $T = \frac{1}{\sqrt{2}} \begin{bmatrix} 1 & -1 \\ 1 & 1 \end{bmatrix}$:

$$TM_2T^{-1} = \begin{bmatrix} & -1 \\ 1 & 0 \end{bmatrix}, \quad TM_\infty T^{-1} = \begin{bmatrix} 1 & 1 \\ & 1 \end{bmatrix}.$$

Considering the Dirichlet domain centered in $z = 2i$, which has trivial stabilizer in $\text{PSL}_2 \mathbb{R}$, we get that a fundamental domain for $\text{PSL}_2 \mathbb{Z}$ is the set

$$D_{2i} \text{PSL}_2 \mathbb{Z} = \{z \in \mathcal{H}: |\Re(z)| \leq 1/2, |z| > 1\}$$

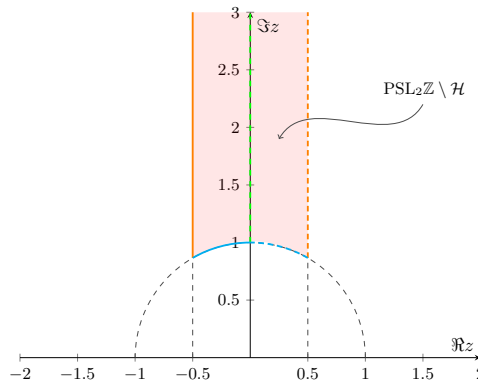


FIGURE 2.4: Fundamental domain of modular surface.

At the link <https://roywilliams.github.io/play/js/s12z/> it is possible to find a visualisation of point-orbits on the tassellation of the plane induced by $\text{PSL}_2 \mathbb{Z}$.

Example 2.2.8: Bolza surface

The *modular surface* is the quotient $\Gamma \backslash \mathcal{H}$ where $\Gamma = \text{PSL}_2 \mathbb{Z}$. The group $\text{PSL}_2 \mathbb{Z}$ is generated by the two matrices

$$g_k = \begin{bmatrix} 1 + \sqrt{2} & (2 + \sqrt{2})\alpha e^{i\frac{k\pi}{4}} \\ (2 + \sqrt{2})\alpha e^{-i\frac{k\pi}{4}} & 1 + \sqrt{2} \end{bmatrix}, \quad \alpha = \sqrt{\sqrt{2} - 1}, \forall k = 0, \dots, 7.$$

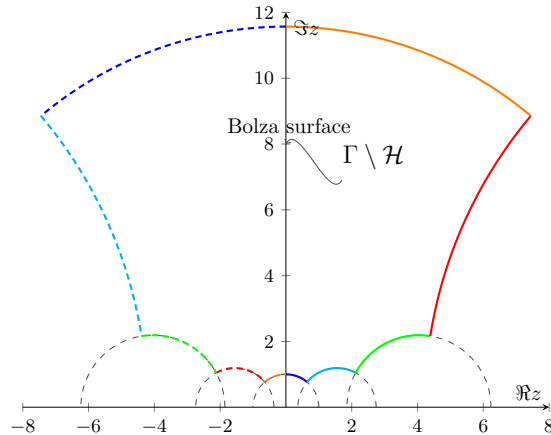


FIGURE 2.5: Fundamental domain of bolza surface in \mathcal{H} .

Considering the Dirichlet domain centered in $\mathcal{D} \ni z = 0$, a fundamental domain for the Bolza surface is given by the hyperbolic octagon with vertices at point $2^{-1/4} \exp(i(\frac{\pi}{8} + \frac{k\pi}{4}))$ for $k = 0, \dots, 7$, with opposite sides identified.



FIGURE 2.6: Bolza surface fundamental domain as subgroup of triangle group $\Delta(2, 3, 8)$ (on the left) and with sides identification (on the right).

There are two interesting facts about Fuchsian groups, which we will not prove ([Kat92]).

Definition 2.2.9 A discrete subgroup $\Gamma < \mathrm{PSL}_2 \mathbb{R}$ is a lattice if it has a fundamental domain D of finite area.

Theorem 2.2.10 (Siegel). If Γ is a lattice, then any Dirichlet fundamental domain has finitely many sides.

Theorem 2.2.11. If Γ is co-compact, i.e. the quotient $\Gamma \backslash \mathcal{H}$ is compact, then Γ has no parabolic element.

The rationale behind this result is that, if the quotient is compact, then it does not have point at extended real axis $\mathbb{R} \cup \{\infty\}$, so it cannot have parabolic elements whose fix elements lie on $\mathbb{R} \cup \{\infty\}$.

2.3 Hyperbolic dynamics

2.3.1 Geodesic flow

The description given above can be regarded as a sort of “discrete” motion induced by $A \in \mathrm{PSL}_2 \mathbb{R}$ on a point of the unit tangent bundle $(z, \tau) \in T^1 \mathcal{H}$. So, the following question would be how to describe the continuous motion of a point z , given a direction τ . This can be achieved by the notion of *geodesic flow*.

Definition 2.3.1 The geodesic flow is a one parameter family of maps

$$a_t: T^1 \mathcal{H} \rightarrow T^1 \mathcal{H}$$

for $t \in \mathbb{R}$, such that for any $(z, \tau) \in T^1 \mathcal{H}$ and $(\gamma(t), \gamma'(t)) = a_t(z, \tau)$ is the unique geodesic parametrised by the arc length satisfying $\gamma(0) = z, \gamma'(0) = \tau$.

In the previous section, we have shown that, for each point (z, τ) there exist one and only one element $G \in \mathrm{PSL}_2 \mathbb{R}$ such that $G(i, i) = (z, \tau)$, which is explicitly given by equation (2.1). So the problem of parameterizing the geodesic starting from z with direction τ can be brought back of parametrizing the geodesic starting from i with direction i . However, we already know that this one is the vertical line it and an arc-length parametrization is given by ie^t . In particular, we have that

$$\begin{aligned} A_t(i, i) &= \begin{bmatrix} \exp(t/2) & \\ & \exp(-t/2) \end{bmatrix} (i, i) \\ &= \left(\frac{\exp(t/2)i}{\exp(-t/2)}, \frac{i}{(0 + \exp(-t/2))^2} \right) = (\exp(t)i, \exp(t)i) \end{aligned}$$

which is the desired parametrization. Hence, for any $(z, \tau) \in T^1 \mathcal{H}$, if $G \in \mathrm{PSL}_2 \mathbb{R}$ is such that $G(i, i) = (z, \tau)$, we have that

$$a_t(z, \tau) = GA_t(i, i).$$

In particular, recalling the Iwasawa decomposition 2.1.1, via the identification of lemma 2.2.1, the geodesic flow is the right action of one parameter family

$$\mathfrak{A} = \left\{ A_t = \begin{bmatrix} \exp(t/2) & \\ & \exp(-t/2) \end{bmatrix}, \quad t \in \mathbb{R} \right\}$$

on the total group $\text{PSL}_2 \mathbb{R}$. There are other two fundamental flows on $T^1 \mathcal{H}$, corresponding to different one parameter subgroups of $\text{PSL}_2 \mathbb{R}$. One is the (*stable*) **horocycle flow** by the one parameter subgroup

$$\mathfrak{U} = \mathfrak{U}^+ = \left\{ U_t = \begin{bmatrix} 1 & t \\ 0 & 1 \end{bmatrix}, \quad t \in \mathbb{R} \right\}$$

and the other one is the *unstable horocycle flow* given by

$$\mathfrak{U}^- = \left\{ U_t = \begin{bmatrix} 1 & 0 \\ t & 1 \end{bmatrix}, \quad t \in \mathbb{R} \right\}$$

In figure 2.7 it's possible to see the simultaneous action of the three groups on the point $(i, e^{i\pi/3})$.

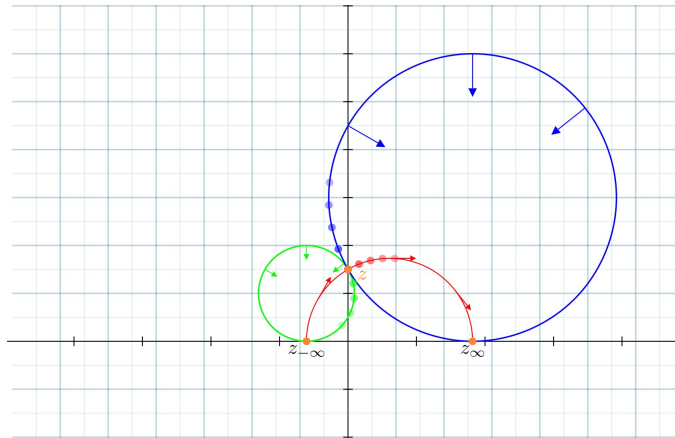


FIGURE 2.7: Action of geodesic, stable and unstable horocycle flow.

2.3.2 Mixing flow on hyperbolic plane

The area form on \mathcal{H}

$$dA = \frac{dx \wedge dy}{y^2}$$

and the volume form on $T^1 \mathcal{H} \simeq \text{PSL}_2 \mathbb{R}$

$$dV = \frac{dx \wedge dy \wedge d\theta}{y^2}$$

are both invariant with respect to the action of the geodesic flow and horocycle flows, by virtue of theorem 2.2.2, so it's interesting to study the corresponding metric system.

We recall the notion of ergodic and mixing dynamical systems 2.3.2 (regarding the case of interest, we will use the continuos-case definitions).

Definition 2.3.2 Let $(X, \mathcal{X}, \mu, R_t)$ a continuos metric dynamical system (in particular $R_{t*}\mu = \mu \forall t \in \mathbb{R}$). Then:

- the flow R_t is **ergodic** if for every measurable set $B \subset X$ which is R_t invariant, $\mu(B) = 0$ or $\mu(X \setminus B) = 0$;

- the flow R_t is **mixing** if for every measurable sets $B, C \subset X$

$$\mu(B \cap R_t^{-1}[C]) \rightarrow \mu(B)\mu(C)$$

holds, when $t \rightarrow \infty$.

These notions describes different manifestations of chaotic behaviour for a classical dynamical system. In particular, the mixing property is stronger than ergodic one: ergodicness of a system only assure that, in certain sense, that for a.e. point the orbit will go through all over the space X ; on the other hand, mixing property regards how much a system “mixes” itself. We will prove the following.

Theorem 2.3.3. *The geodesic and horocyclic flows are mixing.*

This theorem is a direct consequence of a more general result about matrix coefficients of representations of subgroups of $\mathrm{SL}_2 \mathbb{R}$. A unitary representation of a group G on a Hilbert space H is a group homomorphism

$$\pi: G \rightarrow \mathrm{U}(H)$$

where $\mathrm{U}(H)$ denotes the group of unitary transformations. This representation is *strongly continuous* if, for any $\varphi \in H$, the map $g \mapsto \pi(g)\varphi$ is continuous.

Definition 2.3.4 Given $\varphi, \psi \in H$, the function $g \mapsto \langle \pi(g)\varphi, \psi \rangle$ is called a **matrix coefficient** of the representation.

In our situation, π will be a representation of the group $G = \mathrm{SL}_2 \mathbb{R}$ action on the Hilbert space $H = L_2(X)$ with $X = \Gamma \backslash G$, defined by

$$\pi(g)\varphi(h) = \varphi(gh), \quad \forall g \in G, \varphi \in L_2(X).$$

In our context, the above definitions of ergodicity and mixing can be translated as follows.

Definition 2.3.5 Let \mathfrak{U}_t be a one parameter subgroup of $\mathrm{SL}_2 \mathbb{R}$.

- The flow associated to \mathfrak{U}_t is ergodic if and only if for any $t \in \mathbb{R}$, $\pi(\mathfrak{U}_t)$ has no non-trivial invariant vector.
- The flow associated to \mathfrak{U}_t is mixing if and only if for any $\varphi, \psi \in L_2(X)$,

$$\langle \pi(\mathfrak{U}_t)\varphi, \psi \rangle \rightarrow \int_X \varphi \, d\mu \int_X \psi \, d\mu$$

for $t \rightarrow \infty$.

The general result from which we will get the mixing of the geodesic flow is then.

Theorem 2.3.6: Howe-Moore

Let π be a strongly continuous unitary representation of $\mathrm{SL}_2 \mathbb{R}$ on a Hilbert space \mathcal{H} . Assume that π has non-trivial invariant vector in \mathcal{H} . Then, if G_n is a diverging^a sequence in $\mathrm{SL}_2 \mathbb{R}$, then

$$\lim_{n \rightarrow \infty} \langle \pi(G_n)\varphi, \psi \rangle = \int_X \varphi \, d\mu \int_X \psi \, d\mu$$

^aThat is for any compact $K \subset \mathrm{SL}_2 \mathbb{R}$, there exists $N \in \mathbb{N}$ such that $G_n \notin K$ for all $n \geq N$.

Proof. See A.1.3, in Appendix A. ■

In fact, in our case, the group $\mathrm{SL}_2 \mathbb{R}$ acts transitively on X , so, if f a invariant vector with respect to $\mathrm{SL}_2 \mathbb{R}$, it must be constant, hence π has no trivial invariant vector. The geodesic flow and the horocycle flow are given by the action of matrices A_t and $U_{\pm t}$. In both cases, we are given a diverging sequence and so we are done.

A mentioned in chapter 2, this is only a particular case of the more general result due to the Hopf, roughly stated in 1.2.4.

Theorem 2.3.7: Hopf

Let (M, g) be a compact Riemannian manifold with negative sectional curvature. Then the geodesic flow $\Phi_t: TM \rightarrow TM$ is ergodic.

2.3.3 Examples

Although the geodesic flow on an hyperbolic surface is indeed ergodic, this does not prevent the existence of some periodic orbits. Nonetheless, these periodic orbits are very unstable, and little differences in initial condition produces very different behaviour during time evolution.

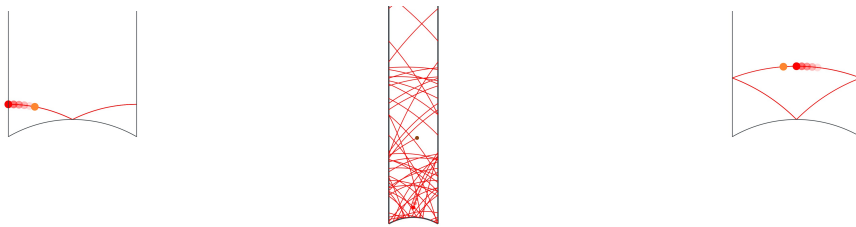


FIGURE 2.8: A typical chaotical orbit on the modular surface (in the center), along with two periodic orbits.

As seen at the end of section 2.2.2, hyperbolic elements $A \in \mathrm{PSL}_2 \mathbb{R}$ have a fixed geodesic, which is its *axis*. We can see periodic orbits on the modular surface as axis of particular hyperbolic elements, see also section 5.3. The two periodic orbits (of periods

4 and 6) in figure 2.8 are given by the two matrices:

$$A_l = \frac{1}{2} \begin{bmatrix} 5^{1/4} - 5^{-1/4} & -(5^{1/4} - 5^{-1/4}) \\ 2/5^{1/4} & 2/5^{1/4} \end{bmatrix} : \text{figure on the left}$$

$$A_r = \frac{1}{6} \begin{bmatrix} 3\sqrt{2}\sqrt[4]{3} & -3\sqrt{2}\sqrt[4]{3} \\ \sqrt{2}3^{3/4} & \sqrt{2}3^{3/4} \end{bmatrix} : \text{figure on the right}$$

Using the *Klein j-function*[†], it is possible to visualize the above motions on the hyperbolic surface on the sphere, getting the images 2.9 (in it are visualized the periodic orbit of matrix A_r and the above ergodic one).

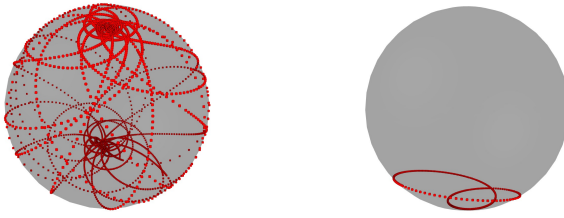


FIGURE 2.9: 3D visualisation of motion on hyperbolic surface.

2.4 Spectra of modular surfaces

The modular group $\mathrm{SL}_2 \mathbb{Z}$ has a particular importance among the fuchsian groups, even if it (or better, its quotient $\mathrm{PSL}_2 \mathbb{Z}$) can be seen just as a triangular group. This group has lots of arithmetic properties and for this reason it has been widely studied, starting from its *principal congruence subgroups* of level N defined by

$$\Gamma(N) = \{G \in \mathrm{SL}_2 : G \equiv_N I\} \quad (2.3)$$

where the congruence “ \equiv ” is taken componentwise. In general, a congruence subgroup of $\Gamma(1) = \mathrm{SL}_2 \mathbb{Z}$ is a subgroup $\Gamma \leq \mathrm{SL}_2 \mathbb{Z}$ for which there exists an N such that $\Gamma \geq \Gamma(N)$ (roughly speaking, it is an “upper subgroup of a principal congruence subgroup”).

The *modular surface of level N* is then defined as

$$X(N) := \Gamma(N) \backslash \mathcal{H}. \quad (2.4)$$

It is, for all $N \geq 1$, a finite-area, non-compact hyperbolic surface. Just to emphasize the relevance of this subgroups, it can be shown that $X(1)$, with its complex structure, can parametrize the space of elliptic curves over \mathbb{C} , [Shi71].

Topologically speaking, the principal modular surface $X(1)$ is a like-sphere surface, with the hyperbolic metric and three “cusp”. Moreover, its hyperbolic surface is equal[‡] to $\pi/3$. To link the next chapter, we can now present the problem of our interest, which is the “quantum-eigenvalue” problem

[†]DA SPIEGARE MEGLIO

[‡]It is possible to use Gauss-Bonnet formula, which states that the hyperbolic area of a $\triangle(a, b, c)$ is equal to $\pi(1 - 1/a - 1/b - 1/c)$.

$$\begin{cases} \Delta \varphi + \lambda \varphi = 0 \\ \varphi(Gz) = \varphi(z) ; \forall G \in \Gamma \\ \int_{\Gamma \backslash \mathcal{H}} |\varphi|^2 d\mu < \text{inf}ty \end{cases} \quad (2.5)$$

with Γ fuchsian group, in particular are extremly important the principal congruence subgroups $\Gamma(N)$. As we will see, the existence of a solution of the problem 2.5 is granted if the quotient space X is compact, which is not the case for subgroups $X(N)$. This matter will be discussed in chapter 7. Avoiding the existence problem, solutions of problem 2.5 are called *Maass forms*.

3 Semiclassical analysis

In this chapter we provide a very brief introduction to basic notions of semiclassical analysis, in particular about symbol quantization. The tools of semiclassical analysis will be essential to understand Weyl’s law and the important Egorov theorem. A comprehensive resource for this subject is [Zwo12], but for a general introductory overview the lecture notes [Dya19] can be very helpful.

3.1 Semiclassical Quantizazion

To be able to relate classical mechanics and its quantum counterpart it is necessary to associate the Hilbert space $H = L^2(M)$ (where M is a manifold) to the mathematical basic structure for classical mechanics, i.e. the cotangent bundle T^*M with its symplectic structure. Moreover, it is necessary to associate operators on H to functions on T^*M .

From a functorial “universal” point of view, there is no procedure to do this [Van51], but there are practical standard and useful ways to do so. One of the most convenient is *Weyl quantization*, which associate classical quantities (*symbols*) $a(x, p) : T^*M \rightarrow \mathbb{C}$ to a quantum observable (pseudodifferential operator) $A(x, hD)$, where x is still the position, but D is a differential and h is a (semiclassical) parameter. In this sense, the limit $h \rightarrow 0$ is to be understood as the classical limit, from the quantum level and for this reason is called *semiclassical limit*. We will now provide the basic notions of this approach.

3.1.1 Semiclassical Fourier transform

From elementary physics, we know that Fourier transform allows us to “change” functions of the position variable q to functions of the momentum p , in the phase space T^*M . Quantization is the tool that allows us to deal with both sets of variables simultaneously in the semiclassical limit. Functions of both q and p variables are called symbols, and are quantized using a sort of “semiclassical Fourier transform”.

We refer to appendix B for the details about classical Fourier transform and the theory of distributions. The latter is a class of important functions related to Fourier transform, in particular we consider the set of *tempered distribution*, which can be viewed as the dual (in the sense of vector spaces) of Schwarz space \mathcal{S} defined by

$$\mathcal{S} = \left\{ f \in C^\infty(\mathbb{R}^n) : \|f\|_{\alpha, \beta} < \infty \quad \forall \alpha, \beta \in \mathbb{N}^n \right\},$$

where $\|\cdot\|_{\alpha,\beta}$ is the seminorm defined in B.1.1. In other words, Schwarz space \mathcal{S} is the set of smooth functions with “rapid decay”. Just to understand the importance of Fourier transform in physics, we will show how it provides the mathematical fundation for the Heisenberg uncertainty principle [Du09].

Example 3.1.9: Heisenberg uncertainty principle in \mathbb{R}

Consider some $\psi \in L^2(\mathbb{R})$ where $x\psi$ and $p\mathcal{F}(\psi) \in L^2(\mathbb{R})$. With the dispersion of ψ defined as

$$\mathcal{D}\psi := \frac{\int_{\mathbb{R}} x^2 |\psi(x)|^2 dx}{\int_{\mathbb{R}} |\psi(x)|^2 dx},$$

we will show, through straightforward computation, that

$$(\mathcal{D}\psi)(\mathcal{D}\mathcal{F}(\psi)) \geq \frac{1}{4}.$$

By integration by parts, we get

$$\begin{aligned} \int_{\mathbb{R}} |\psi(x)|^2 dx &= x |\psi(x)|^2 \Big|_{-\infty}^{\infty} - \int_{\mathbb{R}} x\psi(x)\overline{\psi'(x)} dx - \int_{\mathbb{R}} x\overline{\psi(x)}\psi'(x) dx \\ &= -2\Re \left(\int_{\mathbb{R}} x\overline{\psi(x)}\psi'(x) dx \right), \end{aligned}$$

where the first term is vanished from the decay properties of functions in \mathcal{S} . Squaring both sides and using Schwarz inequality gives

$$\left(\int_{\mathbb{R}} |\psi(x)|^2 dx \right)^2 \leq 4 \left(\int_{\mathbb{R}} |x\overline{\psi(x)}\psi'(x)| dx \right)^2 \leq 4 \left(\int_{\mathbb{R}} x^2 |\psi(x)|^2 dx \right) \left(\int_{\mathbb{R}} |\psi'(x)|^2 dx \right).$$

(i) and (iv) of proposition ?? give $\mathcal{F}(\psi'(x)) = ip\mathcal{F}(\psi)(p)$ and $\|\psi\|^2 = (2\pi)^{-1} \|\mathcal{F}(\psi)\|^2$, so

$$\int_{\mathbb{R}} |\psi'(x)|^2 dx = \frac{1}{2\pi} \int_{\mathbb{R}} p^2 |\hat{\psi}(p)|^2 dp.$$

The thesis follows by last two equalities.

This simple yet fundamental example is explanatory of the following definition, i.e. the semiclassical Fourier transform.

Definition 3.1.1 (semiclassical Fourier transform) For a parameter $h > 0$, the semiclassical Fourier transform $\mathcal{F}_h: \mathcal{S}' \rightarrow \mathcal{S}'$ is defined by

$$\mathcal{F}_h(f)(p) := \mathcal{F}(f) \left(\frac{p}{h} \right) = \int_{\mathbb{R}^n} e^{-\frac{i}{h} \langle q, p \rangle} f(q) dq,$$

with the inverse

$$\mathcal{F}_h^{-1}(f)(q) = h^{-n} \mathcal{F}(f) \left(\frac{q}{h} \right) = \frac{1}{(2\pi h)^n} \int_{\mathbb{R}^n} e^{\frac{i}{h} \langle q, p \rangle} f(p) dp.$$

This different version of Fourier transform has lots of properties similar to the ones of the classical version (see proposition B.1.4).

Proposition 3.1.2. 1. $(h D_p)^\alpha \mathcal{F}_h(\varphi) = \mathcal{F}((-q)^\alpha \varphi)$ and $\mathcal{F}_h((h D_q)^\alpha \varphi) = p^\alpha \mathcal{F}_h(\varphi)$.
2. $\|\varphi\| = (2\pi h)^{-n/2} \|\mathcal{F}_h(\varphi)\|$.

Proof. See [Zwo12]. ■

The aim behind this definition is the desire to control the degree of localization and uncertainty of \mathcal{F} in the semiclassical limit, using a parameter $h > 0$. This is the statement of subsequent theorem 3.1.3.

Theorem 3.1.3 (generalized uncertainty principle). For $j = 1, \dots, n$ and $f \in \mathcal{S}'$, it holds

$$\frac{h}{2} \|f\| \cdot \|\mathcal{F}_h(f)\| \leq \|q_j f\| \cdot \|p_j \mathcal{F}_h(f)\|.$$

Proof. See [Zwo12].

The foregoing theorem 3.1.3 generalizes the previous example 3.1.1. It can be retrieved from theorem 3.1.3 by choosing $n = 1$ and $h = 1/2$. In particular, we can do the following reasoning. Suppose that, in general, we have a function $\psi \in L^2(\mathbb{R}^n)$ where $1 = \|\psi\| = (2\pi h)^{-n/2} \|\mathcal{F}_h(\psi)\|$.

As before, the localization of ψ relative to $x = 0$ can be gauged by $\|q_j \psi\|$ for $j = 1, \dots, n$. For example, suppose that

$$\psi(q) = h^{-\|\alpha\|_1/2} \phi(q_1/h^{\alpha_1}, \dots)$$

for some n -tuple of positive real numbers α , with $\|\alpha\|_\infty \leq 1$, $\phi \in \mathcal{S}$ and $\|\phi\| = 1$. Then, with some computations, it is possible to prove (CITA [Zwo12])

$$\int_{\mathbb{R}^n - N_h(\varepsilon)} |\psi(x)|^2 dx$$

is “very small”, where $N_h(\varepsilon) := \prod_{i=1}^n [-h^{\alpha_i - \varepsilon}, h^{\alpha_i - \varepsilon}]$. Moreover, $\|x_j \psi\| \simeq h^{\alpha_j}$, for all j . On the other hand, the semiclassical Fourier transform gives us

$$\mathcal{F}_h(\psi)(p) = h^{\|\alpha\|_1/2} \mathcal{F}(\psi)(p_1/h^{1-\alpha_1}, \dots, p_n/h^{1-\alpha_n}),$$

which implies that $(2\pi h)^{-n/2} \|p_j \mathcal{F}_h(\psi)\| \simeq h^{1-\alpha_j}$. Again, the localization in q is matched by delocalization in p , and vice-versa.

3.1.2 How to quantize

We will now write down quantization formulas, which are equations that let us associate symbols (classical observables) to h -dependent linear operators (quantum observables) which acts on functions $\varphi(x) \in \mathcal{S}(\mathbb{R}^n)$. We will use variable x for position coordinates, rather than general variable q .

Definition 3.1.4 (symbols and Weyl-quantization) Any function $a = a(x, p) \in \mathcal{S}(\mathbb{R}^{2n})$ in the Schwartz space will be called symbol. The Weyl quantization

$$\text{Op}^W : \mathcal{S}(\mathbb{R}^{2n}) \rightarrow \text{Hom}(\mathcal{S}(\mathbb{R}^n))$$

of symbol a is defined by

$$\text{Op}^W(a)(\varphi)(x) = \frac{1}{(2\pi h)^n} \int_{\mathbb{R}^n} \int_{\mathbb{R}^n} e^{\frac{i}{h}\langle x-y, p \rangle} a\left(\frac{x+y}{2}, p\right) \varphi(y) dy dp, \quad (3.1)$$

where $\varphi \in \mathcal{S}(\mathbb{R}^n)$.

Remark 3.1.1 (Semiclassical pseudodifferential operator). It's possible to define a generalization of Weyl quantization, i.e. the t -quantization for $0 \leq t \leq 1$, given by

$$\text{Op}_t(a)(\varphi)(x) = \frac{1}{(2\pi h)^n} \int_{\mathbb{R}^n} \int_{\mathbb{R}^n} e^{\frac{i}{h}\langle x-y, p \rangle} a(tx + (1-t)y, p) \varphi(y) dy dp.$$

The Weyl quantization is realized for $t = 1/2$, while the *left-right quantization* are obtained for $t = 1, 0$ respectively. The left quantization $\text{Op}^l = \text{Op}_1$ is often called *standard quantization*.

In general, any operator of the form $\text{Op}_t(a)$ is called a *semiclassical pseudodifferential operator* and its dependency on both x, hD is expressed by $\text{Op}_t(a)(x, hD)$.

In view of remark 3.1.1, we see that Weyl-quantization is a sort of “mean” between left and right quantization (it is defined as $\text{Op}_{1/2}$). The Weyl quantization has a number of useful properties.

Example 3.1.10:

Let a a real-valued function (symbol). Then $\text{Op}^W(a)$ is a symmetric operator, i.e.

$$\langle \text{Op}^W(a)(\psi_1), \psi_2 \rangle = \langle \psi_1, \text{Op}^W(a)(\psi_2) \rangle.$$

For this,

$$\begin{aligned} \int \text{Op}^W(a)(\psi_1)(x) \overline{\psi_2(x)} dx &= \iiint e^{\frac{i}{h}\langle x-y, p \rangle} a\left(\frac{x+y}{2}, p\right) \psi_1(y) \overline{\psi_2(x)} dx dy dp \\ &= \iiint e^{\frac{i}{h}\langle x-y, p \rangle} \overline{a\left(\frac{x+y}{2}, p\right)} \psi_1(y) \overline{\psi_2(x)} dx dy dp \\ &= \int \psi_1(y) \overline{\text{Op}^W(a)(\psi_2)(y)} dy. \end{aligned}$$

We will now briefly present some others examples of symbol quantization and some results that will be useful in the following sections ([Zwo12]).

Example 3.1.11: quantizing a p -dependent symbol

If $a(x, p) = p^\alpha$ for a multiindex $\alpha \in \mathbb{N}^n$, then we have

$$\text{Op}_t(a)(\varphi)(x) = a(x, hD)\varphi(x) = (hD)^\alpha \varphi(x)$$

where hD is a semiclassical scaling of the usual differential operator $D^\alpha = i^{-|\alpha|} \partial^\alpha$. If a is “polynomial” in p , with coefficients depending on x , i.e.

$$a(x, p) = \sum_{|\alpha| \leq N} \alpha_\alpha(x) p^\alpha$$

we see why the operators created by quantization maps are called “pseudodifferential”: if a is polynomial in p , we get a standard differential operator.

Example 3.1.12: quantizing a x -dependent symbol

If $a(x, p) = a(x)$, then $\text{Op}_t(a)(\varphi) = a\varphi$. To check this, we take the t -derivative of $\text{Op}_t(a)(\varphi)$:

$$\begin{aligned} \partial_t \text{Op}_t(a)(\varphi) &= \frac{1}{(2\pi h)^n} \iint_{\mathbb{R}^n \times \mathbb{R}^n} e^{\frac{i}{h} \langle x-y, p \rangle} \langle \partial_t a(tx + (1-t)y), x-y \rangle \varphi(y) dy dp \\ &= \frac{h}{i(2\pi h)^n} \int_{\mathbb{R}^n} \text{div}_p \left(\int_{\mathbb{R}^n} e^{\frac{i}{h} \langle x-y, p \rangle} \partial_t a(tx + (1-t)y) \varphi(y) dy \right) dp \\ &= \frac{h}{i(2\pi h)^n} \int_{\mathbb{R}^n} \text{div} \left(e^{\frac{i}{h} \langle x, p \rangle} \mathcal{F}(\psi(p)) \right) dp. \end{aligned}$$

where $\psi(y) = \partial_t a(tx + (1-t)y)\varphi(y)$. The last expression vanishes by rapid decay, and so $\text{Op}_t(a)\varphi = \text{Op}_1(a)\varphi = a\varphi$.

Example 3.1.13: quantizing a linear symbol

Let $a(x, p) = \langle x, \xi \rangle + \langle p, \rho \rangle$ be a linear symbol. From the above examples, $\text{Op}_t(a) = \langle x, \xi \rangle + \langle hD, \rho \rangle$ for all $t \in [0, 1]$.

Proposition 3.1.5 (Properties of quantization). *The followings hold:*

- If $a \in \mathcal{S}(\mathbb{R}^{2n})$, then $\text{Op}_t(a)$ is a continuous map from $\mathcal{S}'(\mathbb{R}^n) \rightarrow \mathcal{S}(\mathbb{R}^n)$ for all $t \in [0, 1]$;
- If $a \in \mathcal{S}'(\mathbb{R}^{2n})$, then $\text{Op}_t(a)$ is a continuous map from $\mathcal{S}'(\mathbb{R}^n) \rightarrow \mathcal{S}'(\mathbb{R}^n)$ for all $t \in [0, 1]$;
- If $a \in \mathcal{S}(\mathbb{R}^{2n})$, then the adjoint operator of $\text{Op}_t(a)$ is $\text{Op}_{1-t}(\bar{a})$: in particular the adjoint operator of the Weyl quantization of a real symbol is itself.

Proof. See [Mar02]. ■

Proposition 3.1.6. *The followings hold:*

- $\text{Op}^W(D_{x_j} a) = [D_{x_j}, \text{Op}^W(a)]$;
- $h \text{Op}^W(D_{p_j} a) = -[x_j, \text{Op}^W(a)]$.

Proof. Let $\varphi \in \mathcal{S}$. We will prove the first statement, as the second is similar. Then by straightforward calculation

$$\begin{aligned}\mathrm{Op}^W(D_{x_j} a) &= \frac{1}{(2\pi h)^n} \iint_{\mathbb{R}^n \times \mathbb{R}^n} D_{x_j} a \left(\frac{x+y}{2}, p \right) e^{\frac{i}{h} \langle x-y, p \rangle} \varphi(y) dp dy \\ &= \frac{1}{(2\pi h)^n} \iint_{\mathbb{R}^n \times \mathbb{R}^n} (D_{x_j} + D_{y_j}) a \left(\frac{x+y}{2}, p \right) e^{\frac{i}{h} \langle x-y, p \rangle} \varphi(y) dp dy\end{aligned}$$

Proposition 3.1.7 (conjugation). *It holds*

$$\mathcal{F}_h^{-1} \mathrm{Op}^W(a)(x, hD) \mathcal{F}_h = \mathrm{Op}^W(a)(hD, -x).$$

Proof. Omitted. ■

3.1.3 Semiclassical Pseudodifferential Operators

From now on, we will only consider Weyl quantization for simplicity. The starting point is the equation

$$\mathrm{Op}^W(a) \mathrm{Op}^W(b) = \mathrm{Op}^W(c) \quad (3.2)$$

for three symbols a, b, c . We want to know under which conditions this equation can hold and compute the correspondent symbol c , which will be denoted by $c := a \otimes_W b$. So we define the *Weyl product* of two symbols a, b as a third symbol c such that equation (3.2) holds.

A linear symbol is a function l of the form

$$l(x, p) = \langle x, \xi \rangle + \langle p, \rho \rangle$$

with $(\xi, \rho) \in \mathbb{R}^{2n}$ fixed. In this sense, there is a bijection between points of \mathbb{R}^n and linear symbols. We first require two lemmas to get the symbol $a \otimes_W b$.

Lemma 3.1.8. *Let $l(x, p) = \langle x, \xi \rangle + \langle p, \rho \rangle$ be a linear symbol. If $a(x, p) = e^{\frac{i}{h} l(x, p)}$ is the exponential of a linear symbol, then*

$$\mathrm{Op}^W(a)(x, hD) = e^{\frac{i}{h} l(x, hD)}$$

where $l(x, hD) = l(x, hD) = \mathrm{Op}^W(l)(x, hD) = \langle x, \xi \rangle + \langle hD, \rho \rangle$ and $e^{\frac{i}{h} l(x, hD)} \varphi(x) := e^{\frac{i}{h} \langle x, \xi \rangle} + e^{\frac{i}{2h} \langle \xi, \rho \rangle} \varphi(x + \rho)$. Furthermore, if l, m are both linear symbols, then

$$e^{\frac{i}{h} l(x, hD)} e^{\frac{i}{h} m(x, hD)} = e^{\frac{i}{h} \sigma(l, m)} e^{\frac{i}{h} (l+m)(x, hD)},$$

for $\sigma((x, p), (y, q)) = \langle y, p \rangle - \langle x, q \rangle$ being the symplectic form on $\mathbb{R}^n \times \mathbb{R}^n$.

Proof. At first, we consider the PDE problem with boundary condition defined by

$$\begin{cases} ih\partial_t v + l(x, hD)v(x, t) = 0 \\ v(x, 0) = u(x), \end{cases}$$

for the function $v(x, t)$ and $u \in \mathcal{S}, t \in \mathbb{R}$. Its unique solution is given by $v(x, t) = e^{\frac{it}{h} l(x, hD)} u$ for $t \in \mathbb{R}$, where the above PDE problem defines the operator $e^{\frac{it}{h} l(x, hD)}$. Now, if $l(x, hD) =$

$\text{Op}^W(l)(x, hD) = \langle x, \xi \rangle + \langle hD, \rho \rangle$, it follows that

$$v(x, t) = e^{\frac{i}{h}\langle x, \xi \rangle} + e^{\frac{it^2}{2h}\langle \xi, \rho \rangle} u(x + t\rho),$$

which gives $e^{\frac{i}{h}l(x, hD)}\varphi(x) = e^{\frac{i}{h}\langle x, \xi \rangle} + e^{\frac{i}{2h}\langle \xi, \rho \rangle} \varphi(x + \rho)$. So we can compute

$$\begin{aligned} \text{Op}^W(e^{\frac{i}{h}l})(u) &= \frac{1}{(2\pi h)^n} \iint_{\mathbb{R}^n \times \mathbb{R}^n} e^{\frac{i}{h}\langle x-y, p \rangle} e^{\frac{i}{h}(\langle p, \rho \rangle + \langle \frac{x+y}{2}, \xi \rangle)} u(y) dy dp \\ &= \frac{1}{(2\pi h)^n} e^{\frac{i}{2h}\langle x, \xi \rangle} \iint_{\mathbb{R}^n \times \mathbb{R}^n} e^{\frac{i}{h}\langle x-y+\rho, p \rangle} e^{\frac{i}{2h}\langle \xi, y \rangle} u(y) dy dp \\ &= \frac{1}{(2\pi h)^n} e^{\frac{i}{2h}\langle x, \xi \rangle} \iint_{\mathbb{R}^n \times \mathbb{R}^n} e^{\frac{i}{h}\langle x-y, p \rangle} e^{\frac{i}{2h}\langle \xi, y+\rho \rangle} u(y+\rho) dy dp \\ &= e^{\frac{i}{h}\langle x, \xi \rangle} e^{\frac{i}{2h}\langle \xi, \rho \rangle} u(x+\rho), \end{aligned}$$

since rescaling the Fourier inversion formula applied to a linear symbol (example 3.1.2) gives (informally)

$$\delta_{xy} = \frac{1}{(2\pi h)^n} \int_{\mathbb{R}^n} e^{\frac{i}{h}\langle x-y, p \rangle} dp$$

in \mathcal{S}' , where $\delta_{x,y}$ is the Dirac delta equal to 1 if $x = y$. We have thus obtained the identity

$$\text{Op}^W(e^{\frac{i}{h}l})(x, hD) = e^{\frac{i}{h}l(x, hD)}.$$

Now we take two linear symbols $l(x, p) = \langle x, \xi \rangle + \langle p, \rho \rangle$ and $m(y, q) = \langle y, \gamma \rangle + \langle q, \eta \rangle$. From the equation above, we have $e^{\frac{i}{h}m(x, hD)}u(x) = e^{\frac{i}{h}\langle x, \gamma \rangle + \frac{i}{2h}\langle \gamma, \eta \rangle} u(x + \eta)$. This implies that

$$e^{\frac{i}{h}l(x, hD)} e^{\frac{i}{h}m(x, hD)} u(x) = \exp\left(\frac{i}{h}\langle x, \xi \rangle + \frac{i}{2h}\langle \xi, \rho \rangle\right) \exp\left(\frac{i}{h}\langle \gamma, x + \rho \rangle + \frac{i}{2h}\langle \gamma, \eta \rangle\right) u(x + \rho + \eta).$$

Since $e^{\frac{i}{h}(l+m)(x, hD)}u(x) = e^{\frac{i}{h}\langle x, \xi + \gamma \rangle + \frac{i}{2h}\langle \xi + \gamma, \rho + \eta \rangle} u(x + \rho + \eta)$, we have

$$e^{\frac{i}{h}(l+m)(x, hD)} u(x) = \exp\left(\frac{i}{2h}\overbrace{\langle \xi, \eta \rangle - \langle \gamma, \rho \rangle}^{=\sigma(l, m)}\right) e^{\frac{i}{h}l(x, hD)} e^{\frac{i}{h}m(x, hD)} u(x).$$

This gives the seeked equation $e^{\frac{i}{h}l(x, hD)} e^{\frac{i}{h}m(x, hD)} =$ ■

The above lemma essentially tell us that the Weyl quantization of the exponentiation of a linear symbol is itself, with the difference that p is substituted by the differential operator hD .

Lemma 3.1.9 (Fourier decomposition of $\text{Op}^W(a)$). If we write

$$\mathcal{F}(a)(l) := \iint_{\mathbb{R}^n \times \mathbb{R}^n} e^{-\frac{i}{h}l(x, p)} a(x, p) dx dp.$$

for $a \in \mathcal{S}$ and $l(x, p) = \langle x, \xi \rangle + \langle p, \rho \rangle$ is a linear symbol. Then the following decomposition formula holds:

$$\text{Op}^w(a)(x, hD) = \frac{1}{(2\pi h)^{2n}} \iint_{\mathbb{R}^n \times \mathbb{R}^n} e^{\frac{i}{h}l(x, p)} \mathcal{F}(a)(l) e^{\frac{i}{h}l(x, hD)} d\xi d\rho.$$

Proof. Sketch of the proof: applying the Fourier inverse formula to $\mathcal{F}(a)$ with the previous lemma, the result follows. See [Zwo12], [Dya19] for details. ■

The following result gives the desired answer for the Weyl product \otimes_W .

Theorem 3.1.10 (quantization composition theorem). *If $a, b \in \mathcal{S}$, then $\text{Op}^W(a) \text{Op}^W(b) = \text{Op}^w(a \otimes_W b)$, where*

$$(a \otimes_W b)(x, p) := e^{ihA(D)}(a(x, p)b(y, q))|_{y=x, q=p}$$

with $A(D) := \frac{1}{2}\sigma(D_x, D_p, D_y, D_q)$ where $\sigma((x, p), (y, q)) = \langle p, y \rangle - psclxq$ is the symplectic form.

Proof. Let l, m be linear symbols. Using lemma 3.1.9, we get

$$\begin{aligned} \text{Op}^w(a)(x, hD) &= \frac{1}{(2\pi h)^{2n}} \iint_{\mathbb{R}^n \times \mathbb{R}^n} \hat{a}(l) e^{\frac{i}{h}l(x, hD)} dl \\ \text{Op}^w(b)(x, hD) &= \frac{1}{(2\pi h)^{2n}} \iint_{\mathbb{R}^n \times \mathbb{R}^n} \hat{b}(m) e^{\frac{i}{h}m(x, hD)} dm \end{aligned}$$

where the integration is intended using the identification between linear symbols and \mathbb{R}^{2n} . Then, using lemma 3.1.8,

$$\begin{aligned} \text{Op}^W(a)(x, hD) \text{Op}^W(b)(x, hD) &= \frac{1}{(2\pi h)^{4n}} \iint_{\mathbb{R}^{2n} \times \mathbb{R}^{2n}} \hat{a}(l) \hat{b}(m) e^{\frac{i}{h}l(x, hD)} e^{\frac{i}{h}m(x, hD)} dm dl \\ &= \frac{1}{(2\pi h)^{4n}} \iint_{\mathbb{R}^{2n} \times \mathbb{R}^{2n}} \hat{a}(l) \hat{b}(m) e^{\frac{i}{2h}\sigma(l, m)} e^{\frac{i}{h}(l+m)(x, hD)} dm dl \\ &= \frac{1}{(2\pi h)^{2n}} \int_{\mathbb{R}^{2n}} \hat{\varphi}_1(r) e^{\frac{i}{h}r(x, hD)} dr \end{aligned}$$

where $\hat{\varphi}_1(r) := \frac{1}{(2\pi h)^{2n}} \int_{l+m=r} \hat{a}(l) \hat{b}(m) e^{\frac{i}{2h}\sigma(l, m)} dl$ is obtained with the change of variable $r = l + m$. We now will show that $\varphi_1 = a \otimes_W b$.

We write $z = (x, p)$, $w = (y, q)$ and $\varphi = a \otimes_W b$, so that

$$\varphi(z) = e^{\frac{i}{2h}\sigma(hD_z, hD_w)} a(z)b(w),$$

and

$$a(z) = \frac{1}{(2\pi h)^{2n}} \int_{\mathbb{R}^{2n}} e^{\frac{i}{h}l(z)} \hat{a}(l) dl, \quad b(w) = \frac{1}{(2\pi h)^{2n}} \int_{\mathbb{R}^{2n}} e^{\frac{i}{h}m(w)} \hat{b}(m) dm.$$

Since* $l(z) = \langle l, z \rangle$ and $m(w) = \langle m, w \rangle$, we have that

$$\exp\left(\frac{i}{2h}\sigma(hD_z, hD_w)\right) \exp\left(\frac{i}{h}(l(z) + m(w))\right) = \exp\left(\frac{i}{h}(l(z) + m(w)) + \frac{i}{2h}\sigma(l, m)\right)$$

implying

$$\begin{aligned} \varphi(z) &= \frac{1}{(2\pi h)^4} \iint_{\mathbb{R}^{2n} \times \mathbb{R}^{2n}} e^{\frac{i}{2h}\sigma(hD_z, hD_w)} e^{\frac{i}{h}(l(z)+m(w))} \Big|_{z=w} \hat{a}(l) \hat{b}(m) dl dm \\ &= \frac{1}{(2\pi h)^4} \iint_{\mathbb{R}^{2n} \times \mathbb{R}^{2n}} e^{\frac{i}{h}(l(z)+m(w))+\frac{i}{2h}\sigma(l, m)} \hat{a}(l) \hat{b}(m) dl dm. \end{aligned}$$

* Again, we are using the abuse of nation of identifying linear symbols with points of \mathbb{R}^{2n} .

Taking the semiclassical Fourier transform of φ gives

$$\begin{aligned}\mathcal{F}_h(\varphi) &= \frac{1}{(2\pi h)^{2n}} \iint_{\mathbb{R}^{2n} \times \mathbb{R}^{2n}} \frac{1}{(2\pi h)^{2n}} \left(\overbrace{\int_{\mathbb{R}^n} e^{\frac{i}{h}(l+m-r)(z)} dz}^{=\delta_{l+m,r}} \right) e^{\frac{i}{2h}\sigma(l,m)} \hat{a}(l) \hat{b}(m) dl dm \\ &= \frac{1}{(2\pi h)^{2n}} \iint_{l+m=r} e^{\frac{i}{2h}\sigma(l,m)} \hat{a}(l) \hat{b}(m) dl dm = \hat{\varphi}_1(r) = \varphi_1(r).\end{aligned}$$

where $\delta_{l+m,r} \in \mathcal{S}'$ is the Dirac delta equals to 1 only if $l + m = r$. Thus $\varphi = \varphi_1$ (they have the same Fourier transform) and we are done. ■

The Weyl product also admits the following integral representation.

Proposition 3.1.11 (integral representation for \otimes_W). *If $a, b \in \mathcal{S}$, then*

$$(a \otimes_W b)(x, p) = \frac{1}{(\pi h)^{2n}} \iint_{\mathbb{R}^{2n} \times \mathbb{R}^{2n}} e^{-\frac{2i}{h}\sigma(w_1, w_2)} a(z + w_1) b(z + w_2) dw_1 dw_2$$

where $z = (x, p)$.

Proof. Omitted. See DS ■

In [Mar02],[Zwo12] is presented a series expansion for the product $a \otimes_W b$ and a first order approximation (in h) is given by

$$a \otimes_W b = ab + \frac{h}{2i} \{a, b\} + O_{\mathcal{S}}(h^2)$$

and, with some computations,

$$[\text{Op}^w(a)(x, hD), \text{Op}^w(b)(x, hD)] = \frac{h}{i} \text{Op}^W(\{a, b\})(x, hD) + O_{\mathcal{S}}(h^3).$$

We begin to recognize the signi-

cance of the classical-quantum correspondence: in the above equation, the commutator of $\text{Op}^W(a)$ and $\text{Op}^W(b)$ is related to the Poisson bracket $\{a, b\}$, a classical quantity. Thus the two worlds relate to each other.

The tools developed here will be now generalized for *symbol classes*, to present, in section 3.2, Egorov theorem and Weyl's law. To summarize, in the current section we have defined quantization procedures, showing that the resulting quantized, pseudodifferential operators form a commutative algebra.

3.1.4 Symbol Classes

The notion of symbol classes was first defined by Hörmander in analyzing PDEs and ψ DO ([Hör83c]). In fact, oftentimes it is useful to organize symbols $a(x, p)$ into *symbol classes*, as this operation allows us to extend symbol calculus to symbols that can depend on the semiclassical parameter h . This section follows the one of Zworski and Hörmander respectively in [Zwo12],[Hör83c]. We only describe the basic definition of symbol classes, stating the principal results without proof, for the sake of brevity.

Definition 3.1.12 (order function) A measurable function $m: \mathbb{R}^{2n} \rightarrow \mathbb{R}_{>0}$ is called an order function if there are constants C and N such that $m(w) \leq Cg(v-w)^N m(v)$ for all $v, w \in \mathbb{R}^{2n}$, where $g(v) = (1 + \|v\|^2)^{1/2}$.

Trivial examples of order functions are the constant function 1 and $g(v)$ itself. It is easy to say that if f_1, f_2 are order functions, then the product $f_1 f_2$ is an order function as well.

Definition 3.1.13 (symbol class) Let $m(z)$ be an order function. The symbol class of $m(z)$ is given by

$$S(m) := \{a \in C^\infty(\mathbb{R}^{2n}): \forall \alpha \in \mathbb{N}^{2n}, \exists C = C(\alpha) \text{ such that } |\partial^\alpha| \leq Cm\}.$$

Likewise, for $\delta \in [0, 1/2]$, we have the (h, δ) -dependent symbol class

$$S(m) := \{a \in C^\infty(\mathbb{R}^{2n}): \forall \alpha \in \mathbb{N}^{2n}, \exists C = C(\alpha) \text{ such that } |\partial^\alpha| \leq Ch^{-\delta|\alpha|}m\}.$$

In particular $S_0(m) = S(m)$. One of the benefits of extending our formulation to symbol classes is that all the previous results still hold. In particular, $\mathcal{S}(\mathbb{R}^{2n}) \subset S(m)$ for any order function m , and it can be shown that Weyl quantization of symbols in $S_\delta(m)$ is also a continuous linear map.

Theorem 3.1.14. If $a \in S_\delta(m)$ with $0 \leq \delta \leq 1/2$ then both

$$\text{Op}^W(a)(x, hD): \mathcal{S}(\mathbb{R}^n) \rightarrow \mathcal{S}(\mathbb{R}^n), \quad \text{Op}^W(a)(x, hD): \mathcal{S}'(\mathbb{R}^n) \rightarrow \mathcal{S}'(\mathbb{R}^n)$$

are continuous linear transformations.

We also retain the quantization composition theorems. As mentioned, we just state the result.

Theorem 3.1.15. Let $a \in S_\delta(m_1)$ and $b \in S_\delta(m_2)$ for $0 \leq \delta \leq 1/2$. The Weyl product $a \otimes_W b$ then lies in $S_\delta(m_1 m_2)$ and $\text{Op}^W(a) \text{Op}^W(b) = \text{Op}^W(a \otimes_W b)$. An approximation for $a \otimes_W b$ is given by

$$a \otimes_W b = ab + \frac{h}{2i} \{a, b\} + O_{S_\delta(m_1 m_2)}(h^{1-2\delta}).$$

The commutator $[\cdot, \cdot]$ and Poisson bracket $\{\cdot, \cdot\}$ are linked by

$$[\text{Op}^W(a)(x, hD), \text{Op}^W(b)(x, hD)] = \frac{h}{i} \text{Op}^W(\{a, b\})(x, hD) + O_{S_\delta(m_1 m_2)}(h^{3(1-2\delta)}).$$

3.2 Two main results: Weyl law and Egorov's Theorem

In this section we will present a first example of Weyl's law and Egorov's theorem, two results mentioned at the beginning of this thesis. The latter put in evidence the correspondence between classical and quantum mechanics, while the former gives informations regarding eigenvalue spacing statistics of the Laplacian. We begin with a real-valued potential function $V \in C^\infty(\mathbb{R}^n)$ and define the Hamiltonian symbol

$$\xi(x, p) := \|p\|^2 + V(x) \tag{3.3}$$

with the corresponding *Schrödinger operator* in n -dimension defined by

$$\Xi(h) := \Xi(x, h D) = -h^2 \Delta + V(x) \quad (3.4)$$

where Δ is the usual euclidian Laplacian and h is the semiclassical parameter. In particular, we can observe that $\text{Op}^W(\xi)(x, h D) = \Xi(h)$. Our goal is to describe the asymptotic distribution of the eigenvalue of Schrödinger operator for $h \rightarrow 0$.

3.2.1 Weyl Law in Euclidian space

As a introductory toy example, we can consider the 1-dimensional potential $V(x) = x^2$ (elastic potential), for a simple harmonic oscillator HO. We consider the case $h = 1$ and so $\Xi = -\partial_{xx} + x^2$. From elementary quantum mechanics, we can define the *creation and annihilation operators* $A := D_x + ix$ and $A^\dagger := D_x - ix$ to get

$$\Xi = AA^\dagger + 1 = A^\dagger A - 1.$$

It is possible to solve the eigenfunction problem related to the HO with the Hermite polynomials

$$H_n(x) := (-1)^n \exp(x^2) \frac{d^n}{dx^n} \exp(-x^2).$$

In particular, the gaussian function $\exp(-x^2/2)$ is the eigenfunction corrisponding to the eigenvalue 1. Moreover, the set of eigenfunctions $\{\psi_n\}_{n \geq 0}$, which are given by $H_n(x) \exp(-x^2/2)$, are orthonormal to each other, so they form a complete set in $L^2(\mathbb{R}^n)$.

In the n -dimensional case, for an HO scaled by semiclassical parameter h , we get that the set of functions

$$\psi_\alpha(x, h) = h^{-n/4} \prod_{i=1}^n H_{\alpha_i}(x_i h^{-1/2}) \exp\left(-\frac{|x|^2}{2}\right), \quad \alpha \in \mathbb{N}^n$$

are eigenfunctions for $\Xi(h)$, with eigenvalue $E_\alpha = (2\|\alpha\|_1 + n)h$. Reindexing the multi-indices, we get that $\Xi(h)\psi_i(x, h) = E_i(h)\psi_i(x, h)$.

Theorem 3.2.1 (Weyl's law for HO). *For $0 \leq a < b < \infty$, it holds*

$$\#\{E(h) : a \leq E(h) \leq b\} = \frac{1}{(2\pi h)^n} (\mu(\{a \leq \|x\|^2 + \|p\|^2\}) + o(1))$$

where $E(h)$ is any eigenvalue of $\Xi(h)$.

Proof. We follow the proof in [Zwo12].

Without loss of generality, let $a = 0$. Since $E(h) = (2\|\alpha\|_1 + n)h$ for some multiindex $\alpha \in \mathbb{N}^n$,

$$\#\{E(h) : 0 \leq E(h) \leq b\} = \#\{\alpha \in \mathbb{N}^n : 0 \leq 2\|\alpha\|_1 + n \leq b/h\} = \#\{\alpha \in \mathbb{N}^n : \|\alpha\|_1 \leq c\}$$

where $c = (b - nh)/2h$. This implies that

$$\#\{E(h) : 0 \leq E(h) \leq b\} = \left| \left\{ x \in \mathbb{R}^n : x_i \geq 0, 1 \leq i \leq n \text{ and } \sum_i x_i \leq c \right\} \right| + o(c^n) = (n!)^{-1} c^n + o(c^n),$$

where the last equality holds because, for $c \rightarrow \infty$, since it can be easily computed that

$$\left| \{x \in \mathbb{R}^n : x_i \geq 0, 1 \leq i \leq n \text{ and } \sum_i x_i \leq 1\} \right| = (n!)^{-1}.$$

Thus, for $h \rightarrow 0$,

$$\#\{E(h) : 0 \leq E(h) \leq b\} = \frac{b^n}{n!(2h)^n} + o(h^{-n}).$$

Now, the measure of the “sphere” $\{\|x\|^2 + \|p\|^2 \leq b\}$ is given by $b^n G(2n)$, where $G(k) = \pi^{k/2} \Gamma(k/2 + 1)^{-1}$. Since $V(2n) = \pi^n (n!)^n$, we have

$$\#\{E(h) : 0 \leq E(h) \leq b\} = \frac{b^n}{n!(2h)^n} + o(h^{-n}) = \frac{1}{(2\pi h)^n} \mu(\{a \leq \|x\|^2 + \|p\|^2\}) + o(h^{-n})$$

as desired. ■

This example gives justification for the following more general result. We will not prove the theorem, because the complexity of its proof is beyond the scope of this thesis, but its statement is nonetheless useful. We suppose that the potential function $V \in C^\infty(\mathbb{R}^n)$ satisfies

$$\begin{cases} |\partial^\alpha V(x)| \leq C \langle x \rangle^k, & \forall \alpha \in \mathbb{N}^n, C = C(\alpha) \in \mathbb{R} \\ V(x) \geq c \langle x \rangle^k, & \|x\| \geq R \end{cases}$$

for certain constants $k, c, R \in \mathbb{R}$.

Theorem 3.2.2. Suppose that V is an admissible potential function, and that $E(h)$ denotes an arbitrary eigenvalue of the operator $\Xi(h) = -h^2 \Delta + V(x)$. Then

$$\#\{E(h) : a \leq E(h) \leq b\} = (2\pi h)^{-n} (\mu(\{a \leq \|p\|^2 + V(x)\}) + o(1))$$

for all $a < b$ in the limit $h \rightarrow 0$.

We will see another form of Weyl’s law in the hyperbolic case, obtained by Selberg trace formula (see chapter 5).

3.2.2 ψ DO on Manifolds

Being the subject very complex, we will focus our discussion on intuition, rather than going in every detail. In this sense, we remark that, for details, the most satisfactory resource for this aim is given by Zworski’s book [Zwo12].

Let M be a smooth Riemannian manifold of dimension n . We will further suppose, in this and the following section, that all manifolds are compact. Let $g: M \subset U_g \rightarrow V_g \subset \mathbb{R}^n$ be a smooth diffeomorphism between open sets and let $\text{Diff}(M)$ the set of all smooth diffeomorphism of M . At first, we will define distributions on manifolds.

Definition 3.2.3 Let $\varphi: C^\infty(M) \rightarrow \mathbb{C}$ be a linear map and let $\Sigma: \mathcal{S}(\mathbb{R}^n) \rightarrow \mathbb{C}$ be defined by

$$\Sigma(f) := \varphi(g^*(\chi f)),$$

where $g \in \text{Diff}(M)$, $\chi \in C_c^\infty(V_g)$. If $\Sigma \in \mathcal{S}'(\mathbb{R}^n)$, then φ is a distribution on M , and write $\varphi \in \mathcal{D}'(M)$.

Definition 3.2.4 If $Q = \sum X_{j_1} \dots X_{j_k}$ where $X_{j_i}: M \rightarrow TM$ is a smooth vector field on M , for all j_i and $1 \leq k \leq m$, then Q is a differential operator on M of order at most m .

We can see that any differential operator P maps the sets

$$C^\infty(M) \rightarrow C^\infty(M), \mathcal{D}'(M) \rightarrow \mathcal{D}'(M).$$

due to mapping properties of vector fields.

We can now define PSO and a quantization procedure on a manifold M . One possible way to approach this would be to use standard pseudodifferential calculus on \mathbb{R}^n and consider then a partition of unity to define quantization operators on M . However:

- this construction depends on local coordinate;
- it depends also on the unit partition.

A key starting question is to determine which symbols are invariant under some diffeomorphism $\phi: \mathbb{R}^n \rightarrow \mathbb{R}^n$: in fact, if the symbol class $S(m)$ is defined by the condition that $\forall \alpha \in \mathbb{N}^n, \exists C = (\alpha) \in \mathbb{R}: |\partial^\alpha a| \leq Cm$, then it may not be true that the pullback of a by the lift of ϕ^{-1} to the cotangent bundle $T^*\mathbb{R}^n$ satisfies the same inequality. It turns out that the appropriate invariant class is given by the following.

Definition 3.2.5 The Kohn-Nirenberg symbol class of order $m \in \mathbb{Z}$ is defined as

$$S^m(\mathbb{R}^{2n}) := \left\{ a \in C^\infty(\mathbb{R}^{2n}): \forall \alpha, \beta \in \mathbb{N}^n, \exists C(\alpha, \beta) \in \mathbb{R}: |\partial_x^\alpha \partial_p^\beta a| \leq C \langle p \rangle^{m - \|\beta\|_1} \right\}$$

Theorem 3.2.6 (Invariance of Kohn-Nirenberg symbols under diffeomorphism).

Let $\theta: \mathbb{R}^n \rightarrow \mathbb{R}^n$ be a diffeomorphism satisfying the inequalities $|\partial^\alpha \theta| \leq C$ and $|\partial^\alpha \theta^{-1}| \leq C$ for C constant depending on the multiindex α . Then, for each symbol $a \in S^m(\mathbb{R}^{2n})$, the pullback $b(x, p) := a(\theta^{-1}(x), \partial\theta(\theta^{-1}(x)) \cdot p)$ under the lift of θ^{-1} is in S^m .

The definition of the Kohn-Nirenberg symbols allows us to define the relevant class of ψ DOs on any smooth manifold.

Definition 3.2.7 (ψ DO on M) A linear map $A: C^\infty(M) \rightarrow C^\infty(M)$ is called a pseudodifferential operator on M of order m if it can be written on each coordinate patch $U_\beta \subset M$ as

$$\varphi A(\psi f) = \varphi \beta^* \text{Op}^W(a_\beta)(x, h D)(\beta^{-1})^*(\psi f)$$

where $\beta \in \text{Diff}(M)$, $\varphi, \psi \in C_c^\infty(U_\beta)$, $f \in C^\infty(M)$, and the symbol a_β is in the Kohn-Nirenberg class $S^m(\mathbb{R}^{2n})$ for some order m . The set of ψ DO of order m on M will be denoted by $\Psi^m(M)$.

Definition 3.2.8 (symbols on T^*M) Let $a \in C^\infty(T^*M)$, $\Phi \in \text{D}(M)$ and $\pi: U_\Phi \times \mathbb{R}^n \rightarrow T^*U_\Phi$ be the natural identification between the open set $U_\Phi \subset M$ and \mathbb{R}^n . If $\Phi^* a \in S^m(U_\Phi \times \mathbb{R}^n)$, then a is a symbol of order m on T^*M , and we write $a \in S^m(T^*M)$.

The above definitions provide the stage for the following two results, which will be used in Egorov's theorem sketch of the proof 3.2.13.

Theorem 3.2.9 (quantization on manifold). If $\Psi^m(M)$ denotes the image $S^m(T^*M)$ under Op^W , then there exist linear maps

$$\sigma: \Psi^m(M) \rightarrow S^m(T^*M)/hS^{m-1}(T^*M)$$

and a “quantizing” operator $\text{Op}^W: S^m(T^*M) \rightarrow \Psi^m(M)$ defined respectively

$$\sigma(A_1 A_2) = \sigma(A_1)\sigma(A_2), \quad \text{and} \quad \sigma(\text{Op}^W(a)) = [a] \in S^m(T^*M)/hS^{m-1}(T^*M),$$

where $[a]$ denotes the equivalence class of a . Then, $a = \sigma(A)$ is the (principal) symbol of the ψ DO A .

Theorem 3.2.10 (Properties of ψ DO). If $A \in \Psi^0(M)$, then $A: L^2(M) \rightarrow L^2(M)$ is bounded. If $A \in \Psi^m(M)$, with $m < 0$, then A is compact.

We will now present how these notions relates with the previous mentioned Weyl’s law. With a choice of local coordinates, we consider the Schrödinger operator $\Xi(h) := -h^2 \Delta + V(x)$ on a compact manifold (M, g) (in this setting $\Delta = \Delta_g$). Using previous examples, we get that the symbol of $\Xi(h)$ is given by

$$\sigma(\Xi(h)) = \xi(x, p) = \|p\|_{g_x}^2 + V(x).$$

Theorem 3.2.11. The pseudodifferential Schrödinger operator $\Xi(h): C_c^\infty(M) \rightarrow C_c(M)$ is essentially self-adjoint. Moreover, for a fixed $h > 0$, there exist a orthogonal basis $\{\psi_k(h)\}_{k \geq 0}$ of $L^2(M)$ made up by Ξ -eigenfunctions such that their eigenvalues tend to ∞ for $k \rightarrow \infty$.

A mirable consequence of this result is the following form of the already mentioned *Weyl’s law*, for planar domains.

Theorem 3.2.12. Let $\Omega \subset \mathbb{R}^2$ be a planar domain in the euclidian plane. If $\Xi = \Xi(1) = -\Delta$, where $V = 0$, and for each Ξ -eigenfunction ψ_j we consider the correspondent eigenvalue E_j , then

$$\lim_{\lambda \rightarrow \infty} \frac{\#\{j: E_j < \lambda\}}{\lambda} = \frac{\text{Area}(\Omega)}{4\pi}.$$

3.2.3 Connection between classical and quantum dynamics: Egorov’s Theorem

Egorov theorem is a very import result in semiclassical analysis which links directly the quantum-mechanical time evolution of a Weyl-quantized operator and the time-evolution of the corrispond symbol along the classical flow. Therefore, Egorov theorem provides a bridge between classical and quantum mechanics.

We will now formulate the theorem. Let (M, g) be a compact smooth Riemannian manifold with metric g and let V be a smooth, real-valued potential on M . Considering local coordinates, the Hamiltonian, as mentioned before, is expressed by

$$\xi(x, p) := \|p\|_{g_x}^2 + V(x)$$

where $(x, p) \in T^*M$. The Hamiltonian flow generated by H is given by (CITARE APPENDICE DA FARE)

$$\Phi^t = \exp(tX_\xi)$$

where X_ξ is the Hamiltonian vector field given by ξ .

From functional analysis theory, by *Stone's theorem* we know that self-adjoint operators are the infinitesimal generators of unitary groups of time evolution operators. So, we denote the unitary group on $L^2(M)$ generated by the self-adjoint operator $\Xi(h)$ as $U(t) = \exp(-it\Xi(h)/h)$.

If $A \in \bigcap_{m \in \mathbb{Z}} \Psi^m(M)$ is another ψ DO, then its quantum time evolution is given by $A(t) = U^{-1}(t)AU(t)$. This is in perfect agreement with Heisenberg picture of quantum mechanics. We are now ready to Egorov's theorem. We now provide a sketch of the proof.

Theorem 3.2.13: Egorov, [Ego69]

Let Φ_t be the Hamiltonian flow of

$$\xi(q, p) = \|p\|_{g_q}^2 + V(q),$$

$U(t)$ the unitary time-evolution operator $\exp(-it\Xi(h)/h)$ and $a_t(q, p) = a(\Phi_t(q, p))$ for some $a \in S^{-\infty}(T^*M)$. If $A = \text{Op}^w(a)(q, hD)$ and $\tilde{A}(t) := \text{Op}^w(a_t)(q, hD)$. Then, it holds

$$\|\text{Op}^w(a_t)(q, hD) - U^{-1}(t)AU(t)\| = \left\| A(t) - \tilde{A}(t) \right\|_{L^2 \rightarrow L^2} = O(h)$$

uniformly respect to t , for any fixed $T > 0$ e for all $0 \leq t \leq T$.

Remark 3.2.1. It is necessary to require that $a \in S^{-\infty}(T^*M)$ to guarantee that a_t is in the same symbol class. In fact, if we only require that $a \in S(T^*M)$, then the symbol class is not preserved by $(\Phi^t)^*$, as the flow of ξ is faster at higher frequencies.

Proof. First of all, $\partial_t a_t = \{\xi, a_t\}$, where $\{\xi, a_t\}$ is the Poisson bracket on T^*M . Let $\sigma(P)$ be the symbol of a ψ DO P ; then

$$\sigma\left(\frac{i}{h}[\Xi(h), B]\right) = \{\xi, \sigma(B)\}$$

for any $B \in \bigcap_{m \in \mathbb{Z}} \Psi^m(M)$. In [Zwo12] and [Mar02], using theorem 3.2.10 and 3.2.9, it is proved that

$$\partial_t \tilde{A}(t) = \frac{i}{h}[\Xi(h), \tilde{A}(t)] + E(t)$$

for $E(t) \in h\Psi^{-\infty}(M)$, with $\|E(t)\|_{L^2 \rightarrow L^2} = O(h)$. Applying now the time-evolution operator on

$$\begin{aligned} \partial_t \left(e^{-\frac{it\Xi(h)}{h}} \tilde{A}(t) e^{\frac{it\Xi(h)}{h}} \right) &= e^{-\frac{it\Xi(h)}{h}} \left(\partial_t \tilde{A}(t) - \frac{i}{h} [\Xi(h), \tilde{A}(t)] \right) e^{\frac{it\Xi(h)}{h}} \\ &= e^{-\frac{it\Xi(h)}{h}} \left(\frac{i}{h} [\Xi(h), \tilde{A}(t)] + E(t) - \frac{i}{h} [\Xi(h), \tilde{A}(t)] \right) e^{\frac{it\Xi(h)}{h}} \\ &= e^{-\frac{it\Xi(h)}{h}} E(t) e^{\frac{it\Xi(h)}{h}} \end{aligned}$$

and as the time-evolution operator is unitary, the last term is $O(h)$. Integrating both sides, this equality gives

$$\left\| U(t)\tilde{A}(t)U^{-1}(t) - A \right\|_{L^2 \rightarrow L^2} = \left\| e^{-\frac{it\Xi(h)}{\hbar}} \tilde{A}(t)e^{\frac{it\Xi(h)}{\hbar}} - A \right\|_{L^2 \rightarrow L^2} = O(h).$$

This implies that

$$\begin{aligned} \left\| \tilde{A}(t) - A(t) \right\|_{L^2 \rightarrow L^2} &= \left\| U(t) \left(\tilde{A}(t) - U^{-1}(t)AU(t) \right) U^{-1}(t) \right\|_{L^2 \rightarrow L^2} \\ &= \left\| U(t)\tilde{A}(t)U^{-1}(t) - A \right\|_{L^2 \rightarrow L^2} = O(h) \end{aligned}$$

uniformly for all $t \in [0, T]$. ■

4 Quantum ergodicity

4.1 Quantum ergodicity

Let (M, g) be a compact Riemannian manifold. We recall some general notions from ergodic theory. The time evolution of any classical system on a Riemannian manifold (M, g) is given by the Hamiltonian flow Φ^t on the phase space T^*M and the flow on each energy shell $\Sigma_c = H^{-1}(c)$ simply identifies with the geodesic flow φ^t on M . Hence, the motion occurs on a hypersurface given by H . We also recall the definition of Liouville measure 1.3.1.

It is possible to discuss the ergodicity of the geodesic flow Φ_t by looking at it as a transformation on the measure space (Σ_c, μ_L^c) and using the discrete definition of ergodicity 1.1.2. In fact, if φ^t is ergodic*, then by Birkhoff's theorem 1.1.5 we have

$$\langle f \rangle_T = \lim_{T \rightarrow \infty} \frac{1}{T} \int_0^T f(\Phi_t(x)) dt = \int_{\Sigma_c} f d\mu_L^c.$$

Moreover, recall the Hamiltonian symbol $\xi: T^*M \rightarrow \mathbb{R}$ given by

$$\xi(q, p) := \|p\|^2 + V(q),$$

for a smooth potential function V , and its (Weyl) quantization $\Xi(h) = -h^2 \Delta + V(x)$, which is the *Schrödinger operator*. In particular, $\text{Op}^W(\xi)(x, hD) = \Xi(h)$. The following definition will be of frequent use.

Definition 4.1.1 (density of a sequence in a set) Given a sequence $\{a_k\}_{k \geq 1}$ of complex numbers, the density of a subsequence a_{k_j} is defined by

$$\lim_{n \rightarrow \infty} \frac{\#\{j: k_j \leq n\}}{n}.$$

We are supposing that the limit does exist.

We begin our “exploration” of different statements of quantum ergodic theorem by quoting the original result of de Verdière, from 1985, which however in is one of the clearest, in our humble opinion. The statement reads as follows.

*For example, if M has sectional negative curvature.

Theorem 4.1.2: QE , Schinrelman and de Védière, CITA

Let M be a compact Riemannian manifold. If the geodesic flow on M is ergodic, then there exists a subsequence of eigenvalues $\{\lambda_{k_i}\}_{i \in \mathbb{N}}$ of density one of the Laplacian $-\Delta$ such that, for any pseudodifferential operator A of order zero with principal symbol a , it holds

$$\lim_{i \rightarrow \infty} \langle A\varphi_{k_i}, \varphi_{k_i} \rangle = \int_{\sigma_c} a \, d\mu_L^c,$$

where φ_{k_i} is a Laplacian's eigenfunction for the eigenvalue λ_{k_i} .

In light of this theorem, it is pretty obvious why negatively-curved Riemannian manifolds are of main interest in this topic: by Hopf's theorem 1.2.4, the geodesic flow on those manifolds is ergodic and, hence, theorem 4.1.2 holds.

An immediate consequence of this theorem is the following.

Corollary 4.1.3 Keeping the notation of theorem 4.1.2 and letting A be a open subset of M , we have

$$\lim_{i \rightarrow \infty} \int_A |\varphi_{k_i}|^2 = \frac{\text{Vol}(A)}{\text{Vol}(M)}.$$

Now several remarks follow.

Remark 4.1.1. • The quantity $\langle A\varphi_n, \varphi_n \rangle$ represents the expectation value of the self-adjoint operator A . So, from this perspective, theorem 4.1.2 states that the expectation value of a quantum observable is just the space-average of its corresponding classical symbol.

- The statement of the theorem can be revised in the sense of measure convergence; in fact, the theorem essentially states that the induced-measures sequence converge to the uniform distribution in the weak*-sense.
- We can give a more striking physical interpretation of theorem 4.1.2. In fact, wavefunctions on a negatively-curved compact domain equidistribute in the high-energy limit. If the classical part of a system, i.e. the geodesic flow, is ergodic, then even in the semiclassical limit $h_n \rightarrow 0$ (or $\lambda_n \rightarrow \infty$) do most eigenfunctions not localize in the phase space.

We will present a more general statement than theorem 4.1.2, involving not only operator Δ , but also the more general Schrödinger operator $\Xi(h)$, to be consistent with the general framework of semiclassical analysis. To introduce the general theorem 4.1.5, we need the following definition.

Definition 4.1.4 (Uniform symbol) Let a be a symbol and let $A = \text{Op}^w(a)(q, hD)$. Then a is uniform if for all $t \in [a, b]$,

$$\alpha := \int_{\Sigma_t} \sigma(A) \, d\mu_L$$

is constant with respect to t , i.e. the averages of a over energy-shells $\xi^{-1}(c)$ are all equal to some α . A ψ DO is uniform if its principal symbol is.

It should be noted that any symbol b can be made uniform, via the application of the correct projection to the set of uniform symbols. This projection Π can be defined in the following way. We refer to METTI ZWORKSI for further details. Assuming that $\|\partial \xi\| > \alpha > 0$ on $\xi^{-1}([a, b])$, we can assure ourselves that $\|\partial \xi\| > \alpha/2$ on $\xi^{-1}[a-\varepsilon, b+\varepsilon]$ for a sufficient small positive parameter $\varepsilon > 0$. If $d = \xi(x, p)$ then we define

$$\Pi(b(x, p)) := b(x, p) - \int_{\Sigma_d} b \, d\mu_L^d$$

for every symbol b . In particular, we have

$$\int_{\xi^{-1}(c)} \Pi(b) \, d\mu_L^c = 0, \quad \forall c \in [a, b].$$

Using a *bump function* $\chi \in C_c^\infty(\xi^{-1}((a-\varepsilon, b+\varepsilon)))$ such that it is equal to 1 on $\xi^{-1}([a, b])$, it is possible to define Π on manifolds M as

$$\Pi: C^\infty(T^*M) \rightarrow C_c^\infty(T^*M), \quad \Pi(b) =$$

In particular, it can be proved, using the equality $\int_{\xi^{-1}(d)} \Pi(b) \, d\mu_L^d = 0$, that Π is indeed a projection, i.e. is idempotent. The previous equality $\int_{\xi^{-1}(c)} \Pi(b) \, d\mu_L^c = 0$ holds for any choice of the symbol b . Thus, Π maps arbitrary symbols to uniform symbols of zero average.

The next theorem is a version of the celebrated QE theorem for operator $\Xi(h)$.

Theorem 4.1.5 (QE, Zelditch and Zworski). *Let (M, g) be a compact Riemannian manifold with ergodic geodesic flow. If $A \in \Psi(M)$ is uniform, with principal symbol $\sigma(A)$, then*

$$(2\pi h)^n \sum_{a \leq \lambda_k \leq b} \left| \langle A\varphi_k, \varphi_k \rangle - \int_{\{a \leq \xi(x, p) \leq b\}} \sigma(A) \, dx \, dp \right|^2 \rightarrow 0,$$

for $h \rightarrow 0$ and $\forall \lambda_k$ eigenvalues of $\Xi(h)$ in the interval $[a, b]$, with correspondent eigenfunctions φ_k .

This theorem can be slightly modified to consider the case $h = 1$ and $\Xi(h) = -\Delta$, implying theorem 4.1.2.

Example 4.1.14: equidistribution of Δ -eigenfunctions

Let (M, g) be a Riemannian manifold such that the geodesic flow is ergodic. Let $\Delta = \Delta_g$ the Laplacian operator on M , with respect to the metric g .

Theorem 4.1.2 assures us that there is a subsequence $k_i \rightarrow \infty$ of density 1 such that

$$\int_M |\varphi_{k_i}^2| f \, dx \rightarrow \int_M f \, dx.$$

This general framework basically sets up the starting point of *quantum unique ergodicity*:

Under the hypothesis of theorem 4.1.5 or 4.1.2, do these probability measures induced by eigenfunctions always converge to the uniform measures?

We approach this point in the next section.

4.2 Quantum unique ergodicity

We will start from a brief heuristic reasoning. The quantum ergodicity theorem gives an answer regarding the asymptotic evolution of Laplacian eigenfunctions, in case of classical ergodicity. In particular, QE theorems examine the quantities $\langle A\varphi_k, \varphi_k \rangle$, where A is a semiclassical ψ DO, corresponding to principal symbol $\sigma(A) = a$. Mathematically and physically, these quantities are the most obvious to consider in the asymptotic limit, because their analytical expression is most certainly impossible to write down. In this sense, these quantities give birth, in a natural way, to sort of “eigenfunction-induced” measure, the **Wigner measures**. The Wigner measure (mentioned in chapter 1) of the state φ_k on T^*M is defined by

$$\mu_k(a) := \langle A\varphi_k, \varphi_k \rangle. \quad (4.1)$$

In fact, the projection of one of this measure to the manifold M is equal to the probability measure $\lambda_k := |\varphi_k(x)|^2 dx$ and for this reason the measure μ_k is called **microlocal lift** of measure λ_k^M . As measures on the phase space T^*M , μ_k also carries with itself informations about the functions φ_k .

Definition 4.2.1 Let $A \in \Psi(M)$ has principal symbol $a = \sigma(A)$. Then, the measure on T^*M defined by

$$\mu(a(x, p)) = \langle A\varphi_k, \varphi_k \rangle$$

is called Wigner measure of eigenfunction φ_k for $\Xi(h)$. The transformation of measures from M to T^*M defined by

$$\mu_k = |\varphi_k|^2 dx \mapsto \langle A\varphi_k, \varphi_k \rangle = \mu_k$$

is called microlocal lift.

Usually, it is an hopeless task to analysize the Wigner measure for a given eigenfunction φ_k . However, again, we could shift our interest to the asymptotic behaviour of this measures. The following definition is fundamental to make more rigourous the concept of “asymptotic behaviour” for measures.

Definition 4.2.2 A sequence of measures $\{\mu_k\}_{k \geq 0}$ on a manifold M converges to a measure μ in the weak-* topology if

$$\lim_{k \rightarrow \infty} \int f d\mu_k = \int f d\mu, \quad \forall f \in C_c^\infty(M)$$

Definition 4.2.3 (Quantum limit) A weak-ast limit μ of a subsequence of Wigner measures is called **quantum limit measure**.

We will take for granted that any quantum limit μ possesses the following two properties:

- μ is a probability measure on any given energy shell σ_c .

- μ is invariant with respect to the geodesic flow Φ_t on M .

In particular, the second statement can be derived directly from Egorov's theorem 3.2.13. Setting the stage for introducing the definition of QUE, we now rewrite the definition of QE as follows.

Definition 4.2.4 If M is a compact Riemannian manifold with ergodic geodesic flow, then there exists a subsequence $\{\varphi_{k_j}\}_{j \geq 0}$ of eigenfunctions of density 1 such that the Wigner measures satisfy $\mu_{k_j} \rightarrow \mu_L^c$ on Σ_c for $j \rightarrow \infty$.

The point is the uniqueness of Liouville measure as the only possible quantum limit.

In this way, it is possible to view that QUE is much stronger than QE: equidistribution occurs not only on the configuration manifold M , but also on the energy surface Σ_c .

If QUE fails, it means that there are some subsequence of Wigner measures, that could be very very sparse among all eigenvalues, that have a different quantum limit, reflecting some particular behaviour of the underlying classical system. The general and most famous conjecture in this field is due to Zeev Rudnick and Peter Sarnak, first formulated in 1993 [RS96]. It reads as follows.

Conjecture 4.2.5: Rudnick, Sarnak

If (M, g) is a Riemannian manifold with negative curvature, then the sequence of Wigner measures μ_k induced by eigenfunctions of operator $\Xi(h)$ converges to the Liouville measure μ_L^c on any energy shell $\Sigma_c = \xi^{-1}(c)$.

A reason behind the difficulty to tackle QUE with respect to QE is that QUE deals with not only with convergence of measures, but also with the elimination of all possible exceptional eigenfunctions. In particular, this aspect defies standard semiclassical tools, as Weyl's law. In fact, it should be necessary to have a control not only on one sequence of eigenfunction, but on every possible sequence.

To present both sides of QUE (when it holds and when it does not), in the next section we briefly present how Hassell managed to prove that QUE fails for the Bunimovich Stadium \mathcal{BS}_l . On the other hand, in the chapter 6, we will present a major result of E. Lindenstrauss, which essentially ensures that QUE holds for hyperbolic surfaces with an additional arithmetical structure.

4.3 Hassell disproof of QUE

The \mathcal{BS}_l billiard has a different behaviour from the geodesic flow on negatively curved surfaces, as it can be seen from figure in chapter 1. Indeed, both of them are ergodic and mixing systems, but the rectangular part of \mathcal{BS}_l gives birth to some interesting, nonetheless trivial, periodic orbits: it is the one-parameter family of orbits that corresponds to billiards bouncing back and forth vertically against the horizontal walls. This situation is called *bouncing ball mode* and the phenomenon of *scarring* involving these modes was studied by Heller as early as 1984. In this sense, this phenomenon gives a heuristical reason for the failure of QUE in \mathcal{BS}_l case. The motion in the \mathcal{BS} is still QE, as those trivial periodic orbits form a set of (Liouville) measure zero, but QUE fails as this regime is still present in the high-eigenvalue limit. (In figure 4.1 it is possible to see 4 of these “bouncing-modes”)

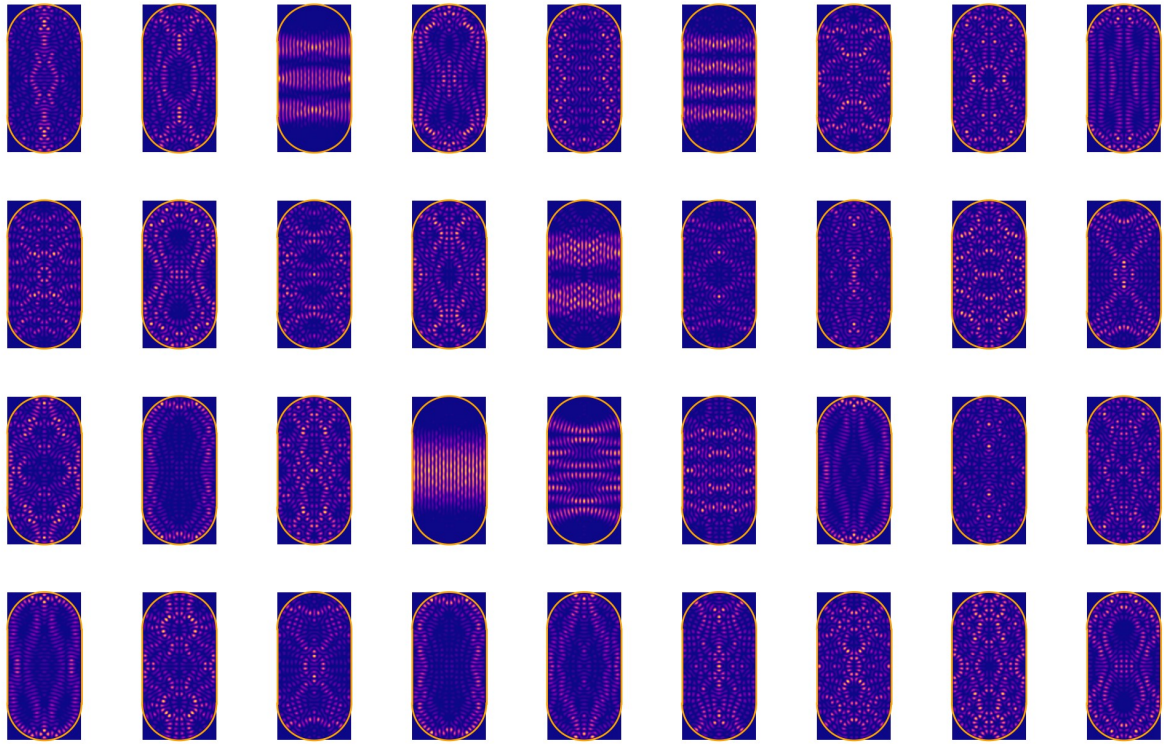


FIGURE 4.1: Bunimovich stadium 36 eigenfunctions, for $\lambda \sim 1000$

In fact, Hassell's main result ([Has10a]) shows that some high-eigenvalue eigenstates of \mathcal{BS}_l do indeed have a positive mass on the bouncing ball orbits.

Theorem 4.3.1: Hassell

For every $\varepsilon > 0$, there exist a subset $B_\varepsilon \subset [1, 2]$ of measure at least $1 - 4\varepsilon$ and a constant $m(\varepsilon) > 0$ with the following property: for every $l \in B_\varepsilon$, there exist a quantum limit formed from Dirichlet eigenfunctions of Δ on the \mathcal{BS}_l that gives probability mass at least $m(\varepsilon)$ to the bouncing ball trajectories.

The result of Hassell was foreshadowed by numerical computations (see also chapter 7) and is based on construction of *quasi-modes*, approximate solutions for eigenfunctions given by Wentzel-Kramers-Brillouin (WKB) methods. The main obstacle in reaching the proof was to show that “bouncing-ball” eigenfunctions (i.e. the corresponding Wigner measures) exist in the high-energy limit. Hassell's proof is a combination of the following techniques:

- the *Heller-Zelditch argument*, mettere referenza:

this method shows that eigenfunctions of Δ localize on any Bunimovich stadium \mathcal{BS}_t , with the (possible) exception of eigenvalues lying in intervals of the form $[n^2 - O(1), n^2 + O(1)]$, with $n \in \mathbb{N}$. It can be proved that, if there really only $O(1)$ eigenvalues in this interval, then eigenfunctions can localize, i.e. “scarring” can occur in momentum space for these intervals (see Tao [Tao08]). Reaching this bound ($O(1)$) is the difficult part of this step;

- the *Hadamard variation formula*:

one of the main difficulties in approaching the previous task is the fact that

Weyl's law has too large error term to get the desired bound. Hassell used this formula, which shows how the eigenvalues of \mathcal{BS}_l vary with the aspect ratio of its rectangular component t . The formula is given by

$$\frac{d}{dl} \lambda_k(l) = - \int_{\partial \mathcal{BS}_l} \frac{\operatorname{sgn}(x)}{2} (Y \cdot \vec{n}) |\partial_{\vec{n}} \varphi_k(x, l)|^2 ds,$$

where (φ_k, λ_k) is an eigenvector-eigenvalue pair of the Laplacian Δ with Dirichlet boundary condition on \mathcal{BS}_l , \vec{n} is the outward unit normal vector at $\partial \mathcal{BS}_l$ and ds is “curvilinear element” on $\partial \mathcal{BS}_l$. Since $\operatorname{sgn}(x)/2(\partial_x \cdot \vec{n}) \geq 0$ always, the formula shows that, as t increases, the magnitude of λ_k decreases instead, for fixed k . One should not be surprised by this, because Weyl's law gives us

$$\lambda_k = \frac{4\pi k}{\operatorname{Area}(\mathcal{BS}_t)} (1 + o(1))$$

and we see that t and λ_k are “almost inversely proportional”. Using this formula, Hassell shows the refinement

$$-\frac{d}{dl} \lambda_k(l) \sim \lambda_k(l)$$

in expectation over k .

- *quantum unique ergodicity:*

this is used to reach a contradiction. More explicitly, if \mathcal{BS}_l is QUE, then by Egorov's theorem 3.2.13 essentially positions and momenta of eigenfunctions in $T^* \mathcal{BS}_l$ are driven by the geodesic flow. At this point, Hassell uses this general argument ([Tao08],[Has10a]): in classical dynamics, all geodesic in \mathcal{BS}_t eventually intersect its boundary, and it can be shown that for any equidistributed eigenfunction, its normal derivative is also equidistributed on $\partial \mathcal{BS}_l$; hence, all eigenfunctions are equidistributed on $\partial \mathcal{BS}_l$ and this would imply that the exponential decay, given by Hadamard formula, holds for every λ_k , and not just in expectation. If this would be the case, it could be shown besides that the Δ -eigenvalues cannot concentrate in interval of the form $[n^2 - O(1), n^2 + O(1)]$ for most $l \in [1, 2]$, else the eigenvalues would lay around n^2 for intervals of t of measure non-zero, getting a contradiction with the exponential decay. The Heller-Zelditch argument then gives a contradiction to QUE assumption.

Remark 4.3.1. It is important to highlight that the Bunimovich Stadium \mathcal{BS}_l is the only known dynamical billiard for which we have a complete understanding of QE and QUE to date. In particular, it is the only one for which we know that QUE does not hold. On the contrary, there many other systems, like the cardioid stadium \mathcal{CS} and Barnett stadium are believed to be QUE.

METTERE FIGURA CARDIOIDE AUTOFUNZIONI?

5 Seldberg trace formula

Trace formulas, in general, establish a connection between geometrical quantities with the spectra of a differential operator. Thus, they have the following form

$$\sum \{\text{spectral terms}\} = \sum \{\text{geometrical terms}\}.$$

We will now consider an introductory example, taken from [Mar12], to introduce this subject.

5.1 Trace formula on \mathbb{S}^1

A first example of a trace formula can be derived from the famous *Poisson summation formula*

$$\sum_{m \in \mathbb{Z}} h(m) = \sum_{n \in \mathbb{Z}} \int_{\mathbb{R}} h(t) e^{2\pi i nt} dt = \sum_{n \in \mathbb{Z}} \hat{h}(n) \quad (5.1)$$

which holds for $h: \mathbb{R} \rightarrow \mathbb{C}$ of class C^2 and such that $|h(t)|$ is of “rapid decay” (as in the Schwarz space \mathcal{S}). Usually, it is used to derive the functional equation of Riemann’s zeta function. We can now read this formula as a *trace formula*.

Consider the Laplacian $-\Delta$ on the unit circle \mathbb{S}^1 . This amounts on studying the equation

$$-\Delta u = \lambda u, \quad u(0) = u(2\pi)$$

which has solutions of the form $\varphi_n(x) = (2\pi)^{-1/2} e^{inx}$ with $\lambda = n^2$. Considering the linear operator L acting on 2π -periodic functions and defined by

$$[Lf](x) := \int_0^{2\pi} k(x, y) f(y) dy$$

where the integral kernel $k(x, y)$ is given by

$$k(x, y) = \sum_{m \in \mathbb{Z}} h(m) \varphi_m(x) \overline{\varphi}_m(y).$$

Then, due to the orthogonality in $L^2([0, 2\pi])$ of eigenfunctions $\varphi_n(x)$, we have

$$L\varphi_n = h(n)\varphi_n$$

and hence the left hand side of equation (5.1) can be read as a “spectral sum” over eigenvalues. In particular, it holds

$$\operatorname{tr} L = \sum_{n \in \mathbb{Z}} \int_{\mathbb{R}} h(t) e^{2\pi i n t} dt.$$

The right hand is of this last equation has an immediate geometric interpretation, as sum over all geodesics (in S^1) of length $2|n|$.

Now, we choose the function $h(t) = (\lambda^2 - t^2)^{-1}$, which appears dealing with the resolvent operator of the Laplacian $(\Delta + \lambda^2)$. For further details we refer to [Mar12]. Poisson summation formula gives

$$\sum_{m \in \mathbb{Z}} \frac{1}{\lambda^2 - m^2} = \sum_{n \in \mathbb{Z}} \int_{\mathbb{R}} \frac{e^{2\pi i n t}}{\lambda^2 - t^2} dt.$$

The integral term can be rewritten as follows. If n is non-positive, then

$$\int_{\mathbb{R}} \frac{e^{2\pi i n t}}{\lambda^2 - t^2} dt = \int_{\mathbb{R}} \frac{e^{-2\pi i |n| t}}{\lambda^2 - t^2} dt$$

while in the other case, with the substitution $t \mapsto -t$,

$$\int_{\mathbb{R}} -\frac{e^{-2\pi i n t}}{\lambda^2 - (-t)^2} dt = \int_{\mathbb{R}} \frac{e^{-2\pi i |n| t}}{\lambda^2 - t^2} dt$$

In conclusion,

$$\sum_{m \in \mathbb{Z}} \frac{1}{\lambda^2 - m^2} = \int_{\mathbb{R}} \frac{e^{-2\pi i |n| t}}{\lambda^2 - t^2} dt$$

Considering the rectangle

$$\gamma = \{t\} \cup \{M + i(t+M)\} \cup \{-t+2Mi\} \cup \{-M + i(M-t)\} = \gamma_1 \cup \gamma_2 \cup \gamma_3 \cup \gamma_4, \quad \forall t \in [-M, M]$$

with $M > 0$ and using the Residue Theorem to compute the integral of $f(t) = \frac{e^{-2\pi i |n| t}}{\lambda^2 - t^2}$ along γ (clockwise) we get

$$\int_{[-M, M]} \frac{e^{-2\pi i |n| t}}{\lambda^2 - t^2} dt = \int_{\gamma_2 \cup \gamma_3 \cup \gamma_4} \frac{e^{-2\pi i |n| z}}{\lambda^2 - t^2} dz + 2\pi i \operatorname{Res}(f, \lambda).$$

It can be shown with simple standard bounding techniques that the integral over the complex segments $\gamma_2 \cup \gamma_3 \cup \gamma_4$ vanishes for $M \rightarrow \infty$. Hence we get

$$\int_{\mathbb{R}} \frac{e^{-2\pi i |n| t}}{\lambda^2 - t^2} dt = 2\pi i \operatorname{Res}(f, \lambda) = 2\pi i \frac{e^{-2\pi i |n| \lambda}}{2\lambda} = \frac{\pi i}{\lambda} e^{-2\pi i |n| \lambda}.$$

So,

$$\sum_{m \in \mathbb{Z}} \frac{1}{\lambda^2 - m^2} = \frac{\pi i}{\lambda} \sum_{n \in \mathbb{Z}} e^{-2\pi i |n| \lambda}.$$

The right hand side is linked to $\cot z$ function on the half plane $\Im(z) < 0$, as

$$\cot z = \frac{\cos z}{\sin z} = i \frac{1 + e^{-2iz}}{1 - e^{-2iz}} = i(1 + e^{-2iz}) \sum_{n=0}^{\infty} e^{-2in} = i \sum_{n \in \mathbb{Z}} e^{-2i|z|}.$$

In the end it is proved

$$\sum_{m \in \mathbb{Z}} \frac{1}{\lambda^2 - m^2} = \frac{\pi}{\lambda} \cot(\pi\lambda)$$

We will now go deeper in trace formula for hyperbolic surfaces, regarding Laplacian eigenfunctions. This form resembles the general structure of a trace formula, where often trigonometric and hyperbolic functions are present. In the general case for h the final formula is the following.

Theorem 5.1.1. *Let $h: \mathbb{C} \rightarrow \mathbb{C}$ a function which is analytic for $|\Im(z)| \leq \sigma$, for a certain $\sigma > 0$. Moreover, suppose that $h(z)$ is such that*

$$|h(z)| \ll (1 + |\Re(z)|)^{-1-\delta}$$

for some $\delta > 0$, uniformly for all z in the strip $|\Im z| \leq \sigma$.

Its proof follows verbatim the previous reasonings.

5.2 Laplacian operator

Driven by the previous example, we now approach the Selberg trace formula for the case of interest. In this situation, as foretold before, our differential operator will be the Laplacian. On the main reasons for the importance of Laplace-Beltrami operator (for brevity, Laplace or Laplacian) is that it's the unique (up to scalar multiplication) second order differential operator that commutes with actions of the isometry group. Thinking about homogeneity and isotropy in physics, this can help explaining its widespread presence in most of partial differential equations (Schrödinger equation, wave equation ecc.) At first, in this chapter, we will introduce main properties of Laplacian on hyperbolic surfaces and will develop, without going in details however, notions of harmonic analysis for this context. The final aim will be to explore the connection between eigen-spectrum of the Laplacian and the dynamical properties of hyperbolic surfaces, namely the Seldberg trace formula.

Explicitly, the Laplace operator on a Riemannian manifold with metric g is given in local coordinate by

$$\Delta f = \frac{1}{\sqrt{|g|}} \partial_i \left(\sqrt{|g|} g^{ij} \partial_j f \right)$$

where $|g|$ is the determinant of metric tensor g and g^{ij} are the components of inverse metric tensor g^{-1} . In the euclidian case we get the usual Laplacian, but in the hyperbolic case (upper-half plane model \mathcal{H})

$$g_{ij} = \frac{\delta_{ij}}{y^2}$$

In this case, $g^{ij} = y^2 \delta^{ij}$ and $\sqrt{|g|} = y^{-2}$. Then with easy computations,

$$\Delta f = y^2(\partial_{xx}f + \partial_{yy}f).$$

The Laplacian can be seen as a differential operator on any hyperbolic surface $M = \Gamma \backslash \mathcal{H}$. However, for simplicity, we will assume M compact and we fix a fundamental domain D for M . In this sense, any $f: D \rightarrow \mathbb{C}$ can be seen as a Γ -invariant function on \mathcal{H} and its integral over D is given by $\int_D f d\mu$.

Lemma 5.2.1. *If $A \in \mathrm{PSL}_2 \mathbb{R}$ and $T_A(f) = f(A^{-1}z)$ for $f \in C^\infty(\mathcal{H})$, then*

$$\Delta T_A = T_A \Delta.$$

Proof. It's sufficient to check the property in case $A = \begin{bmatrix} 0 & -1 \\ 1 & 0 \end{bmatrix}$ or $A = \begin{bmatrix} 1 & x \\ 0 & 1 \end{bmatrix}$, for some $x \in \mathbb{R}$, as these two matrices generates all $\mathrm{PSL}_2 \mathbb{R}$. ■

Remark 5.2.1. Very often, it's considered as the Laplacian the operator $-\Delta$, because in this way the eigenvalues are positive, see the following result.

Theorem 5.2.2. *There exists a sequence $\{\varphi_j\}_{j \in \mathbb{N}}$ of $L^2(M)$ of Laplacian-eigenfunctions*

$$\Delta \varphi_j = \lambda_j \varphi_j$$

with corresponding (positive) eigenvalues λ_j such that $\{\lambda_j\}_j$ is a increasing and diverging sequence of positive real numbers and $\{\varphi_j\}_{j \in \mathbb{N}}$ form a orthonormal basis of $L^2(M)$.

Proof. See [Le 17]. ■

The proof of this theorem is based on the use of spectral decomposition theorem for compact operators. However, as the Laplacian is not compact, it is necessary to use some approximating compact operators (*heat kernel*), showing that the share the same spectrum of the Laplacian. Here are some general properties for the Laplacian.

Proposition 5.2.3. *The followings hold.*

- Δ is a symmetric operator, i.e. $\langle \Delta f, g \rangle = \langle f, \Delta g \rangle$ for any $f, g \in C^\infty(M)$.
- If $f \in C^\infty(M)$ is not constant, then $\langle \Delta f, f \rangle$ is positive.

5.2.1 A brief journey across harmonic analysis on the hyperbolic plane

To prove, in the subsequent sections, the Seldberg trace formula, we will now some notions taken from the field of harmonical analysis (see [Eva10],[Hör83a])

DA FINIRE IL DISCORSO

The starting point is the definition of the *invariant kernel*.

Definition 5.2.4 An invariant kernel is a function $\kappa: \mathcal{H} \times \mathcal{H} \rightarrow \mathbb{C}$ with the following characteristics:

1. $\kappa(\gamma z, \gamma w) = \kappa(z, w)$ for all $\gamma \in \text{Isom}(\mathcal{H}) = \text{PSL}_2 \mathbb{R}$ and for all $(z, w) \in \mathcal{H} \times \mathcal{H}$;
2. $\kappa(\cdot, \cdot)$ is symmetric in its arguments.

Such a kernel carries with it an *invariant integral operator* I defined by

$$If(z) = \int_{\mathcal{H}} \kappa(z, w) f(w) d\mu(w).$$

with f that must satisfy appropriate conditions. This induces an operator on the quotient surface $M = \Gamma \backslash \mathcal{H}$, in particular for f Γ -invariant:

$$If(z) = \sum_{\gamma \in \Gamma} \int_D \kappa(z, \gamma w) f(w) d\mu(w).$$

with D fundamental domain for Γ .

We will consider invariant kernels of the form

$$\kappa(d(z, w))$$

where $\kappa: \mathbb{R} \rightarrow \mathbb{C}$ is an even function. With abuse of notation, we will use $\kappa(z, w)$ for complex z, w or $\kappa(l)$ for real l indifferently, instead of $\kappa(d(z, w))$.

Proposition 5.2.5. *If f is an eigenfunction of the Laplacian of eigenvalue λ , then it is also an eigenfunction of the invariant integral operator I_κ relative to κ . Hence, there exists a function $h: \mathbb{R} \rightarrow \mathbb{C}$ such that*

$$I_\kappa f(z) = \int \kappa(d(z, w)) f(w) d\mu(w) = h(\lambda) f(z).$$

Proof. Let f be an eigenfunction of the Laplacian of eigenvalue λ . We define the corresponding radial function

$$F_z(w) = \int_{S_z} f(Mw) dM$$

where $S_z = \text{Stab}_z$ and dM is the normalised Haar measure on S_z . It is a radial eigenfunction and, by the subsequent lemma 5.2.6 we know that

$$F_z(w) = \varphi_\lambda(z, w) f(z).$$

So we have

$$\begin{aligned} \int_{\mathcal{H}} \kappa(z, w) f(w) d\mu(w) &= \int_{S_z} \int_{\mathcal{H}} \kappa(z, M^{-1}w) f(w) d\mu(w) dM \\ &= \int_{S_z} \int_{\mathcal{H}} \kappa(z, w) f(Mw) d\mu(w) dM \\ &= \int_{\mathcal{H}} \kappa(z, w) F_z(w) d\mu(w). \end{aligned}$$

Hence

$$\int_{\mathcal{H}} \kappa(z, w) f(w) d\mu(w) = h(\lambda) f(z),$$

where the “eigenvalue” $h(\lambda)$ is given by

$$h(\lambda) = \int_{\mathcal{H}} \kappa(z, w) \varphi_\lambda(z, w) d\mu(w).$$

What remains to be proved is that $h(\lambda)$ is independent of z and for any $g \in \mathrm{PSL}_2 \mathbb{R}$:

$$\begin{aligned} \int_{\mathcal{H}} (gz, w) \varphi_{\lambda}(gz, w) d\mu(w) &= \int_{\mathcal{H}} \kappa(z, g^{-1}w) \varphi_{\lambda}(z, g^{-1}w) d\mu(w) = \\ &= \int_{\mathcal{H}} \kappa(z, w) \varphi_{\lambda}(z, w) d\mu(w). \end{aligned}$$

This concludes the proof. ■

Lemma 5.2.6. *For any $\lambda \in \mathbb{C}$ and z in the upper-half plane, there exists a unique function $w \mapsto \varphi_{\lambda}(z, w)$, with radial symmetry centered in z , such that*

1. $\varphi_{\lambda}(z, z) = 1$;
2. $\Delta_g \varphi_{\lambda}(z, w) = \lambda \varphi_{\lambda}(z, w)$.

Proof. Omitted ([Le 17]). ■

We define the Seldberg transform $\mathcal{S}(k)$ of a radiant kernel κ as

$$\mathcal{S}(\kappa)(\lambda) = h(\lambda) = \int_{\mathcal{H}} \kappa(d(i, w)) \varphi_{\lambda}(i, w) d\mu(w). \quad (5.2)$$

We will use the re-parametrisation $\lambda = s(1 - s) = 1/4 + r^2$, with $r \in \mathbb{C}$ we will write indifferently, with abuse of notation, $\mathcal{S}(\kappa)(r)$ and $\mathcal{S}(\kappa)(\lambda)$.

Proposition 5.2.7. *The Seldberg transform $\mathcal{S}(\kappa)$ of a radiant kernel κ can be computed with the Fourier transform of the function*

$$g(u) = \frac{1}{\sqrt{2}} \int_{|u|}^{\infty} \frac{\kappa(\rho) \sinh \rho}{\sqrt{\cosh \rho - \cosh u}} d\rho$$

so that

$$\mathcal{S}(\kappa)(r) = \mathcal{F}(g)(x).$$

Proof. Let $f: \mathbb{C} \rightarrow \mathbb{C}$ defined by $f(z) = y^{1/2+ir}$, for $z = x + iy$ and fixed r . We have that

$$-\Delta_g f(z) = y^2 \cdot \left((1/4 + r^2) y^{1/2-2+ir} \right) = f(z)$$

so it is an eigenfunction of the Laplacian with eigenvalue

$$\lambda = \frac{1}{4} + r^2 = s(1 - s)$$

for a certain $s \in \mathbb{C}$. With abuse of notation, we will write $h(r) = h(\lambda)$, instead of $h(\lambda(r))$. By proposition 5.2.5, we have that

$$h(r) = \int \kappa(d(i, z)) \Im(z)^{1/2+ir}.$$

Let $U(\cosh \rho) = \kappa(\rho)$ so that, using formula for hyperbolic distance

$$U \left(1 + \frac{|z - w|^2}{2\Im(z)\Im(w)} \right) = \kappa(d(z, w)).$$

Hence we have

$$h(r) = \int_{-\infty}^{\infty} \int_0^{\infty} U\left(\frac{1+x^2+y^2}{2y}\right) y^{1/2+ir} \frac{dy}{y^2} dx.$$

Letting $\cosh \rho = (1+x^2+y^2)/2y$ (substitution with respect to variable x) and $y = e^u$, we have

$$x = \pm \sqrt{2e^u \cosh \rho - 1 - e^{2u}}, \quad \sinh \rho d\rho = \frac{x}{y} dx, \quad e^u du = dy$$

and then*

$$h(r) = \int_{-\infty}^{\infty} \int_{|u|}^{\infty} \frac{U(\cosh \rho)}{e^{2u}} \cdot (e^u)^{1/2+ir} \cdot \frac{y \sinh \rho}{x} e^u d\rho du = \frac{1}{\sqrt{2}} \int_{-\infty}^{\infty} \int_{|u|}^{\infty} \frac{\kappa(\rho) \sinh \rho}{\sqrt{\cosh \rho - \cosh u}} e^{ir} d\rho du.$$

The result is proved. ■

It can be also shown that it is possible to revert the Seldberg transform also using Fourier inversion formula, with a different “weight function”.

Proposition 5.2.8. *For a function $h: \mathbb{R} \rightarrow \mathbb{C}$, the Seldberg transform is inverted using the inverse Fourier transform*

$$g(u) = \frac{1}{2\pi} \int_{-\infty}^{\infty} e^{-iru} h(r) dr$$

with

$$\kappa(\rho) = -\frac{1}{\sqrt{2\pi}} \int_{\rho}^{\infty} \frac{g'(u)}{\sqrt{\cosh u - \cosh \rho}} du.$$

Proof. Omitted. ■

5.3 Periodic geodesics

The trace formula is a bridge between spectral property of a system, namely the spectrum of the Laplacian, and its geometrical characteristics, i.e. the set of lengths of closed geodesics.

Let $M = \Gamma \setminus \mathcal{H}$ be a compact hyperbolic surface, so that Γ does not contain any parabolic element. We further assume that M can be considered as a regular Riemann surface, hence Γ has not elliptic elements either.

The spectrum of the Laplacian is denoted by

$$\lambda_j = \frac{1}{4} + \rho_j^2$$

and, as $\lambda_j \in \mathbb{R}$, we have that $|\Im(\rho_j)| \leq 1/2$.

Definition 5.3.1 A periodic or closed geodesic in M is a geodesic $\gamma: \mathbb{R} \rightarrow M$ such that $\exists T > 0$

$$(\gamma(t+T), \gamma'(t+T)) = (\gamma(t), \gamma'(t)), \quad \forall t \in \mathbb{R}.$$

The set of closed geodesic in M will be denoted by $\mathcal{G}(M)$. The smallest $T > 0$ for which this is true, is denoted by $\ell(\gamma)$ and it's called the period or length of the geodesic γ .

*The minimum value of $\cosh \rho$ is $\frac{1+e^{2u}}{2e^u} = \cosh u$ and so $\rho \geq |u|$.

As we said in section METTI SEZIONE, for every hyperbolic element $A \in \Gamma$, there is one and only geodesic invariant with respect to the action of A , namely the *axis* of A , see (2.2). It's possible to prove the following result.

Lemma 5.3.2. *If $M = \Gamma \setminus \mathcal{H}$ is an hyperbolic compact surface, then for every hyperbolic element $g \in \Gamma$ the projection of the axis γ of g in M is a closed geodesic of length ℓ_g .*

Proof. CITA KONSTANTINE ■

It's interesting to see how the length ℓ_g is linked to the matrix g . If

$$g = \begin{bmatrix} a & b \\ c & d \end{bmatrix}$$

then this matrix it's similar to

$$A_\ell = \begin{bmatrix} \exp(\ell/2) & \\ & \exp(-\ell/2) \end{bmatrix}$$

for a certain $\ell > 0$. We have that $d(z, Az) = \ell$ and hence this is still true for g , so ℓ it's exactly the length of the axis of g . In particular we have that

$$2 \cosh \ell = |\operatorname{tr} g|.$$

This relation can be restated with eigenvalues of g : if $1 < \lambda$ and λ^{-1} are g 's eigenvalues, than this equation rewrites as

$$\ell_g = \log \lambda^2.$$

Definition 5.3.3 An element $\gamma \in \Gamma$ is called primitive iff it cannot be expressed in the form δ^k , with $k \geq 2$ and δ is another element of Γ .

Proposition 5.3.4. The set $\mathcal{G}(M)$ can be identified with the set of conjugacy classes in Γ of primitive hyperbolic elements.

Proof. Let $\rho \in \mathcal{G}(M)$ and let C_ρ be the class of geodesics of \mathcal{H} that project on ρ . Let γ be a representative of this class. The stabilizer $\operatorname{Stab}_\gamma$ of γ in $\operatorname{PSL}_2 \mathbb{R}$ is the set of hyperbolic transformations fixing γ . It is conjugate to the diagonal subgroup (see METTI REFERENZA)

$$\left\{ \begin{bmatrix} \exp(t/2) & \\ & \exp(-t/2) \end{bmatrix}, t \in \mathbb{R} \right\}.$$

In particular $\operatorname{Stab}_\gamma \simeq \mathbb{R}$. Hence, the subgroup $\operatorname{Stab}_\gamma \cap \Gamma$ is homomorphic to a discrete subgroup of \mathbb{R} , being Γ a discrete subgroup, and so it's cyclic. Let $\delta \in \Gamma$ such that

$$\operatorname{Stab}_\gamma \cap \Gamma = \langle \delta \rangle.$$

Obviously, δ must be primitive. Any other representative $\hat{\gamma}$ of C_ρ is obtained as $\hat{\gamma} = g\gamma$, with $g \in \Gamma$, and so

$$\operatorname{Stab}_{\hat{\gamma}} \cap \Gamma = \langle g\delta g^{-1} \rangle.$$

Let C_δ be the conjugacy class of δ in Γ . Then, we have built a map $\rho \mapsto (C_\gamma \mapsto C_\delta)$ associating a conjugacy class in Γ of primitive hyperbolic elements to a periodic geodesic, which is one-to-one. ■

At this point, we can establish the approximate growth for the number of closed geodesic (not necessary primitive) with length at most L .

Proposition 5.3.5. *Let $X = \Gamma \setminus \mathcal{H}$ be an hyperbolic compact surface. Then the number of closed geodesics $c_X(L)$ on X with length at most L is $O(e^L)$.*

Proof. Let $x \in X$ be a point on the surface and let w be the correspondent point on \mathcal{H} , so that $\pi(w) = x$. Let D_w be the Dirichlet domain of center w for Γ . If γ is a closed geodesic on X of length at most L , then let γ' be its lifting on \mathcal{H} , passing through a point $q \in D_w$. This curve γ' is a geodesic on \mathcal{H} and it is fixed (as geodesic) by an hyperbolic element $G \in \Gamma$. Let d be the diameter of the domain D_w , which is finite as X is compact. Then we get

$$d(w, Gw) \leq d(w, q) + d(q, Gq) + d(Gq, Gw) \leq L + 2d.$$

Hence, for each geodesic of length at most L , there exist an element $G \in \Gamma$ such that w is sent inside a (hyperbolic) ball of center w and ray $L + 2d$. Hence, $c_X(L)$ is bounded by the number of images of the domain D_w which are distant at most $L + 2d + d$ from w . For L “big enough”, thus the following estimate hold

$$c_X(L) \simeq \frac{\mu_{\mathcal{H}}(B(w, L + 3d))}{\mu_{\mathcal{H}}(D_w)}.$$

Using the Poincaré disk model, a hyperbolic ball of hyperbolic radius of $R = L + 3d$, centered in 0, can be seen as an Euclidian disk with radius $\tanh(R/2)$. Thus, the area is given by

$$\begin{aligned} \mu_{\mathcal{H}}(B(w, R)) &= \mu_{\mathcal{D}}(B(0, R)) = \iint_{B(0, R)} \frac{4}{(1 - |z|^2)} dx dy \stackrel{z=re^{i\theta}}{=} \int_0^{2\pi} \int_0^{\tanh(R/2)} \frac{4r}{(1 - r^2)^2} dr d\theta \\ &= 4\pi \left[\frac{1}{1 - r^2} \right]_0^{\tanh(R/2)} = 4\pi \cosh^2(R/2) \end{aligned}$$

and this gives what desired. ■

5.4 Pretrace formula

The general form of Seldberg is the following: for any “admissible function”[†] h ,

$$\sum_{j=0}^{\infty} h(r_j) = \frac{\text{Area}(M)}{4\pi} \int_{-\infty}^{+\infty} h(r)r \tanh(\pi r) dr + \sum_{\gamma \in \Gamma}$$

where, as in the previous section, $\mathcal{G}(M)$ the set of periodic geodesics of M .

Let $\{\varphi_j\}_{j \in \mathbb{N}}$ be a orthonormal basis of (real) eigenfunctions of Δ on $L^2(M)$, as in theorem 5.2.2.

Proposition 5.4.1. *Let h be the Seldberg transform of radial kernel κ , we have*

$$\sum_{j=0}^{\infty} h(r_j) \varphi_j(z) \varphi_j(w) = \sum_{\gamma \in \Gamma} \kappa(z, \gamma w),$$

[†]In the following will be more precise.

where the convergence is absolute and uniform. When $z = w$, we get

$$\sum_{j=0}^{\infty} h(r_j) |\varphi_j(z)|^2 = \frac{1}{4\pi} \int_{-\infty}^{\infty} h(x) \tanh(\pi x) x \, dx + \sum_{\gamma \in \Gamma \setminus \{e\}} \kappa(z, \gamma z). \quad (5.3)$$

Proof. The eigenfunctions φ_j are Γ -invariant functions on \mathcal{H} , hence by definition of Seldberg transform we have

$$\int_{\mathcal{H}} \kappa(z, w) \varphi_j(w) \, d\mu(w) = h(r_j) \varphi_j(z).$$

At the same time

$$\int_{\mathcal{H}} \kappa(z, w) \varphi_j(w) \, d\mu(w) = \int_D \sum_{\gamma \in \Gamma} k(z, \gamma w) \varphi_j(w) \, d\mu(w).$$

The sequence $\{\varphi_j\}_{j \geq 0}$ form a basis, so

$$\sum_{\gamma \in \Gamma} k(z, \gamma w) = \sum_{j \in \mathbb{N}} \left(\int_D \sum_{\gamma \in \Gamma} k(z, \gamma z') \varphi_j(z') \, d\mu(z') \right) \varphi_j(w) = \sum_{j \in \mathbb{N}} h(r_j) \varphi_j(z) \varphi_j(w),$$

where the series converge in L^2 . In [Hej80], Hejhal proved that the series converge absolutely and uniformly in z, w .

To get (5.3), we first prove that

$$\kappa(z, z) = \frac{1}{4} \int_{-\infty}^{\infty} h(x) \tanh(\pi x) x \, dx.$$

We start by writing the inverse Seldberg transform[‡]

$$\kappa(z, z) = \kappa(d(z, z)) = \kappa(0) = -\frac{1}{\pi\sqrt{2}} \int_0^\infty \frac{g'(u)}{\sqrt{\cosh u - 1}} \, du = -\frac{1}{2} \int_0^\infty \frac{g'(u)}{\sinh(u/2)} \, du$$

where $g(u)$ is the inverse Fourier transform

$$g(u) = \frac{1}{2\pi} \int_{-\infty}^{\infty} h(r) e^{-iu\rho} \, d\rho.$$

Substituting and using Fubini theorem (thanks to rapid decay condition of h), we get

$$\begin{aligned} \kappa(z, z) &= \frac{1}{4\pi^2} \int_0^\infty \int_{-\infty}^{\infty} h(\rho) \frac{\sin(u\rho)}{\sinh(u/2)} \rho \, d\rho \, du \\ &= \frac{1}{4\pi^2} \int_{-\infty}^{\infty} h(\rho) \left(\int_0^\infty \frac{\sin(u\rho)}{\sinh(u/2)} \, du \right) \rho \, d\rho. \end{aligned}$$

We now rewrite the term $1/\sinh(u/2)$ as a series

$$\frac{1}{\sinh(u/2)} = \frac{2}{e^{u/2}(1 - e^{-u})} = 2e^{-u/2} \sum_{n=0}^{\infty} e^{-nu}$$

[‡]See 5.2.8

and using its absolute convergence, we can interchange integration and summation

$$\begin{aligned} \int_0^\infty \frac{\sin(u\rho)}{\sinh(u/2)} du &= 2 \sum_{n \geq 0} \int_0^\infty e^{-(2n+1)u/2} \sin(u\rho) du \\ &= 2 \sum_{n \geq 0} \frac{4\rho}{4\rho^2 + (2n+1)^2} = \sum_{n \in \mathbb{Z}} \frac{4\rho}{4\rho^2 + (2n+1)^2}. \end{aligned}$$

Moreover, we have the Fourier correspondence

$$\int_{-\infty}^\infty e^{-2\pi ix\zeta} \frac{2\rho}{\rho^2 + \zeta^2} d\zeta = 2\pi e^{-2\pi\rho|x|}$$

and we can use Poisson summation formula (5.1)

$$\sum_{n \in \mathbb{Z}} f(n) = \sum_{n \in \mathbb{Z}} \int_{-\infty}^\infty e^{-2\pi in\xi} f(\xi) d\xi$$

finally getting

$$\sum_{n \in \mathbb{Z}} \frac{\rho}{\rho^2 + (n+1/2)^2} = \pi \sum_{n \in \mathbb{Z}} e^{i\pi n} e^{-2\pi\rho|n|} = \pi \frac{1 - e^{-2\pi\rho}}{1 + e^{-2\pi\rho}} = \pi \tanh(\pi\rho).$$

To sum up, we have obtained that

$$\int_0^\infty \frac{\sin(u\rho)}{\sinh(u/2)} du = \pi \tanh(\pi\rho)$$

and so the proof is complete. ■

Remark 5.4.1. Even if Poisson summation formula could have appear to be a “fictitious” tool to introduce Seldberg trace formula in section 5.1, in this proof one can see that these two subjects actually are linked together.

To prove the complete version of Seldberg trace formula, it is necessary to integrate equation (5.3) over a fundamental domain D (for example, a Dirichlet domain). We have

$$\sum_{j=0}^\infty h(r_j) |\varphi_j(z)|^2 = \frac{\text{Area}(M)}{4\pi} \int_{-\infty}^\infty h(x) \tanh(\pi x) x dx + \sum_{\gamma \in \Gamma \setminus \{e\}} \int_D \kappa(z, \gamma z) d\mu(z).$$

We would like to rewrite the last term as a sum over closed geodesics. To this, we will group the terms by conjugacy classes $[\gamma]$, with $\gamma \in \Gamma$. If $\gamma_0 \in [\gamma]$, then there exist a $g \in \Gamma$ such that $\gamma_0 = g^{-1}\gamma g$. So

$$\begin{aligned} \int_D \kappa(z, \gamma_0 z) d\mu(z) &= \int_D \kappa(z, g^{-1}\gamma g z) d\mu(z) = \int_D \kappa(gz, \gamma gz) d\mu(z) \\ &= \int_{gD} \kappa(z, \gamma z) d\mu(z). \end{aligned}$$

Hence we have

$$\sum_{\gamma \in \Gamma \setminus \{e\}} \int_D \kappa(z, \gamma z) d\mu(z) = \sum_{[\gamma] \neq [e]} \int_{D_\gamma} \kappa(z, \gamma z) d\mu(z),$$

where

$$D_\gamma = \bigcup_{g \in C_{\gamma, \Gamma} \setminus \Gamma} gD$$

with $C_{\gamma, \Gamma}$ being the centralizer of γ in Γ , i.e. the set

$$C_{\gamma, \Gamma} = \{g \in \Gamma : g\gamma = \gamma g\} \quad (5.4)$$

We are now ready to prove the following result.

Lemma 5.4.2. *Given $\gamma \in \Gamma$, it does exist a unique primitive element $\delta \in \Gamma$ such that $\gamma^n = \gamma$ for some $k \geq 1$, and moreover the centralizer is $C_{\gamma, \Gamma} = \langle \delta \rangle$.*

Proof. The last part of the result is an immediate consequence of the first part, so we will only prove this one.

In the proof of proposition 5.3.4 we have seen that the subgroup of Γ fixing the axis a_γ is cyclic and generated by a primitive element δ , so $\gamma = \delta^n$. Any other primitive element δ' such that $\gamma = \delta'^k$, has the same axis of γ . Hence it is in the subgroup $\langle \delta \rangle$, but δ and δ' are both primitive, so $\delta = \delta'$. ■

Using lemma 5.4.2, it is possible to decompose the summation over conjugacy classes of primitive elements, which correspond to elements of $\mathcal{G}(M)$ in view of proposition 5.3.4. In the end

$$\sum_{[\gamma] \neq e} \int_{D_\gamma} \kappa(z, \gamma z) d\mu(z) = \sum_{\gamma \in \mathcal{G}(M)} \sum_{n=1}^{\infty} \int_{D_\gamma} \kappa(z, \gamma^n z) d\mu(z).$$

It should be noticed that the set D_γ is nothing than the fundamental domain for the hyperbolic cylinder $C_{\gamma, \Gamma} \setminus \mathcal{H}$.

5.4.1 Hyperbolic terms

We now fix a primitive element $\gamma \in \Gamma$. Up to a conjugation by an isometry, which does not change the value of the integral we are considering, we can suppose WLOG that

$$\gamma = A_\ell,$$

where $\ell = \ell_\gamma$ is the length of the isometry. A fundamental domain for the quotient $C_{\gamma, \Gamma} \setminus \Gamma$ is given by the strip

$$\{z \in \mathcal{H} : 1 \leq \Im(z) < e^\ell\}$$

We now use the function $U(\cosh \rho) := \kappa(\rho)$, where $\rho = d(\cdot, \cdot)$. For $z' = e^{n\ell} z$, by using lemma 2.2.4, we have

$$\cosh d(z, \gamma^n z') = 1 + \frac{|z - z'|^2}{2\Im(z)\Im(z')} = 1 + 2 \frac{|z|^2 \sinh^2(n\ell/2)}{y^2}$$

so that ($z = x + iy$)

$$\begin{aligned} \int_{D_\gamma} \kappa(z, \gamma^n z) d\mu(z) &= \int_1^{e^\ell} \int_{-\infty}^{\infty} U(1 + 2 \sinh^2(n\ell/2)) \left(1 + \frac{x^2}{y^2}\right) \frac{dx dy}{y^2} \\ &\stackrel{q=x/y}{=} \int_1^{e^\ell} \frac{1}{y} dy \int_{-\infty}^{\infty} U(1 + 2 \sinh^2(n\ell/2)(1 + q^2)) dq \\ &\stackrel{*_1}{=} \frac{\ell}{\sinh(n\ell/2)} \int_{\sinh(n\ell/2)}^{+\infty} \frac{U(1 + 2u)}{\sqrt{u - \sinh^2(n\ell/2)}} du \\ &\stackrel{*_2}{=} \frac{\ell}{\sinh(n\ell/2)\sqrt{2}} \int_{n\ell}^{+\infty} \frac{\kappa(\rho) \sinh \rho}{\sqrt{\cosh \rho - \cosh(n\ell)}} d\rho \end{aligned}$$

where $*_1$ is true for the substitution $u = \sinh^2(n\ell/2)(1 + q^2)$ and $*_2$ for the hyperbolic duplication formula $1 + 2 \sinh^2(t/2) = \cosh(t)$ for $t = n\ell$. We thus have proved, in view of subsection 5.2.1,

$$\int_{D_\gamma} k(z, \gamma^n z) d\mu(z) = \frac{\ell g(n\ell)}{2 \sinh(n\ell/2)},$$

where g is the “kernel” of Seldberg transform 5.2.7. Putting all together, we thus have proved

$$\sum_{j \in \mathbb{N}} h(r_j) = \frac{\text{Area}(M)}{4\pi} \int_{-\infty}^{\infty} h(\rho) \tanh(\pi\rho) \rho d\rho + \sum_{\gamma \in \mathcal{G}(M)} \sum_{n=1}^{\infty} \frac{\ell g(n\ell)}{2 \sinh(n\ell/2)},$$

which is the desired form of Seldeberg trace formula.

5.5 An application: Weyl's law

For our interest, we will see one main consequence of the Seldberg trace formula is the Weyl's law, in the hyperbolic context, already mentioned in chapter 4 for the Euclidian case.

Theorem 5.5.1 (Weyl law, hyperbolic case). Let $N(\lambda) = \#\{j \in \mathbb{N}: \lambda_j \leq \lambda\}$ be the number of eigenvalues smaller than λ . We have the asymptotic law

$$N(\lambda) \sim \frac{\text{Area}(M)}{4\pi} \lambda$$

when $\lambda \rightarrow +\infty$.

In order to prove this result, we need the following lemmas, which are just two result of the greater framework of Tauberian theorems ([Kor04]).

Lemma 5.5.2 (Karamata). Let $\{a_n\}_{n \geq 0}$ be a divergent sequence of positive real numbers such that

$$\lim_{r \rightarrow 0} \sum_{n=0}^{\infty} e^{-ra_n} = \frac{c}{r}.$$

Then it holds

$$\lim_{n \rightarrow \infty} \frac{\#\{n: a_n \leq N\}}{N} = c.$$

Proof. Omitted. See CITA ■

Lemma 5.5.3 (tauberian lemma). Let $\{a_n\}_{n \geq 0}$ be a divergent non-decreasing sequence of positive real numbers, such that the number

$$\#\{n: a_n \leq N\}$$

has an exponential growth, i.e. $O(e^L)$. Then the serie

$$\sum_{n=0}^{\infty} \frac{a_n}{e^{(1+\varepsilon)a_n} - e^{\varepsilon a_n}}$$

converges $\forall \varepsilon > 0$.

Proof. Omitted. See ■

The proof of theorem 5.5.1 is then.

Proof. We apply Seldberg formula

$$\sum_{j \in \mathbb{N}} h(r_j) = \frac{\text{Area}(M)}{4\pi} \int_{-\infty}^{\infty} h(\rho) \tanh(\pi\rho) \rho d\rho + \sum_{\gamma \in \mathcal{G}(M)} \sum_{n=1}^{\infty} \frac{\ell g(n\ell)}{2 \sinh(n\ell/2)},$$

to the function of rapid decay $h(r) = e^{-\varepsilon r^2}$. We have that

$$g(u) = \frac{1}{\sqrt{4\pi\varepsilon}} e^{-u^2/(2\varepsilon)}.$$

We get that

$$\sum_{n=0}^{\infty} e^{-\varepsilon r_n^2} = \frac{\text{Area}(M)}{4\pi} \int_{-\infty}^{\infty} r e^{-\varepsilon r^2} \tanh(\pi r) dr + \frac{1}{\sqrt{4\pi\varepsilon}} \sum_{\gamma \in \mathcal{G}(M)} \sum_{n=1}^{\infty} \frac{\ell_{\gamma}}{e^{n\ell_{\gamma}/2} - e^{-\ell_{n\gamma}}} e^{-\frac{(n\ell_{\gamma})^2}{4\varepsilon}}$$

The last term on the right side could appear different from the one of before, but it is just the expansion of function $\sinh(x)$. It can be, moreover, re-written as

$$\sum_{\gamma \in \mathcal{CG}(M)} \frac{\ell_{\delta}}{e^{\ell_{\gamma}/2} - e^{-\ell_{\gamma}/2}} e^{-\frac{\ell_{\gamma}^2}{4\varepsilon}}$$

if $\mathcal{CG}(M)$ is the set of closed geodesic (not necessarily primitive) and δ is the primitive element such that $\gamma = \delta^n$. We will now show that the second term will decay to zero, for $\varepsilon \rightarrow 0$. Let ℓ_0 be the shortest geodesic on X ($\ell_0 > 0$ because M is compact). We can observe that, if we choose $\varepsilon < \ell_0/8$, then

$$\frac{\ell_{\gamma}^2}{4\varepsilon} = \frac{\ell_{\gamma}^2}{8\varepsilon} + \frac{\ell_{\gamma}^2}{8\varepsilon} \geq \frac{\ell_{\gamma}^2}{8\varepsilon} + \frac{\ell_0}{8\varepsilon} \ell_{\gamma} \geq \frac{\ell_0}{8\varepsilon} + \ell_{\gamma}.$$

Hence we have that

$$\frac{1}{\sqrt{4\pi\varepsilon}} \sum_{\gamma \in \mathcal{CG}(M)} \frac{\ell_{\delta}}{e^{\ell_{\gamma}/2} - e^{-\ell_{\gamma}/2}} e^{-\frac{\ell_{\gamma}^2}{4\varepsilon}} \leq \frac{1}{\sqrt{4\pi\varepsilon}} e^{-\frac{\ell_0}{4\varepsilon}} \sum_{\gamma \in \mathcal{CG}(M)} \frac{\ell_{\delta}}{e^{\ell_{\gamma}/2} - e^{-\ell_{\gamma}/2}} e^{-\ell_{\gamma}}.$$

If ε approaches zero, the quantity

$$\frac{1}{\sqrt{4\pi\varepsilon}} e^{-\frac{\ell_0}{4\varepsilon}}$$

goes to zero, hence it is enough proving that the series converges. We have

$$\sum_{\gamma \in \mathcal{CG}(M)} \frac{\ell_\delta}{e^{\ell_\gamma/2} - e^{-\ell_\gamma^2/2}} e^{-\ell_\gamma} \leq \sum_{\gamma \in \mathcal{CG}(M)} \frac{\ell_\gamma}{e^{\ell_\gamma/2} - e^{-\ell_\gamma^2/2}} e^{-\ell_\gamma}$$

as $\gamma = \delta^n$. In 5.3.5 we have proved that the number of closed geodesics in X of length at most L is approximately $O(e^L)$. Then we are done with lemma 5.5.3, with $\varepsilon = 1/2$.

Now we focus on the first term. Integrating by parts, we get

$$\int_{-\infty}^{\infty} r e^{-\varepsilon r^2} \tanh(\pi r) dr = \frac{1}{\varepsilon} \int_{-\infty}^{\infty} e^{-\varepsilon r^2} \frac{\pi}{2 \cosh(\pi r)^2} dr.$$

Using the series expansion of exponential function and exchanging integral and sum symbols due to monotone convergence theorem, we get

$$\begin{aligned} \int_{-\infty}^{\infty} \sum_{n=0}^{\infty} \frac{(-\varepsilon r^2)^n}{n!} \frac{\pi}{2 \cosh(\pi r)^2} dr &= \sum_{n=0}^{\infty} \int_{-\infty}^{\infty} \frac{(-\varepsilon r^2)^n}{n!} \frac{\pi}{2 \cosh(\pi r)^2} dr \\ &= \int_{-\infty}^{\infty} \frac{\pi}{2 \cosh(\pi r)^2} dr + \sum_{n=1}^{\infty} \int_{-\infty}^{\infty} \frac{(-\varepsilon r^2)^n}{n!} \frac{\pi}{2 \cosh(\pi r)^2} dr \\ &= \underbrace{\frac{\tanh(\pi r)}{2} \Big|_{-\infty}^{\infty}}_{=1} - \varepsilon \int_{-\infty}^{\infty} \sum_{n=1}^{\infty} \frac{(-\varepsilon)^{n-1} r^{2n}}{n!} \frac{\pi}{2 \cosh(\pi r)^2} dr. \end{aligned}$$

For the second term of this last equality

$$\begin{aligned} 0 &\leq \int_{-\infty}^{\infty} \sum_{n=1}^{\infty} \frac{(-\varepsilon)^{n-1} r^{2n}}{n!} \frac{\pi}{2 \cosh(\pi r)^2} dr \leq \int_{-\infty}^{\infty} r^2 \frac{\pi}{2 \cosh(\pi r)^2} \sum_{n=1}^{\infty} \frac{(-\varepsilon)^{n-1} r^{2(n-1)}}{n!} dr \\ &= \int_{-\infty}^{\infty} r^2 \frac{\pi}{2 \cosh(\pi r)^2} e^{-\varepsilon r^2} dr = \int_{-\infty}^{\infty} \underbrace{r^2 e^{-\varepsilon r^2}}_{\leq 1} \frac{\pi}{2 \cosh(\pi r)^2} dr \leq 1 \end{aligned}$$

and so

$$\int_{-\infty}^{\infty} e^{-\varepsilon r^2} r^2 \frac{\pi}{2 \cosh(\pi r)^2} dr = 1 + O(\varepsilon)$$

from which

$$\int_{-\infty}^{\infty} r e^{-\varepsilon r^2} \tanh(\pi r) dr = \frac{1}{\varepsilon} (1 + O(\varepsilon)).$$

We can conclude that

$$\sum_{n=0}^{\infty} e^{-\varepsilon r_n^2} = \frac{\mathrm{Area}(X)}{4\pi\varepsilon} (1 + O(1))$$

and now we are done again with lemma 5.5.2. ■

5.6 The case of $\mathrm{PSL}_2 \mathbb{Z}$

As mentioned before, the trace formula just proved holds only for compact groups, in particular it does not apply to $\mathrm{PSL}_2 \mathbb{Z}$. In fact, the difference is that this group has indeed elliptic elements (it does have cusps). As proved in [Sar11] and [Gut90],

the trace formula for $X(1)$ has a more complex form than the one presented. For $X(1)$, if $g \in C_c^\infty(\mathbb{R})$ is an even smooth function of compact support and $h(\xi) = \hat{g}(\xi/2\pi)$ is the anti-Fourier transform of h (h is an entire function), the trace formula reads as follows ($\lambda_j = 1/4 + t_j^2$):

$$\begin{aligned} & \sum_{j \in \mathbb{N}} h(t_j) - \frac{1}{2\pi} \int_{-\infty}^{\infty} h(t) \left(\frac{\varphi'}{\varphi} \right) \left(\frac{1}{2} + it \right) dt = \\ &= \frac{\text{Area}(X(1))}{2\pi} \int_{-\infty}^{\infty} h(r) \tanh(\pi r) r dr - \frac{1}{\pi} \int_{-\infty}^{\infty} h(r) \left(\frac{\Gamma'}{\Gamma} \right) (1 + it) dr - 2 \ln(2g(0)) + h(0) \\ &+ \sum_{[\delta]} \sum_{1 \leq \nu \leq m-1} \frac{2}{m \sin(\pi\nu/m)} \int_{-\infty}^{\infty} \frac{h(r) e^{-\frac{\pi\nu}{m}r}}{1 + e^{-2\pi r}} dr + \sum_{\gamma \in \mathcal{G}(X(1))} + \sum_{n=1}^{\infty} \frac{\ell g(n\ell)}{2 \sinh(n\ell/2)} \end{aligned} \quad (5.5)$$

where Γ is the Euler's function and $\varphi(s) = \Lambda(2s-1)/\Lambda(2s)$ with

$$\Lambda(s) = \pi^{-s/2} \Gamma(s/2) \zeta(s) = \Lambda(1-s)$$

is the function which gives birth to the functional equation of the Riemann zeta function. We will now describe the formula.

The term on the left hand side, next to the term of the standard Seldberg trace formula ([Gut90]), is the “winding number” of function φ (this function is the eigenfunction relative to the eigenvalue $1/4$) and does take into account the continuous spectrum. On the right hand side the new sum is over the elliptic conjugacy classes $[\delta]$ of which, in $X(1)$, there are two (one of order 2 and one of order 3).

The trace formula (5.5) has, on the left hand side, the sum over the discrete and continuous spectrum, while on the other side there is the geometric side. The fact that the latter side is explicit is at the heart of many modern applications of the general trace formula, one strategy being that one computes explicitly the geometric sides for quotients $\Gamma \backslash G$ and $\Gamma' \backslash G'$. In particular, correspondence of geometrical sides implies the same for the spectrum.

Considering the special case, it is possible to use the formula (5.5) for $h(t) = H(t/T)$, where H is a fixed function and T will go to infinity. It is possible to prove that, for $T \rightarrow \infty$, the contribution coming from first term on the right hand side is leading hence we get

$$\sum_{j \in \mathbb{N}} H(t_j/T) - \frac{1}{2\pi} \int_{-\infty}^{\infty} H(t/T) \left(\frac{\varphi'}{\varphi} \right) \left(\frac{1}{2} + it \right) dt \sim \frac{\text{Area}(X(1))}{2\pi} \int_{-\infty}^{\infty} H(r/T) \tanh(\pi r) r dr$$

and in similar way as in the previous section, this leads to the approximation

$$\sum_{t_j \leq T} 1 - \frac{1}{2} \int_{-T}^T \left(\frac{\varphi'}{\varphi} \right) \left(\frac{1}{2} + it \right) dt \sim \frac{\text{Area}(X(1))}{2\pi} T^2$$

Using the fact the $\varphi(s) = \Lambda(2s-1)/\Lambda(2s)$, it is possible to prove that the leading term on the left hand side is the summation, hence $X(1)$ is *essentially cuspidal* (see the final part of chapter 7). For details, see [Sar03], [Shi71].

6 Arithmetic Quantum Unique Ergodicity

6.1 Lindenstrauss' result

Let $M = \Gamma \backslash \mathcal{H}$ be a finite area hyperbolic surface. What we will say is true for Γ being an *arithmetical lattice*, but for the sake of clarity we fix $\Gamma = \mathrm{PSL}_2 \mathbb{Z}$, which is a good example. We could do the same with Bolza surface 2.2.3. Moreover, we have mentioned that, if M is compact, then $L^2(M)$ has an orthonormal basis of Laplacian eigenfunctions, but $M = \mathrm{PSL}_2 \mathbb{Z} \backslash \mathcal{H}$ is not compact. So we suppose that this is true even in this case (see [EW10] and last section for details).

As mentioned in chapter 1, the main result due to Lindenstrauss relies on the arithmetical structures of arithmetic surfaces, encoded in Hecke operators. We will define them in this chapter.

Theorem 6.1.1: Lindenstrauss, Arithmetic QUE

If we assume that the Laplacian eigenfunctions φ_j on M are also eigenfunctions for a Hecke operator, then the only possible quantum limit is the Liouville measure.

Using the additional symmetries, Lindenstrauss was able to prove the QUE conjecture for a Hecke basis of eigenfunctions on compact arithmetic surfaces. He and Brooks [Lin06] extended result to the above statement, regarding any joint basis of the Laplacian and a single Hecke operator.

Up to date, it is still an open question whether QUE holds for every orthonormal basis of eigenfunctions of just the Laplacian (which might not be a Hecke basis). For details [Dya22].

The result of Lindenstrauss is a consequence of the following result, which is the main tool developed by Lindenstrauss to tackle the problem. We will assume that M is compact.

Theorem 6.1.2 (Lindenstrauss' measure rigidity theorem). *Let Γ be an arithmetic lattice in $\mathrm{PSL}_2 \mathbb{R}$ and let μ be a probability measure on $X = \Gamma \backslash \mathrm{PSL}_2 \mathbb{R}$. Moreover, μ is such that:*

- μ is invariant under the geodesic flow;
- μ is p -Hecke recurrent for a prime number p ;
- μ has positive entropy on every ergodic component;

We these assumptions, μ is the normalized Liouville measure (Haar measure) on X .

We will not go in depth into this problem, but we make some observations. By Egorov's theorem, the distributions I_{φ_j} are invariant under the geodesic flow. If M is compact as we have supposed, every possible quantum limit is an invariant probability measure. If M is not compact, there could be some *escape of mass* at infinity such that the limit has still mass 1. This possibility was excluded by Soundararajan, see [Sou10a],[Sou10b]. We will now check that these quantum limits of I_{φ_j} are p -Hecke recurrent. For the other point, we refer to [EW10].

6.1.1 Microlocal lift revised

We will re-write what developed in section 4.2, in this planar hyperbolic context, in particular regarding Wigner measures. In this framework, the *microlocal lift* of an eigenfunction φ for the (hyperbolic) Laplacian Δ is presented with some slight differences. As mentioned in chapter 2, the unit tangent space $T^1\mathcal{H}$ is equivalent to the group $G = \mathrm{SL}_2\mathbb{R}$, and so it convenient to fully exploit its structure as *Lie algebra*.

Definition 6.1.3 (Lie algebra of $\mathrm{SL}_2\mathbb{R}$) The Lie algebra of $\mathrm{SL}_2\mathbb{R}$ is given by

$$\mathfrak{G} = \{X \in M_{2 \times 2}(\mathbb{R}) : \forall t \in \mathbb{R} \exp(tX) \in \mathrm{SL}_2\mathbb{R}\}.$$

Using the formula $\det(\exp(X)) = \exp(\mathrm{tr} X)$, we get that \mathfrak{G} coincides with the set of 2×2 matrices with null trace. The differentiation in the direction $X \in \mathfrak{G}$, on the point $g \in G$ is given by

$$D_x : C^\infty(G) \rightarrow C^\infty(G), \quad D_X f(g) = \left. \frac{d}{dt} f(g \exp(tX)) \right|_{t=0}$$

With this, it is possible to view a generic flow on $T^1\mathcal{H}$ choosing a particular direction X :

- *geodesic flow:* $X = A_1 = \begin{pmatrix} 1/2 & \\ & -1/2 \end{pmatrix}$
- *stable horocycle flow:* $X = U^+ = \begin{pmatrix} 1 & \\ & 1 \end{pmatrix}$
- *unstable horocycle flow:* $X = U^- = \begin{pmatrix} & 1 \\ 1 & \end{pmatrix}$

We define the *Casimir operator* as

$$\Omega = D_{A_1} D_{A_1} + \frac{1}{2} D_{U^+} D_{U^-} + \frac{1}{2} D_{U^-} D_{U^+}$$

which has the followings properties.

Lemma 6.1.4

The Casimir operator commutes with all differential operators.

Recalling $\mathcal{H} \times \mathbb{S}^1 \simeq \mathrm{PSL}_2\mathbb{R}$, the restriction of Ω to S^1 -invariant functions coincides with the Laplacian Δ on \mathcal{H} .

For S^1 -invariant functions we mean that following. Let

$$R_\theta = \begin{pmatrix} \cos \theta & -\sin \theta \\ \sin \theta & \cos \theta \end{pmatrix},$$

we define the space of S^1 -eigenfunctions of weight $2n$ as

$$K_{2n} = \{f \in C^\infty(\Gamma \setminus G) : f(gR_\theta = e^{2in\theta}f(g))\},$$

so that the space of S^1 -invariant functions is the space K_0 . By Fourier decomposition it can be seen that it holds the decomposition in direct sum

$$\overline{\bigoplus_{n \in \mathbb{Z}} A_{2n}} = C^\infty(\Gamma \setminus G).$$

A function f is called S^1 -finite if there exists an $N \in \mathbb{N}$ such that

$$f \in \bigoplus_{n=-N}^N A_{2n}.$$

Finally, we define the *raising* and *lowering operators* E^+ and E^- as

$$E^+ := \frac{1}{2} \begin{pmatrix} 1 & i \\ imi & -1 \end{pmatrix}, \quad E^- := \frac{1}{2} \begin{pmatrix} 1 & -i \\ -imi & 1 \end{pmatrix}.$$

Now, we fix an L^2 -normalised eigenfunction φ of the Laplacian, of eigenvalue $\lambda = \frac{1}{4} + t^2$. As mentioned before, φ can be seen as a S^1 -invariant function. In this context, the lift is constructed in the following way. We define inductively the functions $\psi_n(g)$ on $G = \mathrm{PSL}_2 \mathbb{Z}$ as

$$\begin{aligned} \psi_0(g) &= \psi(gS^1) \in A_0 \\ \psi_{2n-2} &= \frac{1}{it + \frac{1}{2} + n} E^+ \varphi_{2n}, \quad n \leq 0 \\ \psi_{2n+2} &= \frac{1}{it + \frac{1}{2} - n} E^- \varphi_{2n}, \quad n \geq 0 \end{aligned}$$

It can be shown that each one of the eigenfunctions ψ_{2n} is a Ω -eigenfunction, corresponding to the eigenvalue λ , i.e. $\Omega \psi_{2n} = \lambda \psi_{2n}$.

We can define the *microlocal lift* as

$$I_\varphi(f) := \left\langle f \sum_{n \in \mathbb{Z}} \psi_{2n}, \psi_0, . \right\rangle$$

It can be shown ([Zel87]) that this definition indeed coincides with one given in section 4.2 arising from the Weyl-quantization procedure and Wigner measures, i.e.

$$I_\varphi(f) = \int_M f |\varphi|^2 d\mu.$$

In this framework, the QE theorem 4.1.5 reads as follows (remember that the semiclassical limit $h \rightarrow 0$ can be read as $\lambda \rightarrow \infty$).

Theorem 6.1.5: QE on hyperbolic surfaces

For any K -finite function $f \in C^\infty(\Gamma \setminus \mathfrak{G})$ and any $l > 0$,

$$\frac{1}{N(L, l)} \sum_{j: |\lambda_j - L| < \varepsilon} \left| I_{\varphi_j}(f) - \frac{1}{|\Gamma \setminus \mathfrak{G}| \int_{\Gamma \setminus \mathfrak{G}} f(g) dg} \right|^2 \rightarrow 0,$$

when $L \rightarrow \infty$ and $N(L, \varepsilon) = \#\{j: |\lambda_j - L| < l\}$

The immediate corollary is the following (see also example 4.1 for comparison)

Corollary 6.1.6. *There exists a diverging subsequence of eigenvalues λ_{j_k} of density 1 so that for any K -finite function f it holds the limit*

$$\lim_{k \rightarrow \infty} I_{\varphi_{j_k}}(f) \rightarrow \frac{1}{|\Gamma \setminus \mathfrak{G}|} \int_{\Gamma \setminus \mathfrak{G}} f(g) dg.$$

In particular,

$$|\varphi_{j_k}|^2 d\mu_{\mathcal{H}} \rightharpoonup d\mu_{\mathcal{H}}$$

where the convergence is weakly.

6.2 Hecke recurrence

6.2.1 The p -adic extension of $\Gamma \setminus \mathrm{PSL}_2 \mathbb{R}$

Our aim is to build up, for each point in $X = \mathrm{PGL}_2 \mathbb{Z} \backslash \mathrm{PGL}_2 \mathbb{R}$ a set of points with a tree structure.

We recall some basic informations about p -adic numbers. We refer to [Q G20] for details. The p -adic numbers, for a fixed prime number p , are another way to complete* the field \mathbb{Q} to the set \mathbb{Q}_p . Their construction follows. For $r \in \mathbb{Q}$, we can write $r = p^k \frac{m}{n}$ with $p \nmid mn$ ($k \in \mathbb{Z}$ can be negative). We define the p -adic norm as

$$|r|_p := r^{-k}.$$

The field \mathbb{Q}_p is the completion of \mathbb{Q} with respect to the p -adic norm $|\cdot|_p$. To have a manageable expression at hand, we can observe that every p -adic number x has an infinite expansion

$$x = \sum_{k=-m}^{\infty} x_k p^k, \quad 0 \leq x_k < p.$$

We define the set of p -adic integers as

$$\mathbb{Z}_p = \left\{ x \in \mathbb{Q}_p : |x|_p \leq 1 \right\},$$

* Actually the real line \mathbb{R} and \mathbb{Q}_p are the only two ways to complete \mathbb{Q} , see Ostrowski theorem.

which can be also viewed as p -adic number with an infinite expansion with powers p^k with $k \geq 0$. The set

$$\mathbb{Z}\left[\frac{1}{p}\right] := \left\{ x = \pm \sum_{k=-m}^n x_k p^k : mn, \in \mathbb{N} \text{ and } 0 \leq x_k < p \right\}$$

is a ring and it is dense in both \mathbb{Q}_p and \mathbb{R} .

Definition 6.2.1 (General PGL group) For a ring R , with R^* be the group of units, we define

$$\mathrm{PGL}_2 R = \left\{ \gamma \in \begin{pmatrix} a & b \\ c & d \end{pmatrix} : a, b, c, d \in R, \det \gamma \in R^* \right\}.$$

Now we need the following decomposition.

Proposition 6.2.2. The diagonal embedding $\mathrm{PGL}_2(\mathbb{Z}[1/p])$ is a lattice and it gives the isomorphism

$$\mathrm{PGL}_2 \mathbb{Z} \setminus \mathrm{PGL}_2 \mathbb{R} \simeq (\mathrm{PGL}_2 \mathbb{Z}[1/p] \setminus \mathrm{PGL}_2 \mathbb{R}) \times (\mathrm{PGL}_2 \mathbb{Q}_p / \mathrm{PGL}_2 \mathbb{Z}_p)$$

Proof. CITA APPENDICI, DA SISTEMARE ■

The ratio behind this result is the main diagonal embedding

$$\mathbb{Z}[1/p] \hookrightarrow \mathbb{R} \times \mathbb{Q}_p$$

given by $x \mapsto (x, x)$ which is discrete and co-compact. Setting,

$$\begin{aligned} G &= \mathrm{PGL}_2 \mathbb{R}, \quad \Gamma = \mathrm{PGL}_2 \mathbb{Z} \\ G_p &= \mathrm{PGL}_2 \mathbb{Q}_p, \quad H_p = \mathrm{PGL}_2 \mathbb{Z}_p, \quad \Gamma_p = \mathrm{PGL}_2 \mathbb{Z}[1/p] \end{aligned}$$

proposition 6.2.2 gives

$$\Gamma \setminus G \simeq \Gamma_p \setminus G \times G_p / H_p.$$

We can consider a point $\Gamma g \in \Gamma \setminus G$. By the above proposition it is identified with a point

$$\Gamma_p(g, e) H_p \in \Gamma_p \setminus G \times G_p / \Gamma_p.$$

Now, the orbit of this point under the action of G_p is given by

$$\{\Gamma_p(g, h) H_p : h \in G_p\}$$

can be identified to G_p / H_p , as the stabilizer is

$$\mathrm{Stab}_{\Gamma_p(g, e) H_p} = H_p.$$

In the end we have built a foliation of $\Gamma \setminus G$ where the leaves are these orbits. Now the following main result shows that the leaves G_p / H_p have a tree structure.

A lattice in \mathbb{Q}_p^2 is a discrete subgroup $L \subset \mathbb{Q}_p^2$ of the form $L = \mathbb{Z}_p v_1 + \mathbb{Z}_p v_2$ where $\{v_1, v_2\}$ is a basis of \mathbb{Q}_p^2 . We define an equivalence relation \sim between lattices by

$$L_1 \sim L_2 \Leftrightarrow L_1 = \alpha L_2, \alpha \in \mathbb{Q}_p \setminus \{0\}. \quad (6.1)$$

Essentially, we are identifying lattices where one is a scaling of the other one. We define X_p as the collection of all equivalence classes $[L]$ in \mathbb{Q}_p^2 . We will now introduce the structure of a graph to X_p , where its points (equivalence classes) are vertices. Two vertices $[L_1, L_2]$ are *adjacent* if for some representatives L_1, L_2 we have

$$pL_1 \subset L_2 \subset L_1.$$

By p -multiplication, we see that this condition is symmetric. An equivalent definition of *adjacency* is to require that, given two representatives L_1, L_2 , we have

$$[L_1 : L_2] = p.$$

Indeed, if $pL_1 \subset L_2 \subset L_1$, taking the quotient by pL_1 we get

$$\{0\} \subset L_2/pL_1 \subset L_1/pL_1 \simeq (\mathbb{Z}_p/p\mathbb{Z}_p)^2 \simeq (\mathbb{Z}/p\mathbb{Z})^2.$$

Thus, there is a bijection between subgroups L_2 such that $pL_1 \subsetneq L_2 \subsetneq L_1$ and subgroups H such that $\{0\} \subsetneq H \subsetneq (\mathbb{Z}/p\mathbb{Z})^2$, both $(L_2$ and $H)$ of index p . However, there are $p+1$ subgroups of index p in $(\mathbb{Z}/p\mathbb{Z})^2$, thus X_p is a $p+1$ regular graph, as each one of its vertices has $p+1$ adjacent vertices. However, the following stronger statement holds.

Proposition 6.2.3. $X_p = \mathrm{PGL}_2 \mathbb{Q}_p / \mathrm{PGL}_2 \mathbb{Z}_p$ is a $p+1$ regular tree.

Proof. See [Ber16],[EW10]. ■

One way to see this is to use Cartan decomposition.

Proposition 6.2.4 (Cartan decomposition). It holds

$$\mathrm{GL}_2 \mathbb{Q} = \mathrm{GL}_2 \mathbb{Z}_p \left\{ \begin{pmatrix} p^m & \\ & p^n \end{pmatrix} : m, n \in \mathbb{Z}, m \leq n \right\} \mathrm{GL}_2 \mathbb{Z}_p.$$

Proof. We first start from a matrix $g = \begin{pmatrix} a & b \\ c & d \end{pmatrix}$. First, we can multiply from the right by $\begin{pmatrix} 0 & 1 \\ 1 & 0 \end{pmatrix} \in \mathrm{GL}_2 \mathbb{Z}_p$ to assume that $|a|_p \geq |b|_p$, in particular $b/a \in \mathbb{Z}_p$. Hence we can multiply from the right by $\begin{pmatrix} 1 & -b/a \\ 0 & 1 \end{pmatrix}$ to get a matrix $\begin{pmatrix} a & 0 \\ c & d' \end{pmatrix}$. We now multiply from the left by $\begin{pmatrix} 1 & 0 \\ \alpha & 1 \end{pmatrix}$, for $\alpha \in \mathbb{Z}[1/p]$, getting $\begin{pmatrix} a & 0 \\ c' & d' \end{pmatrix}$, with $c' = a\alpha + c$. By density (in \mathbb{Q}_p) of $\mathbb{Z}[1/p]$, we choose $\alpha \in \mathbb{Z}[1/p]$ “near” $-c/a$ such that $|c'|_p$ is small, hence ensuring $|c'|_p \leq |d'|_p$. Like before, we multiply (from the left) by the matrix $\begin{pmatrix} 1 & 0 \\ -c'/d' & 1 \end{pmatrix} \in \mathrm{GL}_2 \mathbb{Z}_p$, thus getting a diagonal form $\begin{pmatrix} a & 0 \\ 0 & d' \end{pmatrix}$.

We conclude observing that each $a \in \mathbb{Q}_p$ can be written as $a = \alpha p^n$, with $\alpha \in \mathbb{Z}_p^*$, form $n \in \mathbb{Z}$. ■

Using this result, recalling $X_p = G_p/H_p = \mathrm{PGL}_2 \mathbb{Q}_p / \mathrm{PGL}_2 \mathbb{Z}_p$, we have

$$X_p = G_p/H_p = \mathrm{PGL}_2 \mathbb{Z}_p \left\{ \begin{pmatrix} p & \\ & p^n \end{pmatrix} : n \in \mathbb{N} \right\}.$$

The vertices of distance n in the tree from the origin $[\mathbb{Z}_p^2]$ are the classes

$$[h \begin{pmatrix} 1 & \\ & p^n \end{pmatrix} \mathbb{Z}_p^2], \quad \forall h \in \mathrm{PGL}_2 \mathbb{Z}_p.$$

6.2.2 Hecke operators

Now we will introduce the Hecke operators. Thanks to the previous section, for each point $x \in X = \mathrm{PGL}_2 \mathbb{Z} \backslash \mathrm{PGL}_2 \mathbb{R}$, we can define the set $\mathfrak{X}_p \subset X$ with a tree structure, called the *Hecke tree*. A remarkable points is that it is possible to give a general definition for a Laplacian operator on graphs: under this general definition, the Hecke operator is indeed a Laplacian ([EW10]).

We denote the distance of two points $x_1, x_2 \in \mathfrak{X}_p(x)$ with $d_p(x_1, x_2)$, such that $d_p(x_1, x_2) = 1$ iff $x_{1,2}$ are neighbours in $\mathfrak{X}_p(x)$. Now let $\mathfrak{X}_p^n(x)$ be

$$\mathfrak{X}_p^n(x) := \{y \in \mathfrak{X}_p(x) : d_p(x, y) = n\}. \quad (6.2)$$

So, we can define the *Hecke operators* T_{p^n} for any $n \geq 1$ as

$$T_{p^n} f(x) = \sum_{y \in \mathfrak{X}_p^n} f(y),$$

for any function $f: X \rightarrow \mathbb{C}$. The following relations hold.

- Lemma 6.2.5.** • $T_p^2 = T_{p^2} + (p+1)I$;
- $T_p T_{p^n} = T_{p^n}$;
 - T_{p^n} is self adjoint for $n \geq 1$;
 - T_{p^n} commutes with the action of $\mathrm{PSL}_2 \mathbb{R}$ and hence we all differential operators.

We can now give an explicit formula for T_p in the case of the modular surface. The neighbours of the origin $[\mathbb{Z}_p^2]$ are of the form

$$[h \begin{bmatrix} 1 & \\ & p^n \end{bmatrix} \mathbb{Z}_p^2], \quad \forall h \in \mathrm{PGL}_2 \mathbb{Z}_p.$$

There are only $p+1$ possible classes, corresponding to index p subgroups of \mathbb{Z}_p^2 . These classes are of the form $[g\mathbb{Z}_p^2]$, where g is one of the $p+1$ matrices

$$\begin{bmatrix} 1 & \\ & p \end{bmatrix}, \quad \begin{bmatrix} p & -b \\ & 1 \end{bmatrix}, \quad \text{with } 0 \leq b < p$$

which corresponds to possible remainder classes in the division by p , plus the diagonal subgroup. The final formula for $f: \mathrm{PSL}_2 \mathbb{Z} \backslash \mathrm{PSL}_2 \mathbb{R} \simeq \Gamma \backslash \mathcal{H} \rightarrow \mathbb{C}$ is

$$T_p f(z) = f(pz) + \sum_{b=0}^{p-1} f\left(\frac{z+b}{p}\right) \quad (6.3)$$

6.2.3 Hecke invariance

The Hecke operator T_p can be seen as the analog of the Laplacian on the $p+1$ -regular tree previously described. The first step is the following abstract result, of which we will give only a sketch of the proof.

- Proposition 6.2.6.** Let f be a function on a $p+1$ -regular tree, and T_p be the operator defined by

$$T_p f(z) = \sum_{y: d_p(x,y)=1} f(y),$$

with d_p being the distance of x, y on the tree. If $T_p f = \lambda f$, then there exist a constant $c > 0$ such that

$$\sum_{y: d_p(x,y) \leq n} |f(y)|^2 \geq cn |f(x)|^2, \quad \forall n \geq 1.$$

Proof. By Cauchy-Schwarz inequality we have

$$\begin{aligned} \left| \sum_{i=0}^n T_{p^i} f(x) \right| &= \left| \sum_{y: d_p(x,y) \leq n} f(y) \right| \leq \left(\sum_{y: d_p(x,y) \leq n} |f(y)|^2 \right)^{1/2} \# \{y: d_p(x,y) \leq n\}^{1/2} \\ &\leq Cp^{n/2} \left(\sum_{y: d_p(x,y) \leq n} |f(y)|^2 \right)^{1/2}, \end{aligned}$$

where C is a constant of proportionality for the “sphere” $\{y: d_p(x,y) \leq n\}$. By lemma 6.2.5, f is an eigenfunction of T_{p^i} , for all $i \geq 1$, with respect to eigenvalues λ_i defined inductively by

$$\lambda_1 = \lambda, \quad \lambda_2 = \lambda^2 - p - 1, \quad \lambda_{i+1} = \lambda \lambda_i - p \lambda_{i-1} \quad \forall i \geq 3.$$

We note that

$$\left| \sum_{i=0}^n T_{p^i} f(x) \right| = \left| \sum_{i=0}^n \lambda_i |f(x)| \right|$$

and so we need to estimate $|\sum_{i=0}^n \lambda_i|$. Using standard techniques for recurrence sequences, we can observe that, if $c_{1,2} = \frac{\lambda + \sqrt{\Delta}}{2}$ are the two solutions of equation $t^2 - t\lambda + p = 0$, then

$$\lambda_i = ac_1^i + bc_2^i$$

with

$$a = \frac{4}{-p\sqrt{\Delta}} \left(p \left(c_2 - \frac{\lambda}{4} \right) + c_2 \right), \quad b = \frac{4}{-p\sqrt{\Delta}} \left(p \left(\frac{\lambda}{4} - c_1 \right) - c_1 \right).$$

In case $|\lambda| > 2\sqrt{p}$ (*non-tempered case*), both c_1, c_2 are real and it is possible to give a straightforward estimation, while in the other case $|\lambda| < 2\sqrt{p}$ (*tempered case*) the computation require much more attention and it is more involved. We refer to [EW10], proposition 3.22 for the details. In both cases, the estimation gives the thesis. ■

Definition 6.2.7 (Hecke recurrence) A measure ν on X is called Hecke-recurrent if for every ν -measurable set $B \subset X$ and ν -a.e. $x \in B$ it holds

$$\mathfrak{X}_p^n(x) \cap B \neq \emptyset,$$

for infinitely many $n \in \mathbb{N}$.

The next theorem can be applied to the microlocal lifts I_{φ_j} of joint eigenfunctions of the Laplacian and the Hecke operator T_p , for some prime p . This justify Lindenstrauss assumption regarding Hecke recurrence.

Theorem 6.2.8. Let $\{\varphi_k\}_{k \geq 0}$ be a sequence of eigenfunctions of T_p , such that $\|\varphi_k\|_2 = 1$ for all k . If $d\mu_k = |\varphi(g)|^2 dg$, the any weak limit ν of μ_k is Hecke recurrent.

Proof. From proposition 6.2.6 and using the fact that T_p is self-adjoint, we have

$$\left\langle \sum_{i=0}^n T_{p^i} f, |\varphi|^2 \right\rangle = \left\langle f, \sum_{i=0}^n T_{p^i} |\varphi|^2 \right\rangle \geq Cn \left\langle f, |\varphi|^2 \right\rangle$$

for a certain constant C . Making $k \rightarrow \infty$, we get

$$\int_X \left(\sum_{i=0}^n T_{p^i} f \right) d\nu \geq Cn \int_X f d\nu.$$

As smooth functions are dense in the set of L^2 -measurable functions, this last inequality holds for every measurable function $f \geq 0$. Now let $B \subset X$ be a measurable set. We define

$$B_k = \left\{ x \in B : B \cap \mathfrak{X}_p^k(x) = \emptyset \right\}$$

and

$$C_h = \bigcap_{k \geq h} B_k.$$

Then $\bigcup_{h \geq 1} C_h$ is the set of points in B such that, after some times, do not come back to B ever again. We will show that this set is of null-measure.

We fix a h . For any $z \in X$ the set $Xtree_p(z) \cap C_h$ contains at most $(p+1) \cdot p^{h-1}$ vertices ($p+1$ points for each level). Hence,

$$\sum_{i=0}^{\infty} T_{p^i} \mathbb{1}_{C_h} \leq (p+1)p^{h-1}$$

We now apply the previous inequality for the (measurable) function $\mathbb{1}_{C_h}$, getting

$$Cn\nu(C_h) \leq \int_X \left(\sum_{i=0}^n T_{p^i} f \right) d\nu \leq (p+1)p^{h-1}\nu(C_h).$$

As this should hold for all n , we have $\nu(C_h) = 0$ and then, by sub-additivity

$$\nu \left(\bigcup_{h \geq 1} C_h \right) \leq \sum_{h \geq 1} \nu(C_h) = 0,$$

and we are done. ■

6.3 Existence

The existence problem of Maass forms for the modular surface is by no means a problem of easy solution and this task has been taken seriously. The starting point is the Weyl's law. As mentioned in chapter 4, this result can be generalized to Riemannian manifolds of any dimensions, but we restrict ourselves to the finite-area non-compact case.

The main difference between the compact and the non-compact case is that the latter has also a *continuous spectrum*, which "hide" the interesting discrete part. The continuous spectrum can be, however, ruled out, via theory of Eisenstein series and their analytical continuation [Shi71]. In particular, for general hyperbolic surfaces $X_\Gamma = \Gamma \backslash \mathcal{H}$,

the spectra consist of the interval $[1/4, \infty)$ with multiplicity the number of cusps of X_Γ .

In the Hilbert space $L^2(X_\Gamma)$ the orthogonal complement to the continuos (and residual) spectrum of X_Γ is the so-called cuspidal space $L^2_{\text{cusp}}(X_\Gamma)$. A maass form which lie in $L^2_{\text{cusp}}(X_\Gamma)$ is called **Maass cusp form**. Coming back to the case $\Gamma = X(N)$, the existence of Maass cusp forms is tied with the dimension of the cuspidal space $L^2_{\text{cusp}}(X(1))$.

Another remarkable accomplishment of the trace formula for $\text{PSL}_2 \mathbb{Z}$ was actually the proof that modular surfaces $X(N)$ are endowed of an abundance of Maass cusp forms. In [Sar03], it is shown that for $X(N)$ holds the limit

$$N_{\Gamma(N)}^{\text{cusp}}(\lambda) \sim \frac{\text{Area}(X(N))}{4\pi} \lambda$$

which is the usually form of Weyl's law. Thus, in the end, solutions to the problem 2.5 exist and there are many of them. A surface X for which this asymptotic law holds is called *essentially cuspidal*.

7 Frontiers in Quantum chaology

7.1 Numerical simulations

The difficulties of even just approaching QUE conjecture by Rudnick and Sarnak, for example, led researches in this area to, at least, find numerical evidence for it. In this sense, a major contribution arrived from Alex Barnett, who worked in the past ten years frequently with Peter Sarnak. He developed numerical methods for investing spectral properties of quantum system derived from billiards and his most notable project was the simulation of $\simeq 30000$ eigenfunctions of the Barnett billiard (and for this reason Sarnak gave his name to this kind of billiard). In particular, this project produced evidence that QUE holds in this case. Barnett studied the rate of equidistribution of Laplacian eigenfunctions (with Dirichlet boundary condition) by analyzing the diagonals element of the *matrix coefficient* (see section 2.3.2) $\langle A\varphi_m, \varphi_n \rangle$, where A is a suitable test ψ DO and φ_n are eigenfunctions of eigenvalues λ_n .

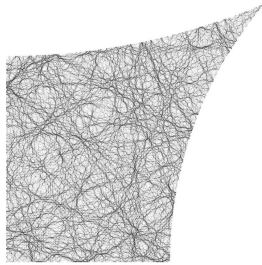


FIGURE 7.1: The density eigenfunction $|\varphi_n|^2$ for $n \simeq 5 \times 10^4$ and the correspondent $\lambda_n \simeq 10^6$. Computed by Alex Barnett.

Barnett examined these quantities up to $n, m \simeq 7 \times 10^5$, getting a 10^2 improvement of eigenvalue magnitude over the state of art. Moreover, he developed a free MATLAB tool to plot efficiently eigenfunctions on complex domains (MPSPACK, see <https://github.com/ahbarnett/mpspack>).

Another essential support to this field, mainly about Maass forms and quantum chaos problems relative to the modular group and its subgroups arrived, starting from the work of [Hej99], recently from Friderik Stromberg ([Str19]), who succeeded in calculating the first 10.000 eigenvalues for $X(1)$. Moreover, Holger Then, with the joint

work of already mentioned Barnett, managed to compute and plot eigenfunctions with an high accuracy ([Bar06],[The05]).

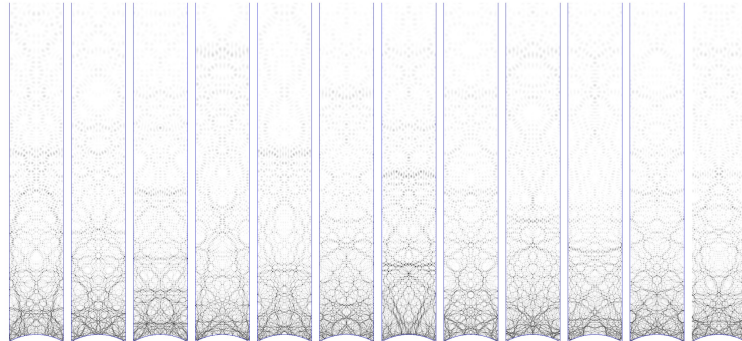


FIGURE 7.2: 12 consecutive Maass forms (5600th eigenvalue and so on), i.e. laplacian eigenfunctions on the modular surface, computed by Holger Then and Alex Barnett

Not to forget is the breakthrough contributions due to Strohmaier and Uski, who computed with very high accuracy, the first 1000 eigenvalues of Laplacian on Bolza surface, using a different algorithm described in [SU13] best suited for compact surfaces of genus 2, 3, 4 (thus very different cases from the modular surface).

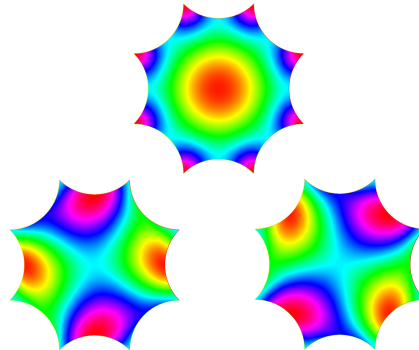


FIGURE 7.3: The three eigenfunctions on Bolza surface, corrisponding to the first eigenvalue $\lambda = 3.8388872\dots$. See [SU13]

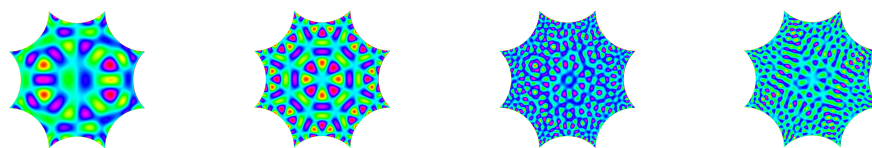


FIGURE 7.4: Bolza surface is an arithmetic hyperbolic surface, thus eigenfunctions equidistributes on the surface.



FIGURE 7.5: The first two eigenfunctions of the modular surface, see on the Poincaré disk model \mathcal{D} . The corresponding eigenvalues are $\lambda_1 = 91.12\dots$ and $\lambda_2 = 148.43\dots$, see [Sar03].

METTI ALTRE FIGURE EIGENFUNCTIONS FATTE DA TE

7.1.1 Numerical methods

The first attempts to investigate the spectrum of the modular surface $X(1)$ were carried out in [Car71]. After those not-so-successfully attempts, other simulations were made and, among the eigenvalues $1/4 + t^2 = \lambda$, some Riemann zeros $1/2 + it$ suddenly appeared. The reason was later discovered by Hejhal [Hej99], who also developed a useful (heuristic) method to compute spectra of modular surfaces, and later improved by the already mentioned Friderik Stromberg, in his PhD thesis.

The reason behind the presence of Riemann zeta's zeros was the following: the numerical methods used until then were faulty in allowing the eigenfunctions to have logarithmic singularities. Obviously, these were not real eigenfunctions. The method developed by Hejhal is now known as “collocation”. The eigenfunctions, i.e. cusp forms, considered have a Fourier expansion in $z = x + iy$ given by

$$\varphi^+(z) = \sum_{n=1}^{\infty} \rho_\varphi(n) y^{1/2} K_{it_\varphi}(2\pi ny) \cos(2\pi nx)$$

and

$$\varphi^-(z) = \sum_{n=1}^{\infty} \rho_\varphi(n) y^{1/2} K_{it_\varphi}(2\pi ny) \sin(2\pi nx)$$

where $\varphi^\pm(z)$ are, respectively, even and odd eigenfunctions respect to the vertical axis $\Re(z) = 0$ (see [Sta84],[Sar03] for details) and the eigenvalue is $\lambda = 1/4 + t_\varphi^2$. The unknowns in these expressions are the coefficients $\rho_\varphi(n)$ and the eigenvalue parameter t_φ . We will roughly described a main method un this subject, due to Hejhal, which is suited for “not-so-big” eigenvalue parameters t_φ , but there are other modern methods, due to Stark, Barnett, Stromberg and Strohmaier among the others, which cover different cases.

The Bessel function $K_{it_\varphi}(y)$ is exponentially decreasing for $y \gg |t_\varphi|$, so that the series expressing φ^\pm is approximated with an accuracy of $O(e^{-2\pi M})$ for $y \geq \frac{\sqrt{3}}{2}$, when

both series are truncated at $n = M$. The functions $\varphi(z)$ are already 1-periodic* so what is missing is the J -invariance, i.e. the condition $\varphi(-1/z) = \varphi(z)$.

This method is “good” to get eigenvalues of $X(1)$ such that $\lambda \lesssim 250000$. At first, truncate the series at $n = M$ and choose evenly distributed points $z_1, \dots, z_M \in D_{2i}$ ($z_i = x_i + iy_i$), where D_{2i} is the Dirichlet fundamental domain of $X(1)$ with center $2i$. The condition $\varphi(-1/z) = \varphi(z)$ for the truncated series $\varphi^{(M)}(z)$ and the chosen sample gives the system of equations

$$\varphi^{(M)}(z_j) = \varphi^{(M)}(-1/z_j), \forall i = 1, \dots, M$$

which is a homogeneous linear system of M equations with M unknowns. Each equation is of the form

$$\sum_{n=1}^M \rho(n) A_{n,j}(t) = 0$$

where[†]

$$A_{n,j}(t) = A_n(z_j, t) := \sqrt{Jy_j} K_{it}(2\pi n J y_j) \cos(2\pi n J x_j) - \sqrt{y_j} K_{it}(2\pi n y_j) \cos(2\pi n x_j).$$

One way to go on, at this point, is to seek solutions $t \leq T$ of the equation

$$\det A(t) = 0$$

where A is the matrix obtained by elements $A_{n,j}(t)$. However, to speed up the process it is more convenient to choose a second set of points w_2, \dots, w_M and to solve the double system of equation (setting $\rho(1) = 1$)

$$\begin{cases} \sum_{n=2}^M \rho^{(z)}(n) A_n(z_j, t) & -A_1(z_j, t) \\ \sum_{n=2}^M \rho^{(z)}(n) A_n(w_j, t) & -A_1(w_j, t) \end{cases}, \quad \forall j = 2, \dots, M. \quad (7.1)$$

For a true eigenvalue parameter t_φ it should hold

$$\rho^{(z)}(n) = \rho^{(w)}(n), \quad \forall n = 2, \dots, M.$$

but it is not granted for approximated values t . Hence one chooses the t 's for which this condition holds. This works well until $T \simeq 500$, but after this points the system (7.1) becomes ill conditioned.

7.2 Spectral statistics and Random Matrix Theory

In order to tackle the problem, without getting involved in complications to the geometrical constraint (symmetry groups, different metric and so and so forth), this field has encountered the method of *SPECTRAL STATISTICS*.

In this case, the approach is exactly the contrary: obtaining geometrical informations from the spectra of the Laplacian, with tools from, for example, the Random Matrix Theory RMT. In particular, getting analytical informations about the spectra of the

*The eigenfunctions have to be $\text{PSL}_2 \mathbb{Z}$ -invariant and $\text{PSL}_2 \mathbb{Z} = \langle J, S \rangle$, where $Jz = -1/z$ and $Sz = z + 1$, see section 2.2.3.

[†]We consider the even case for φ .

Laplacian is an hopeless task, but nonetheless it is possible to get asymptotical informations, starting from statistical knowledge of the correspondent classical underlying billiard. In this sense, Weyl's law is a good example, as it lets to recover the area of the domain, from the distribution of the eigenvalues.

For this reason (distribution of the eigenvalues) the *Nearest Neighbour Spacing Distribution* is introduced: it a function that counts the fraction of eigenvalues λ_n less than a fixed real λ , which are distant from the next eigenvalue λ_{n+1} at most s . In other words, the expression of the NNSD is

$$P(s, N) := \frac{1}{N} \sum_{j=1}^N \mathbb{1}_{\{s > \lambda_{n+1} - \lambda_n\}}.$$

In general, the sequence λ_n is sufficiently randomized, so it "should exist" a limit distribution $p(s) = \lim_{N \rightarrow \infty} P(s, N)$ so that

$$\lim_{N \rightarrow \infty} \int_0^\infty p(s, N) h(s) ds = \int_0^\infty p(s) h(s) ds$$

for a smooth function h with compact support. In this context, we can find the true starting point of the modern Quantum Chaos, which is the *Berry-Tabor conjecture*.

Conjecture 7.2.1: Berry-Tabor, 1977

For "generic integrable systems" the limit distributions $P(s)$ of the NNSD is equal to the waiting time distribution coincides with the corresponding quantity for a sequence of uncorrelated levels (the Poisson ensemble), i.e. the waiting time distribution of a Poisson process: $p(s) = ce^{-cs}$, with $c = \text{Area}/4\pi$.

Another dramatic insight about the possible forms of the quantity $p(s)$ is given by the following conjecture, regarding the chaotic, ergodic case.

Conjecture 7.2.2: Bohigas, Giannoni, and Schmit, 1984

If the underlying classical dynamics is ergodic, then $p(s)$ coincides with the corresponding quantity for the eigenvalues of a suitable ensemble of *random matrices*.

Until now the conjecture has not been proved in its generality. However, there is a vast list of numerical studies based on a wide variety of systems that support its validity; of particular interest are, of course, hyperbolic dynamical systems arising from arithmetical groups (like the modular surface and the bolza surface) and an exstensive analysis is developed in [Bog+97] and [Bog03], a work by Bogolmy, Bohigas, Giannoni, and Schmit which gives this thesis title.

Remark 7.2.1. It is a curious thing, object of undergoing studies, that the statistics of conjecture 7.2.2 is similar to the distribution of the zeros of Riemann's zeta function $\zeta(z)$.

A mathematically rigorous formulation of the now-so-called Random Matrix Theory RMT was established by Freeman Dyson in a series of papers. He introduced the classification of the Gaussian random matrix ensembles according to their invariance properties under time reversal. In particular, he proved the existence of only three

classes for such matrices. He said:

What is here requiered is a new kind of statistical mechanics, in which we renounce exact knowledge not of the state of the system but of the system itself. We picture a complex nucleus as a “black box” in which a large number of particles are interacting according to unknown laws. The problem then is to define in a mathematically precise way an ensemble of systems in which all possible laws of interaction are equally possible.

-Freeman Dyson

Definition 7.2.3 (Gaussian Random Matrix) The Gaussian random matrix H is a matrix from an ensemble of matrices with probability distribution $P(H)$, such that

- the probability distribution have to be invariant under a prescribed transformations W , $P(H) = P(W^{-1}HW)$;
- matrix elements of H are statistically independent.

The possible Gaussian random matrix ensembles are then:

- 1) **Gaussian Orthogonal Ensemble** GOE: related to time-reversal systems, this ensemble is invariant under orthogonal trasformations. The matrix H mirroring the Hamiltonian of the system is real symmetric and has $N(N + 1)/2$ indipendent real components.
- 1) **Gaussian Unitary Ensemble** GUE: related to non time-reversal systems, this ensemble is invariant under unitary trasformations. The matrix H mirroring the Hamiltonian of the system is complex Hermitian and has N^2 indipendent real components.
- 1) **Gaussian Symplectic Ensemble** GSE: related to time-reversal systems with particular features, this ensemble is invariant under symplectic trasformations. The matrix H mirroring the Hamiltonian of the system is quaternionic Hermitian and has $N(2N - 1)$ indipendent components. This ensample is used only for very particular systems.

After suitable normalization, the NNSD for the three Gaussian ensembles are given by:

- GOE : $p(s) = \frac{\pi}{2} \exp\left(-\frac{\pi}{4}s^2\right);$
- GUE : $p(s) = \frac{32}{\pi^2}s^2 \exp\left(-\frac{4}{\pi}s^2\right);$
- GSE : $p(s) = \left(\frac{64}{9\pi}\right)^3 s^4 \exp\left(-\frac{64}{9\pi}s^2\right).$

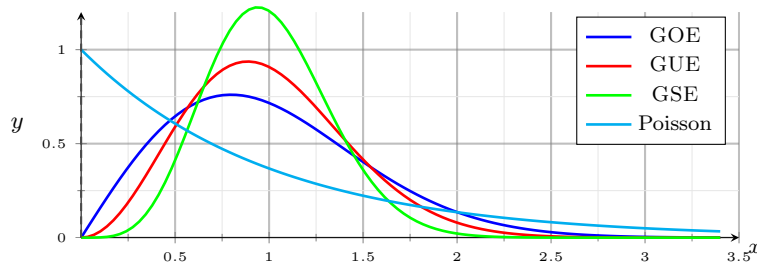


FIGURE 7.6: Different distributions from Random Matrix Theory.

Quite remarkably, the distribution eigenvalues on the modular surface $X(1) = \text{PSL}_2 \mathbb{Z}$ follows a Poisson distribution ([Rud07]).

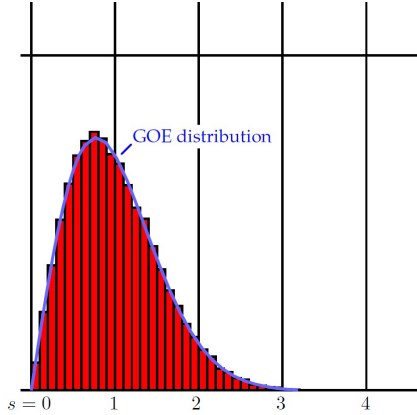


FIGURE 7.7: From [Rud07]. Normalized gaps between roughly 50000 sorted eigenvalues for the Barnett's stadium 7.1. The distributions follows the GOE distribution.

On the contrary, the distribution is expected, by enormous numerical simulations by Odlyzko [OF], to follow the rare GUE distribution ([Rud07]).

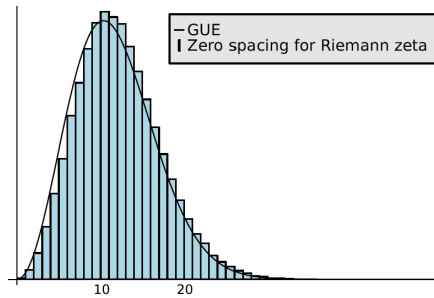


FIGURE 7.8: From [Rud07], computations by [OF]. Distributions of zeros of Riemann zeta function.

For further details, we refer to CITA. The hope of this approach is to increase the understanding about how integrable and chaotic systems differ in the semiclassical limit.

7.3 Conclusion

To be done

7.3.1 Billiard and spectral simulations

A Ergodic notions

A.1 Mixing

In this section, we will prove theorem 2.3.6

Lemma A.1.1. *If $\varphi \in \mathcal{H}$ such that the sequence $\{\pi(A_{t_n})\varphi\}_{n \geq 0}$ converges weakly to an element φ_0 . Then φ_0 is itself invariant to the action of the group \mathfrak{U} .*

Proof. Let a_s Be simple matrix multiplications, we get

$$A_{-t} U_s A_t = U_{s e^{-t}}.$$

Then, for any $\psi \in H$,

$$\begin{aligned} \langle \pi(U_s)\varphi_0 - \varphi_0, \psi \rangle &= \lim_{n \rightarrow \infty} \langle \pi(U_s A_{t_n})\varphi - \pi(A_{t_n})\varphi, \psi \rangle \\ &= \lim_{n \rightarrow \infty} \langle \pi(A_{-t_n} U_s A_{t_n})\varphi - \varphi, \pi(A_{-t_n})\psi \rangle \\ &= \lim_{n \rightarrow \infty} \langle \pi(U_{s e^{-t_n}})\varphi - \varphi, \pi(A_{-t_n})\psi \rangle \\ &\leq \lim_{n \rightarrow \infty} \|\pi(U_{s e^{-t_n}})\varphi - \varphi\| \|\psi\| \end{aligned}$$

where last inequality follows from Cauchy-Schwarz inequality and $U_{s e^{-t_n}} \rightarrow I$. This concludes the proof. ■

Lemma A.1.2 (Mautner phenomenon). *If $\varphi \in \mathcal{H}$ is invariant under the action of U , then it's invariant under $\mathrm{SL}_2 \mathbb{R}$.*

Proof. For any matrix $G \in \mathrm{SL}_2 \mathbb{R}$, we define the function

$$F(G) = \langle \pi(G)\varphi, \varphi \rangle.$$

Function F is nothing else then a matrix coefficient METTI RIFERIMENTO. We note that φ is bi- U -invariant. In fact:

$$F(UGU') = \langle \pi(UGU')\varphi, \varphi \rangle = \langle \pi(G)\varphi, \pi(U^{-1})\varphi \rangle = F(G) \quad \forall U, U' \in \mathfrak{U}.$$

We consider the matrix

$$B = \begin{pmatrix} 1 & r \\ 1 & \varepsilon \end{pmatrix} \begin{pmatrix} 1 & s \\ \varepsilon & 1 \end{pmatrix} \begin{pmatrix} 1 & s \\ 1 & 1 \end{pmatrix} = \begin{pmatrix} 1 + \varepsilon r & r + s + rs\varepsilon \\ \varepsilon & 1 + s\varepsilon \end{pmatrix}.$$

Let $r = (e^t - 1)/\varepsilon$, for fixed $t \in \mathbb{R}, \varepsilon > 0$. So $B = \begin{pmatrix} e^t & \\ \varepsilon & e^{-t} \end{pmatrix}$. This means that, for any $\varepsilon, t > 0$

$$F\left(\begin{pmatrix} 1 & \\ \varepsilon & 1 \end{pmatrix}\right) = F\left(\begin{pmatrix} e^t & \\ \varepsilon & e^{-t} \end{pmatrix}\right).$$

By continuity of representation, if $\varepsilon \rightarrow 0$, we have

$$\langle \varphi, \varphi \rangle = \lim_{\varepsilon \rightarrow 0} F(B) = F\left(\begin{pmatrix} e^t & \\ & e^{-t} \end{pmatrix}\right).$$

This means that $F(A_t) = \langle \pi(A_t)\varphi, \varphi \rangle = \|\varphi\|^2$ and hence the equality case in Cauchy-Schwarz inequality holds. This is possible only if $\pi(A_t)\varphi$ and φ are linear dependent and but putting $t = 0$, we get $\pi(A_t)\varphi = \varphi$. Using the same reasoning, it is possible to prove that F is bi- \mathfrak{A} -invariant. In an analogous way as before, we set

$$D = A_{-t} \begin{pmatrix} 1 & \\ s e^{-t} & 1 \end{pmatrix} A_t = \begin{pmatrix} 1 & \\ s & 1 \end{pmatrix},$$

to get that

$$F\left(\begin{pmatrix} 1 & \\ s e^{-t} & 1 \end{pmatrix}\right) = F\left(\begin{pmatrix} 1 & \\ s & 1 \end{pmatrix}\right)$$

Again, by a continuity argument, we get

$$F\left(\begin{pmatrix} 1 & \\ s & 1 \end{pmatrix}\right) = \|\varphi\|$$

and thus the invariance of φ under \mathfrak{U}^- . So φ is invariant under the diagonal group \mathfrak{A} and under the groups \mathfrak{U}^\pm , hence it must be invariant under the action of all group $\mathrm{PSL}_2 \mathbb{R}$. ■

We are now ready to prove the main result.

Theorem A.1.3 (Howe-Moore). *Let π be a strongly continuous unitary representation of $\mathrm{SL}_2 \mathbb{R}$ on a Hilbert space \mathcal{H} . Assume that π has non-trivial invariant vector in \mathcal{H} . Then, if G_n is a diverging^a sequence in $\mathrm{SL}_2 \mathbb{R}$, then*

$$\lim_{n \rightarrow \infty} \langle \pi(G_n)\varphi, \psi \rangle = \int_X \varphi d\mu \int_X \psi d\mu$$

^aThat is for any compact $K \subset \mathrm{SL}_2 \mathbb{R}$, there exists $N \in \mathbb{N}$ such that $G_n \notin K$ for all $n \geq N$.

Proof. As a first step, we will show that the converging thesis holds for the diagonal subgroup \mathfrak{A} . Suppose there exist φ, ψ and a sequence $t_n \rightarrow \infty$ such that $\langle \pi(A_{t_n})\varphi, \psi \rangle$ does not converge to $\int_X \varphi d\mu \int_X \psi d\mu$.

We have $\|\pi(A_{t_n})\varphi\| = \|\varphi\|$, so (by Banach-Alaoglu theorem) we can find a subsequence that is weakly convergent to some φ_0 . By lemmas A.1.1 and A.1.2, φ_0 is $\mathrm{SL}_2 \mathbb{R}$ -invariant, hence φ_0 is constant. This is a contradiction, because the considered subsequence. Then, necessarily $\forall \phi, \psi \in H$, we have $\langle \pi(A_t)\psi, \phi \rangle \rightarrow \int_X \varphi d\mu \int_X \psi d\mu$ for $t \rightarrow \infty$.

For a general diverging sequence $G_n \in \mathrm{SL}_2 \mathbb{R}$, there exists (for fixed n) $k_n, k'_n \in \mathrm{SO}_2 \mathbb{R}$ and a sequence $t_n \rightarrow \infty$ such that

$$G_n = K_n A_{t_n} K'_n, \quad K_n, K'_n \in \mathrm{SO}_2 \mathbb{R}.$$

This is only a sort of “hyperbolic-polar decomposition” of elements G_n . As K_n, K'_n are bounded elements in $\mathrm{SL}_2 \mathbb{R}$, using multiple diagonal argument, we can choose a subsequence

(which will be still denoted by index n) such that $K_n \rightarrow K$ and $K'_n \rightarrow K'$. So

$$\langle \pi(G_n)\varphi, \psi \rangle = \langle \pi(A_{t_n})\pi(K'_n)\varphi, \pi(K_n)^{-1}\psi \rangle$$

has the same limit as

$$\langle \pi(A_{t_n})\pi(K')\varphi, \pi(K)^{-1}\psi \rangle.$$

However, the limit of this last term is 0,

B Fourier transform

In this appendix we briefly review some notions and properties of the *Fourier transform*.

B.1 Basic notions

We will present Fourier transform on \mathbb{R}^n , keeping in mind that it can be extended to general smooth manifolds using *partition of unity*.

A suitable space for the Fourier transform is the so-called *Schwarz space*, i.e. the space of *rapidly decaying functions*. More precisely, we give the following definition, ([Hör83a])

Definition B.1.1 We define the seminorm $\|\cdot\|_{\alpha,\beta}$ for a smooth function f on \mathbb{R}_n as

$$\|f\|_{\alpha,\beta} := \|x^\alpha \partial^\beta f\|_\infty$$

for fixed multiindices $\alpha \in \mathbb{N}^n$ and β , where*

$$x^\alpha = \prod_i x_i^{\alpha_i}, \quad \partial^\beta = \prod_{i=1}^n \partial_{x_i^{\beta_i}}.$$

The Schwarz space (in \mathbb{R}^n) is the set $\mathcal{S} = \mathcal{S}(\mathbb{R}^n) = \left\{ f \in C^\infty(\mathbb{R}^n) : \|f\|_{\alpha,\beta} < \infty \forall \alpha, \beta \in \mathbb{N}^n \right\}$. The space $(\mathcal{S}, \|\cdot\|_{\alpha,\beta})$ is a Fréchet space over \mathbb{C} and we say $f_j \rightarrow f$ in \mathcal{S} if $\|f_j - f\|_{\alpha,\beta} \rightarrow 0$ for all multiindices α, β .

Definition B.1.2 The Fourier is defined by $\mathcal{F}: \mathcal{S} \ni f \mapsto \hat{f} \in \mathcal{S}$ (we will also use the notation \hat{f} for the Fourier transform of f) and

$$\hat{f}(p) = \int_{\mathbb{R}^n} e^{-i\langle p, x \rangle} f(x) dx,$$

with the inverse given by

$$\mathcal{F}^{-1}(f)(x) = \frac{1}{(2\pi)^n} \int_{\mathbb{R}^n} e^{i\langle x, p \rangle} f(p) dp.$$

The Fourier transform can be defined also for larger spaces, see for example Plancherel theorem. A useful result is the following.

*We are implicitly using the fact that the derivatives commute.

Lemma B.1.3. Let be given a real, symmetric and positive-definite quadratic form $x^T Q x$, where Q is a $n \times n$ -matrix. Then

$$\mathcal{F}\left(e^{-\frac{1}{2}x^T Q x}\right) = \frac{(2\pi)^{n/2}}{(\det Q)^{1/2}} e^{-\frac{1}{2}\langle Q^{-1} p, p \rangle}.$$

Proof. Using the spectral theorem, we can choose an orthogonal basis v_1, \dots, v_n for \mathbb{R}^n that makes Q diagonal, with diagonal elements $\lambda_1^2, \dots, \lambda_n^2$, where each element is positive. Hence, if A is the coordinate-change matrix and $D = \text{diag}(\lambda_1^2, \dots, \lambda_n^2)$, using Einstein notation, from a straightforward computation we get that

$$\begin{aligned} \mathcal{F}(e^{-\frac{1}{2}x^T Q x}) &= \int_{\mathbb{R}^n} e^{-\frac{1}{2}\left(\lambda_i^2 v_i^2 - 2iv_i(a_{ji}p_j) - \frac{(a_{ji}p_j)}{\lambda_i^2}\right) - \frac{1}{2}\frac{(a_{ji}p_j)^2}{\lambda_i^2}} dv \\ &= e^{-\frac{1}{2}\frac{(a_{ji}p_j)^2}{\lambda_i^2}} \int_{\mathbb{R}^n} e^{-\frac{1}{2}\left(\lambda_i v_i - i\frac{(a_{ji}p_j)}{\lambda_i}\right)^2} dv. \end{aligned}$$

The external term $e^{-\frac{1}{2}\frac{(a_{ji}p_j)^2}{\lambda_i^2}}$ can be seen as $\langle AD^{-1}A^T p, p \rangle$. But, from $A^T Q A = D$, we get that $Q^{-1} = AD^{-1}A^T$, hence we get $e^{-\frac{1}{2}\langle Q^{-1} p, p \rangle}$. The integral part can be computed by separating each v_i and using the substitution $y_i = \lambda_i v_i - i\frac{(a_{ji}p_j)}{\lambda_i}$ we get standard gaussian integral. The final result is

$$e^{-\frac{1}{2}\frac{(a_{ji}p_j)^2}{\lambda_i^2}} \int_{\mathbb{R}^n} e^{-\frac{1}{2}\left(\lambda_i v_i - i\frac{(a_{ji}p_j)}{\lambda_i}\right)^2} dv = e^{-\frac{1}{2}\frac{(a_{ji}p_j)^2}{\lambda_i^2}} \prod_{i=1}^n \frac{(2\pi)^{1/2}}{\lambda_i} = \frac{(2\pi)^{n/2}}{(\det Q)^{1/2}} e^{-\frac{1}{2}\frac{(a_{ji}p_j)^2}{\lambda_i^2}},$$

and we are done. ■

The main properties of the Fourier transform are summarized by the following.

Proposition B.1.4. The Fourier transform $\mathcal{F}: \mathcal{S} \rightarrow \mathcal{S}$ is an isomorphism of topological vector spaces. Moreover, for all $f, g \in \mathcal{S}$ hold:

1. $\mathcal{D}_p^\alpha(\mathcal{F}(f)) = \mathcal{F}((-x)^\alpha f)$ and $\mathcal{F}(\mathcal{D}_x^\alpha(f)) = p^\alpha \mathcal{F}(f)$, where $\mathcal{D}_x^\alpha := \frac{\partial^\alpha}{i^{|\alpha|}}$.
2. $\mathcal{F}(f * g) = (2\pi)^{-n} \mathcal{F}(f) * \mathcal{F}(g)$, where $*$ is the standard convolution.
3. $\langle \mathcal{F}(f), g \rangle = \langle f, \mathcal{F}(g) \rangle$.
4. the Fourier transform is an L^2 -isometry.

B.2 Distributions

Another tool linked to the Fourier transform is the notion of *distribution*. In general, a *distribution* on \mathbb{R}^n is a linear functional $\varphi: C_c^\infty(\mathbb{R}^n) \rightarrow \mathbb{R}$ such that $\varphi(f_n) \rightarrow \varphi(f)$, if $f_n \rightarrow f$ with the respect to the previously introduced seminorm, in $C_c^\infty(\mathbb{R}^n)$. The set of all distributions generalizes and forms a vector space dual to $C_c^\infty(\mathbb{R}^n)$. Often, the distribution are improperly denoted by some functions, when they are actually applications.

The vector space of tempered distributions \mathcal{S}' is defined by duality from the Schwartz space \mathcal{S} . Introducing tempered distributions gives, among other things, the correct vector space for a rigorous formulation of the Fourier transforms of nonsmooth functions.

Definition B.2.1 Let the space of tempered distributions \mathcal{S}' be the set of all continuous linear functionals $\varphi: \mathcal{S} \ni f \mapsto \varphi(f)$. We say that $\varphi_j \rightharpoonup \varphi$ in \mathcal{S}' if there the convergence componentwise (i.e. for each function $f \in \mathcal{S}$). Moreover, we define, for each multiindex $\alpha \in \mathbb{N}^n$:

- $D^\alpha \varphi(f) := (-1)^{|\alpha|} \varphi(D^\alpha f)$.
- $(x^\alpha \varphi)(f) := \varphi(x^\alpha f)$.

Finally, \mathcal{F} extends to \mathcal{S}' by setting $\mathcal{F}(\varphi)(f) := \varphi(\mathcal{F}(f))$, $\forall \varphi \in \mathcal{S}', f \in \mathcal{S}$.

Example B.2.15: Fourier transform of Dirac distribution

The Dirac distribution is defined by $\delta_0(f) = f(0)$. Viewed as a tempered distribution, its Fourier transform is

$$\mathcal{F}(\delta_0)(f) = \delta_0 \mathcal{F}(f) = \text{Fourier}(f)(0) = 1.$$

Using distributions, it is possible to prove the following result. We omit the proof, as it is a little involved.

Proposition B.2.2. Let be given a real, symmetric and invertible quadratic form $x^T Q x$, where Q is a $n \times n$ -matrix. Then

$$\mathcal{F}\left(e^{-\frac{1}{2}ix^T Q x}\right) = \frac{(2\pi)^{n/2} e^{i\frac{\pi}{4} \operatorname{sgn} Q}}{|\det Q|^{1/2}} e^{-\frac{1}{2}i\langle Q^{-1} p, p \rangle}.$$

where $\operatorname{sgn} Q$ is the signature of Q .

C Flows and integrable systems

C.1 Ergodic notions

Theorem C.1.1. If Φ_t is ergodic on $(\Sigma_c, \chi, \mu_L^c)$, then

$$\lim_{T \rightarrow \infty} \int_{\Sigma_c} \left(\langle f \rangle_T - \bar{f} \right)^2 d\mu_L^c = 0,$$

for all $f \in L^2(\Sigma_c)$, where \bar{f} denotes the mean integral.

Theorem C.1.2 (Birkhof's theorem). If Φ_t is ergodic on $(\Sigma_c, \chi, \mu_L^c)$, then...

METTERE HOPF

Source codes

C.1 Billiard simulation in Bunimovich stadium	99
C.2 Eigenfunctions of modular surface	107

C.2 Python codes

C.2.1 Billiards

Put your Codes here.

```

1 import numpy as np
2 from manim import *
3
4 from intersect import intersection
5 import matplotlib.pyplot as plt
6 from math import sqrt, acos, tan
7 from scipy import sparse
8 from scipy.sparse import linalg as sla
9 from numpy import sin, cos, pi, linspace, abs, sign, subtract,
   random
10
11 """
12 :type direction: [vx,vy] directional vector
13 :type b_point: bouncing point
14 :type center: center of the circle
15 """
16
17 #costants
18 #SIZEX=3000
19 #SIZEY=1000
20
21
22 BKground=(196,203,211)
23 INF = 1000
24 EPS = 1e-11
25
26 def getTrajectory(p,v): # p is the position, v is the velocity
   vector
   #xc=x+y*m
28   return [p,v] #[xc,0,math.sqrt((xc-x)**2+y**2)]
29
30 def bounce_circle(direction, b_point, center):
31     """
32         Calculate the new direction after a bouncing with a circled wall
33         """

```

```

34     F1 = [[b_point[0]-center[0], b_point[1]-center[1]], [b_point[1]-
35         center[1], center[0]-b_point[0]]]
36     F2 = [[-1, 0], [0, 1]]
37     F3 = [[center[0]-b_point[0], center[1]-b_point[1]], [-(b_point[1]-
38         center[1]), b_point[0]-center[0]]]
39     #F3 = [[b_point[0]-center[0], b_point[1]-center[1]], [-b_point[1]+
40         center[1], -b_point[0]+center[0]]]
41     F3 = -np.dot(1/((b_point[0]-center[0])**2+(b_point[1]-center[1])-
42         **2), F3)
43     return np.dot(np.matmul(np.matmul(F1, F2), F3), direction)
44
45 #print("prova:", np.dot([[0,1],[-1,0]],[2,3]))
46 #print("nuova direzione", bounce_circle([1,1],[np.sqrt(Radius)+WIDTH/
47     /2,np.sqrt(Radius)],[WIDTH/2,0]))
48
49 def upper_wall_intersection(p,v,Radius):
50     l, r = 0, INF
51     while r-l > EPS:
52         m = (l+r)/2
53         if p[1]+m*v[1] > Radius:
54             r = m
55         else:
56             l = m
57     return l
58
59 def lower_wall_intersection(p,v,Radius):
60     l, r = 0, INF
61     while r-l > EPS:
62         m = (l+r)/2
63         if p[1]+m*v[1] < -Radius:
64             r = m
65         else:
66             l = m
67     return l
68
69 def sgn(x):
70     return int(x > 0) - int(x < 0)
71 def norm(v):
72     return np.sqrt(np.dot(v, v))
73
74 def right_c_intersection(p, v, L, Radius):
75     c = [L / 2, 0]
76     #if v[0] >= 0:
77     #l, r = 0, (2 * (Radius) + L)
78     test_p = p + np.multiply(np.dot(np.subtract(c, p), v), v)
79     #print("Norma prova: ", norm(test_p-c))
80     #print("prodotto direzione prova: ", np.dot(np.subtract(c, p), v))
81     #print("Punto prova: ",test_p)
82     if norm(test_p-c) > Radius:
83         return INF
84     elif np.dot(np.subtract(c, p), v) < 0:
85         return INF
86     else:

```

```

86     t = np.dot(np.subtract(c, p), v)+np.sin(acos(norm(test_p-c)/
Radius))*Radius
87     test_p = p + np.multiply(t, v)
88     if test_p[0] > c[0]:
89         return t
90     else:
91         return INF
92     #l, r = np.dot(np.subtract(c, p), v), 2*Radius
93     #while r - l > EPS:
94     #    m = (l + r) / 2
95     #    new_p = p + np.multiply(m, v)
96     #    if new_p[0] > c[0]:
97     #        r = m
98     #    else:
99     #        l = m
100    #return l
101
102
103 def left_c_intersection(p, v, L, Radius):
104     c = [-L / 2, 0]
105     #if v[0] >= 0:
106     #l, r = 0, (2 * (Radius) + L)
107     test_p = p + np.multiply(np.dot(np.subtract(c, p), v), v)
108     #print("Norma prova: ", norm(test_p-c))
109     #print("prodotto direzione prova: ", np.dot(np.subtract(c, p), v))
110
111     #print("Punto prova: ", test_p)
112     if norm(test_p-c) > Radius:
113         return INF
114     elif np.dot(np.subtract(c, p), v) < 0:
115         return INF
116     else:
117         t = np.dot(np.subtract(c, p), v)+np.sin(acos(norm(test_p-c)/
Radius))*Radius
118         test_p = p + np.multiply(t, v)
119         if test_p[0] < c[0]:
120             return t
121         else:
122             return INF
123
124
125
126 def billiard(p, v, n_col, L, Radius):
127     point_list=[[p[0], p[1], 0]]
128     for i in range(n_col):
129         times = [upper_wall_intersection(p, v, Radius),
130                  lower_wall_intersection(p, v, Radius),
131                  left_c_intersection(p, v, L, Radius),
132                  right_c_intersection(p, v, L, Radius)]
133         hit_wall = times.index(min(times))
134         #print('tempi:', times)
135         #print("muro:", hit_wall, times[hit_wall])
136         new_p = p+np.multiply(times[hit_wall], v)
137         #print("nuova posizione", new_p[0], new_p[1])
138         if hit_wall == 0 or hit_wall == 1:
139             v[1] = -v[1]
140         elif hit_wall == 2:
141             v = bounce_circle(v, new_p, [-L/2, 0])

```

```

140         else:
141             v = bounce_circle(v, new_p, [L/2, 0])
142             p = new_p
143             point_list.append([p[0], p[1], 0])
144             return point_list
145
146
147 def time(p1, p2, velocity): #computes the distance done and the
148     time of the path between two points
149     #sequence = billiard(p, v, num_col, L, Radius)
150     length = 0
151     #for i in range(1,num_col+1):
152     #    length = length + norm(np.subtract(p1, p2))
153     #return length/norm(v)
154     return norm(np.subtract(p1, p2))/velocity
155
156
157 def stop(p1, p2, perc):
158     p1 = np.array(p1,dtype='float64')
159     p2 = np.array(p2,dtype='float64')
160     return np.array([[1,0],[0,1],[0,0]],dtype='float64') @ ((1-perc)
161 *p1+perc*p2)
162
163
164 class Draw_single(Scene):
165     def construct(self):
166         self.camera.background_color = WHITE##ece6e2"
167
168         stadium_back = WHITE##c2c4c6##f2f4f6###8598a7###069fd9
169 "##05014a"
170         stadium_bord = "#353c42"
171         col_orbi = "#0000ff"###05014a"
172
173         M = [[1, 0], [0, 1], [0, 0]]
174         reduc = [[1,0,0],[0,1,0]]
175         velocity = 1
176         # the b are the ball object for manim, optional
177         p1 = [0, 0]
178         theta1 = PI / 4
179         v1 = [velocity * np.cos(theta1), velocity * np.sin(theta1)]
180         r_ball1 = 0.08
181         b1_start = Dot(np.dot(M, p1), radius=r_ball1).set_color(
182         col_orbi)
183         b1 = Dot(np.dot(M, p1), radius=r_ball1).set_color(col_orbi)
184
185         # p2 = [-1.5, 0]
186         # theta2 = PI-PI / 3
187         # v2 = [velocity * np.cos(theta2), velocity * np.sin(theta2)
188     ]
189
190         # b2_start = Dot(np.dot(M, p2), radius=0.05).set_color(PINK)
191         # b2 = Dot(np.dot(M, p2), radius=0.05).set_color(PINK)
192         #
193         # p3 = [1,1.5]
194         # theta3 = PI / 3
195         # v3 = [velocity * np.cos(theta3), velocity * np.sin(theta3)
196     ]
197         # b3 = Dot(np.dot(M, p3), radius=0.05).set_color(BLUE)

```

```

193
194     num_col = 10
195     num_animation = 10
196     L = 4*1.3
197     Radius = 2*1.3
198     #r1 = 4
199     #r2 = 10
200
201     render1 = billiard(p1, v1, num_col, L, Radius)
202     #time1 = time(p1, v1, num_col, render1)/6
203     #render2 = billiard(p2, v2, num_col, L, Radius)
204     #time2 = time(p2, v2, num_col, render2)/6
205     #print("tempi: ",time1, time2)
206     # trace lascia la traccia, opacity can be an array
207     trace1 = TracedPath(b1.get_center, stroke_opacity=0.3,
208     stroke_color=b1.get_color(), stroke_width=2)
209     #trace2 = TracedPath(b2.get_center, stroke_opacity=0.3,
210     stroke_color=b2.get_color(), stroke_width=2)#, dissipating_time
211     #=0.5)
212     #trace1 = VMobject()
213     #trace2 = VMobject()
214     #trace3 = VMobject()
215
216     # filling the billiard
217     rect = Rectangle(color=stadium_back, width=L, height=2*
Radius).set_fill(stadium_back, opacity=1)
218     stadi = AnnularSector(color=stadium_back, fill_opacity=1,
inner_radius=0, outer_radius=Radius, angle=-PI, start_angle=3 *
PI / 2, arc_center=[-L / 2, 0, 0])
219     stad2 = AnnularSector(color=stadium_back, fill_opacity=1,
inner_radius=0, outer_radius=Radius, angle=-PI, start_angle=PI / 2,
arc_center=[L / 2, 0, 0])
220     self.add(rect, stadi, stad2)
221     # drawing the billiard
222
223     #self.add(b1, b2, trace1, trace2, b1_start, b2_start)
224     self.add(trace1, b1_start)
225     self.add(Line([-L / 2, Radius, 0], [L / 2, Radius, 0],
stroke_width=5, color=stadium_bord))
226     self.add(Line([-L / 2, -Radius, 0], [L / 2, -Radius, 0],
stroke_width=5, color=stadium_bord))
227     self.add(Arc(Radius, 3 * PI / 2, -PI, arc_center=[-L / 2, 0,
0], stroke_width=5, color=stadium_bord))
228     self.add(Arc(Radius, PI / 2, -PI, arc_center=[L / 2, 0, 0],
stroke_width=5, color=stadium_bord))
229
230     num_start_balls=6
231     centers = [stop(np.dot(reduc, render1[0]), np.dot(reduc,
render1[1]), p) for p in linspace(0,0.2,num_start_balls)]
232     opty = linspace(0.5,0,num_start_balls)
233     starting_balls = VGroup(*[
234         Circle(arc_center=centers[i], radius=r_ball1, color=
col_orb1, fill_opacity=opty[i], stroke_width=0)
235         for i in range(num_start_balls)])
236     self.add(starting_balls)
237
238     perc = 0.6
239
240     Anim1 = Succession(

```

```

238     *[
239         AnimationGroup(
240             Create(Line(start=render1[i - 1], end=render1[i],
241                 stroke_width=2, color=b1.get_color())),
242                 #MoveAlongPath(b1, Line(start=render1[i - 1],
243                 end=render1[i]), rate_func=linear)
244             )
245             for i in range(1, num_animation)
246         ],
247         AnimationGroup(
248             Create(Arrow(start=render1[num_animation - 1],
249                         end=stop(np.dot(reduc, render1[
250                             num_animation - 1]), np.dot(reduc, render1[num_animation]), perc),
251                         stroke_width=2, color=b1.get_color(),
252                         buff=0, max_tip_length_to_length_ratio=r_ball1)
253                     ),
254                     #MoveAlongPath(b1,
255                     #Line(start=render1[num_animation -
256                         1],
257                         #end=stop(np.dot(reduc, render1[
258                             num_animation - 1]), np.dot(reduc, render1[num_animation]), perc))
259                     #
260             )
261             #
262             #.set_color(PINK)
263             # Anim2 = Succession(
264             #     *[
265                 #         AnimationGroup(
266                 #             Create(Line(start=render2[i - 1], end=render2[i],
267                     #                 stroke_width=2).set_color(PINK)),
268                     #                 MoveAlongPath(b2, Line(start=render2[i - 1],
269                     end=render2[i]), rate_func=linear).set_run_time(
270                         #                             time(render2[i - 1], render2[i], 3 *
271                         velocity))
272                         #
273                         for i in range(1, num_animation)
274                     ],
275                     #         AnimationGroup(
276                     #             Create(Line(start=render2[num_animation - 1],
277                         #                 end=stop(np.dot(reduc, render2[
278                             num_animation - 1]), np.dot(reduc, render2[num_animation]), perc),
279                         #                         stroke_width=2, color=b2.get_color()))
280                     ,
281                     #                     MoveAlongPath(b1,
282                     #                     Line(start=render1[num_animation -
283                         1],
284                         #                         end=stop(np.dot(reduc, render2[
285                             num_animation - 1]), np.dot(reduc, render2[num_animation]), perc))
286                         #
287                         )
288                     #
289             )
290             #
291             for i in range(1, num_animation+1):
292                 print(render1[i-1], render1[i])
293
294             #self.play(Anim1, Anim2)
295             self.play(Anim1)
296
297
298
299
300
301
302
303
304
305
306
307
308
309
310
311
312
313
314
315
316
317
318
319
320
321
322
323
324
325
326
327
328
329
330
331
332
333
334
335
336
337
338
339
340
341
342
343
344
345
346
347
348
349
350
351
352
353
354
355
356
357
358
359
360
361
362
363
364
365
366
367
368
369
370
371
372
373
374
375
376
377
378
379
380
381
382
383

```

```

284
285 class Draw_image_multiple(Scene):
286     def construct(self):
287         self.camera.background_color = WHITE # "#ece6e2"
288
289         stadium_back = WHITE # "#c2c4c6"#f2f4f6"###8598a7"###069fd9
290 "###05014a"
291         stadium_bord = "#353c42"
292 #col_orb1 = "#0000ff" # "#05014a"
293
294         M = [[1, 0], [0, 1], [0, 0]]
295         reduc = [[1, 0, 0], [0, 1, 0]]
296         velocity = 1
297         r_ball1 = 0.08
298
299         Num_points = 6
300         Max_val_binom = 20
301         x_rnd = np.random.binomial(Max_val_binom, 0.5, Num_points)
302 #y_rnd = np.random.binomial(Max_val_binom, 0.5, Num_points)
303 #print(((x_rnd)/Max_val_binom-0.5)*0.3/0.5)
304 # binomial distribution with ray of 0.3 and centered in 0
305         x_rnd = ((x_rnd) / Max_val_binom - 0.5) * 0 / 0.5
306 #y_rnd = ((y_rnd) / Max_val_binom - 0.5) * 0.5 / 0.5
307 # use this line to set vertical points with same direction
308         y_rnd = [a for a in linspace(-0.15,0.15,Num_points)]
309         p_list = [np.add([-1, 1], [x_rnd[i], y_rnd[i]]) for i in
310 range(Num_points)]
311         #p_list = [-1, 0]
312 # theta list is a list of angles between PI*a and PI*b where
313 #linspace(a,b,Num_points)
314         theta_list = [PI*m for m in linspace(0, 0, Num_points)]
315         v_list = [[velocity*np.cos(a), velocity*np.sin(a)] for a in
316 theta_list]
317         List = [] # list of lists of points
318
319
320         num_col = 12
321         num_animation = 12
322         L = 7
323         Radius = 3.2
324
325         for l in range(Num_points):
326             List.append(billiard(p_list[l], v_list[l], num_col, L,
Radius))
327
328             #b1 = Dot(np.dot(M,p1),radius=0.02).set_color(ORANGE)
329             #k2 = VMobject() #element to draw previous segment behind a
ball
330             dots = VGroup(*[Dot(np.dot(M, p_list[i]), radius=r_ball1)
for i in range(Num_points)])
331             dots.set_color_by_gradient(ORANGE, PINK) #color by gradient
332             #dots.set_color(BLUE)
333             # Traccie dietro le palline, da usare SOLO CON POCHE PALLINE
334             # (MAX 15 con MAX 10 PALLINE)
335             traces = VGroup(*[TracedPath(b.get_center, stroke_opacity
=0.2, stroke_color=b.get_color(), stroke_width=2,
dissipating_time=3) for b in dots])
336
337             #traces = VGroup(*[VMobject() for i in range(Num_points)])

```

```

333         self.add(traces, dots) #, traces)
334
335
336     num_start_balls = 6
337     for l in range(Num_points):
338         centers = [stop(np.dot(reduc, List[l][0]), np.dot(reduc,
339             List[l][1]), p) for p in
340                 linspace(0, 0.2, num_start_balls)]
341         opty = linspace(0.5, 0, num_start_balls)
342         starting_balls = VGroup(*[
343             Circle(arc_center=centers[i], radius=r_ball1, color=
344             dots[l].get_color(), fill_opacity=opty[i], stroke_width=0)
345             for i in range(num_start_balls)])
346         self.add(starting_balls)
347
348     perc = 0.6
349
350     TotalAnim = AnimationGroup(
351         *[
352             Succession(
353                 *[
354                     AnimationGroup(
355                         Create(Line(start=List[l][i - 1], end=
356                             List[l][i], stroke_width=2, color=dots[l].get_color())),
357                             # MoveAlongPath(b1, Line(start=render1[i -
358                             1], end=render1[i]), rate_func=linear)
359                             )
360                         for i in range(1, num_animation)
361                     ],
362                     AnimationGroup(
363                         Create(Arrow(start=List[l][num_animation -
364                             1],
365                             end=stop(np.dot(reduc, List[l][
366                             num_animation - 1]),
367                             np.dot(reduc, List[l][
368                             num_animation])), perc),
369                             stroke_width=2, color=dots[l].
370                             get_color(), buff=0,
371                             max_tip_length_to_length_ratio
372                             =0.04)
373                             ),
374                             # MoveAlongPath(b1,
375                             # Line(start=render1[
376                             num_animation - 1],
377                             # end=stop(np.dot(reduc,
378                             render1[num_animation - 1]), np.dot(reduc,
379                             render1[num_animation]), perc))
380                             #
381                         )
382                     )
383                 )
384             )
385         ]
386     )
387     self.play(TotalAnim)
388     self.add(Line([-L / 2, Radius, 0], [L / 2, Radius, 0],
389             stroke_width=6, color=stadium_bord))
390     self.add(Line([-L / 2, -Radius, 0], [L / 2, -Radius, 0],
391             stroke_width=6, color=stadium_bord))

```

```

377     self.add(Arc(Radius, 3 * PI / 2, -PI, arc_center=[-L / 2, 0,
378     0], stroke_width=6, color=stadium_bord))
      self.add(Arc(Radius, PI / 2, -PI, arc_center=[L / 2, 0, 0],
      stroke_width=6, color=stadium_bord))

```

SCRIPT C.1: Billiard simulation in Bunimovich stadium

C.2.2 Quantum eigenfunctions

C.3 FreeFem++

```

1 int n=20 ; //number of modes
2 int nev=30; //number of eigenvalues to be calculated
3
4 string fnm = "modular_surface_100nev . txt " ; //file name for
   saving
5
6 // vertices = (0,0.26607724526008814), (0,0), (\pm
   0.14062592996432,0)
7
8
9 real yc = 1;//2.0121921726123;//1;//1.0000648650767; // radius of
   circle
10 real xc = 2;//3.6258450075213;//2;
11 real r = 2; //4.0001297343609; // centre of circle on x-axis
12 real R = 4;//16.1956693580892;
13 real angle = pi/3; //(2-sqrt(3))
14 real T = 2-sqrt(3);//0.14062592996432;//2-sqrt(3)
15
16
17 //border G1 (t=0,-pi/6){ x=-2+sqrt(r)*cos(t) ; y=yc+sqrt(r)*sin(t);
   label=1;};
18 border G1 (t=0,-T){ x = t ; y=yc-sqrt(R-(t+xc)^2); label=1;};
19
20
21 border G2 ( t=-T,0){ x = t; y=0; label=2;};
22 border G3 ( t=0,T){ x = t; y=0; label=3;};
23 //border G2 (t=pi/6,0){ x=-2+r*cos(t) ; y=-1+2*sin(t); label=2;};
24 border G4 ( t=T,0) { x= t; y=yc-sqrt(R-(t-xc)^2); label=4;};
25
26
27 //border G3 ( t=0,(2-sqrt(3)+0.0001)) { x= t; y=0; label=3;};
28 //border G3 (t=pi,5*pi/6){ x=2+r*cos(t) ; y=-1+r*sin(t); label=3;};
29
30 //border G4 (t=7*pi/6,pi) { x=2+sqrt(r)*cos(t) ; y=yc+sqrt(r)*sin(t)
   ; label=4;};
31
32
33 plot (G1(n)+G2(n)+G3(n)+G4(n));
34
35 mesh Th=buildmesh(G1(2*n)+G2(n)+G3(n)+G4(2*n),fixeborder=true);
36
37 plot (Th,wait=true,fill=true);
38

```

```

39
40
41 //Adapting the mesh messes up the periodic boundary conditions
42 func metric = 4/(1-x^2-y^2)^2;
43 //mesh ATh = adaptmesh(Th,metric);
44 //Th = adaptmesh(Th,metric);
45
46 //plot (Th,wait=true,fill=true);
47 fespace Vh(Th,P2,periodic=[[1,y],[4,y],[2,y-x],[3,x-y]]);
48 //fespace Vh(Th,P2);
49
50
51
52 //glues opposite sides such that orientation is preserved
53 Vh u1,u2;
54
55
56 real sigma=200; // value of the shift
57
58
59 varf op(u1,u2)=int2d(Th)(dx(u1)*dx(u2)+dy(u1)*dy(u2)-sigma*(u1*u2)*
  metric); //+on(G1,u1=0)+on(G2,u1=0)+on(G3,u1=0)+on(G4,u1=0);
60 varf b([u1],[u2])=int2d(Th)((u1*u2)*metric);
61
62 matrix OP = op(Vh,Vh,solver=LU,factorize=1);
63 matrix B = b(Vh,Vh,solver=CG,eps=1e-20);
64
65 real[int] ev(nev);
66 Vh[int] eV(nev);
67
68 int k=EigenValue(OP,B,sym=true, sigma=sigma, value=ev, vector=eV,
  tol=1e-12, maxit=0, ncv=0);
69
70 for(int i=0; i<k;i++){
71   u1=eV[i];
72   real gg = int2d(Th)(dx(u1)*dx(u1)+dy(u1)*dy(u1));
73   real mm= int2d(Th)(u1*u1);
74
75   ofstream Eva(fnm,append);
76   Eva << ev[i] << "\n";
77   cout << "lambda[" << i << "] = " << ev[i] << ", err= " << int2d(Th
    )(dx(u1)*dx(u1) + dy(u1)*dy(u1) - ((ev[i])*u1*u1)*4/(1-x^2-y^2)
    ^2) << endl;
78   plot(ev[i], cmm="Eigen Vector "+i+" value =" +ev[i], wait=true,
    value=true, fill=true); //, hsv=colorhsv);
79 //cout << "----<<i<<" << ev[i] << "err=" << dx(u1)*dx(u1)+dy(u1)*dy(u1)
  -(ev[i])*u1*u1 << "----" << endl; plot(ev[i], cmm="EigenVector"+i+
  valeur=" +ev[i], wait=1,value=1);
80 //uncomment the above two lines to display level sets for each
  eigenfunction
81 }

```

SCRIPT C.2: Eigenfunctions of modular surface

List of Figures

1	First 24 eigenfunctions on Bunimovich Stadium	iii
1.1	Billiard trajectories on a circle and an ellipse. The underlying system is conservative, hence the motion is not “everywhere distributed”.	5
1.2	Billiard trajectories on the Bunimovich stadium.	6
1.3	Barnett’s billiard.	6
1.4	Billiard trajectories in the Cassini’s oval and Cardioid.	7
1.5	Ergodic orbit on the modular surface.	8
2.1	Action of an hyperbolic matrix on three point. In purple the <i>axis</i> , see the end of this section.	18
2.2	Action of a parabolic matrix on three point.	19
2.3	Action of an elliptic matrix on three point.	19
2.4	Fundamental domain of modular surface.	22
2.5	Fundamental domain of bolza surface in \mathcal{H} .	23
2.6	Bolza surface fundamental domain as subgroup of triangle group $\Delta(2, 3, 8)$ (on the left) and with sides identification (on the right).	23
2.7	Action of geodesic, stable and unstable horocycle flow.	25
2.8	A typical chaotical orbit on the modular surface (in the center), along with two periodic orbits.	27
2.9	3D visualisation of motion on hyperbolic surface.	28
4.1	Bunimovich stadium 36 eigenfunctions, for $\lambda \sim 1000$	52
7.1	The density eigenfunction $ \varphi_n ^2$ for $n \simeq 5 \times 10^4$ and the corrispondent $\lambda_n \simeq 10^6$. Computed by Alex Barnett.	81
7.2	12 consecutive Maass forms (5600th eigenvalue and so on), i.e. laplacian eigenfunctions on the modular surface, computed by Holger Then and Alex Barnett	82
7.3	The three eigenfunctions on Bolza surface, corrisponding to the first eigenvalue $\lambda = 3.8388872\dots$ See [SU13]	82
7.4	Bolza surface is an arithmetic hyperbolic surface, thus eigenfunctions equidistributes on the surface.	82
7.5	The first two eigenfunctions of the modular surface, see on the Poincaré disk model \mathcal{D} . The corrisponding eigenvalues are $\lambda_1 = 91.12\dots$ and $\lambda_2 = 148.43\dots$, see [Sar03].	83
7.6	Different distributions from Random Matrix Theory.	86

7.7	From [Rud07]. Normalized gaps between roughly 50000 sorted eigenvalues for the Barnett's stadium 7.1. The distributions follows the GOE distribution.	87
7.8	From [Rud07], computations by [OF]. Distributions of zeros of Riemann zeta function.	87

Bibliography

- [Ana09] N. Anantharaman. “Chaotic vibrations and strong scars”. In: *News. Euro. Math. Soc.* 74 (2009), pp. 19–24.
- [Arn78] V.I. Arnold. *Mathematical Methods of Classical Mechanics*. Springer, 1978.
- [Bar06] A. Barnett. “Asymptotic rate of quantum ergodicity in chaotic Euclidean billiards”. In: *Comm. Pure Appl. Math* 59 (2006), pp. 1457–1488.
- [Ber03] M. Berry. “Quantum chaology”. In: (2003). URL: http://www.phy.bris.ac.uk/people/berry_mv/the_papers/berry358.pdf.
- [Ber16] N. Bergeron. *The Spectrum of Hyperbolic Surfaces*. Universitext. Springer International Publishing, 2016. ISBN: 9783319276649.
- [Ber89] M. Berry. “Quantum scars of classical closed orbits in phase space”. In: *Proc. Roy. Soc. London* 423 (1989), pp. 219–231.
- [Bog+97] E. B. Bogomolny et al. “Arithmetical Chaos”. In: *Phys. Rep.* 291 (1997), pp. 219–324.
- [Bog03] E. B. Bogomolny. “Quantum and Arithmetical Chaos”. 2003.
- [Bun79] L. Bunimovich. “On the ergodic properties of nowhere dispersing billiards”. In: *Comm. Math. Phys.* 65 (1979), pp. 292–312.
- [Cag20] A. Cagnetta. “Approcci Tauberiani al Teorema dei Numeri Primi”. 2020.
- [Car71] P. Cartier. “Computers in Number Theory”. In: *Academic Press* (1971), pp. 37–48.
- [Col85a] Y. Colin de Verdière. “Ergodicité et fonctions propres du Laplacien”. In: *Comm. Math. Phys.* 102 (1985), pp. 497–502.
- [Col85b] Y. Colin de Verdière. “Ergodicité et fonctions propres du laplacien”. In: *Comm. Math. Phys.* 102 (1985), pp. 497–502.
- [Coo18] Joseph Cook. “Properties of Eigenvalues on Riemann Surfaces with Large Symmetry Groups”. PhD thesis in Mathematics. Loughborough University, Feb. 2018. URL: <https://core.ac.uk/download/288357815.pdf>.
- [DS99] M. Dimassi and J. Sjöstrand. *Spectral Asymptotics in the Semi-Classical Limit*. Vol. 268. Lecture Note Series. Cambridge UP, 1999.

- [Du09] W. Du. “Fourier analysis and the uncertainty principle”. 2009. URL: <http://www.math.uchicago.edu/~may/VIGRE/VIGRE2009/%20REUPapers/Du.pdf>.
- [Dya16] S. Dyatlov. *Lecture notes on quantum ergodicity*. 2016. URL: <https://math.mit.edu/~dyatlov/files/2016/qenotes.pdf>.
- [Dya19] S. Dyatlov. *Lecture notes on semiclassical analysis*. 2019. URL: <https://math.mit.edu/~dyatlov/semisnap/>.
- [Dya22] S. Dyatlov. “Around quantum ergodicity”. In: *Ann. Math. du Québec* 46 (2022), pp. 11–26.
- [Eas20] Alex Eastman. “Quantum Ergodicity on Hyperbolic Surfaces”. Lecture notes. 2020. URL: <https://perso.u-cergy.fr/~elemasson/qchyp.pdf>.
- [Ego69] Y. Egorov. “The canonical transformations of pseudodifferential operators”. In: *Uspehi. Mat. Nauk.* 24.5 (1969), pp. 235–236.
- [Eva10] L. Evans. *Partial Differential Equations*. 2nd ed. Graduate Studies in Mathematics. AMS, 2010.
- [EW10] M. Einsidler and T. Ward. “Arithmetic Quantum Unique Ergodicity for $\Gamma \backslash \mathbb{H}$ ”. Lecture notes for Arizona Winter School 2010. 2010.
- [GL08] S. Geninska and E. Leuzinger. “A geometric characterization of arithmetic Fuchsian groups”. In: *Duke Math. J.* 142 (2008), pp. 111–125.
- [Gut90] M.C. Gutzwiller. *Chaos in Classical and Quantum Mechanics*. Vol. 1. Interd. App. Math. Springer, 1990.
- [Has10a] A. Hassell. “On the ergodic properties of nowhere dispersing billiards”. In: *Ann. Math.* 171.1 (2010), pp. 605–618.
- [Has10b] A. Hassell. “What is quantum unique ergodicity?” In: *Techninical Papers* (2010).
- [Has11] A. Hassell. “What is quantum unique ergodicity?” In: *Aus. Math. Soc. Gazette* 35 (2011), pp. 158–167.
- [Hej80] D. Hejhal. “The Selberg trace formula for $\mathrm{PSL}_2 \mathbb{Z}$ ”. In: *Springer-Verlag* 1001 (1980).
- [Hej99] D. Hejhal. “On eigenfunctions of the Laplacian for Hecke triangle groups”. In: *Emerging Applications of Number Theory* 109 (1999), pp. 291–305.
- [Hör83a] L. Hörmander. *The Analysis of Linear Partial Differential Operators I: Distribution Theory and Fourier Analysis*. Vol. 257. A Series of Comprehensive Studies in Mathematics. Springer-Verlag, 1983.
- [Hör83b] L. Hörmander. *The Analysis of Linear Partial Differential Operators II: Differential Operators with Constant Coefficients*. Vol. 257. A Series of Comprehensive Studies in Mathematics. Springer-Verlag, 1983.

- [Hör83c] L. Hörmander. *The Analysis of Linear Partial Differential Operators III: Pseudo-Differential Operators*. Vol. 257. A Series of Comprehensive Studies in Mathematics. Springer-Verlag, 1983.
- [Kat92] S. Katok. *Fuchsian groups*. Chicago Lec. in Math. Chicago Univ. Press, 1992.
- [Klé17] Riku Klén. “Hyperbolic distance between hyperbolic lines”. In: *Annales Mathematicae et Informaticae* 47 (2017), pp. 129–139.
- [Kog18] C. Kogler. “Closed Geodesics on Compact Hyperbolic Surfaces”. 2018.
- [Kor04] Jacob Korevaar. *Tauberian Theory - A Century of Development*. Springer, 2004.
- [LB03] E. Lindenstrauss and J. Bourgain. “Entropy of quantum limits”. In: *Comm. Math. Phys.* 40.1 (2003), pp. 153–171.
- [Le 17] E. Le Masson. “Quantum Chaos on hyperbolic surfaces”. Lectures notes. 2017. URL: <https://perso.u-cergy.fr/~elemasson/qchyp.pdf>.
- [Lin06] E. Lindenstrauss. “Invariant measures and arithmetic quantum unique ergodicity”. In: *Annals of Mathematics* 163 (2006), pp. 165–219.
- [Mar02] A. Martinez. *An Introduction to Semiclassical and Microlocal Analysis*. Universitext. Springer, 2002.
- [Mar06] J. Marklof. “Arithmetic Quantum Chaos”. In: 2006.
- [Mar12] J. Marklof. *Selberg’s Trace Formula: An Introduction*. Vol. 397. Lecture Note Ser. Cambridge Univ. Press, 2012.
- [Mor01] Dave Witte Morris. *Introduction to Arithmetic Groups*. 2001. DOI: [10.48550/ARXIV.MATH/0106063](https://doi.org/10.48550/ARXIV.MATH/0106063). URL: <https://arxiv.org/abs/math/0106063>.
- [Nat21] Y. Natsume. *Quantum Chaos with Python*. Dec. 2021. URL: <https://medium.com/@natsunoyuki/quantum-chaos-with-python-f4adfe4ab62c>.
- [OF] A. Odlyzko and P.J. Forrester. “A nonlinear equation and its application to near est neighbor spacings for zeros of the zeta function and eigenvalues of random matrices”. In: *Proc. of the Organic Math. Workshop* (). URL: <http://www.cecm.sfu.ca/~pborwein/>.
- [Pet37] H. Petersson. “Über die eindeutige bestimmung und die erweiterungsfähigkeit von gewissen grenzkreisgruppen”. In: *Abh. Math. Sem.* 12.1 (1937), pp. 180–199.
- [Q G20] Q. Q. Gouvéa. *p-adic Numbers*. 3rd ed. Universitext. Springer Cham, 2020.
- [RS96] Z. Rudnick and P. Sarnak. “The behaviour of eigenstates of arithmetic hyperbolic manifolds”. In: *Comm. Math. Phys.* 161.1 (1996), pp. 195–213.
- [Rud07] Z. Rudnick. “What is Quantum Chaos?” In: vol. 55. 1. 2007.
- [Sar03] P. Sarnak. “Spectra of Hyperbolic Surfaces”. In: *Bulletin (New Series) of the American Mathematical Society* 40.4 (2003), pp. 441–478.

- [Sar11] P. Sarnak. “Recent progress on the quantum unique ergodicity conjecture”. In: *Bullettin of the American Mathematical Society* 48 (2011), pp. 211–228.
- [Shi71] G. Shimura. *Introduction to the arithmetic theory of automorphic functions*. Princeton Univ. Press, 1971.
- [Sou10a] Kannan Soundarajan. “Quantum unique ergodicity for $\mathrm{SL}_2 \mathbb{Z} \backslash \mathcal{H}$ ”. In: *Ann. of Math.* 172.2 (2010), pp. 1529–1538.
- [Sou10b] K. Soundararajan. “Quantum Unique Ergodicity and Number Theory”. Lecture notes for Arizona Winter School 2010. 2010.
- [Sta84] H. Stark. “Fourier coefficients of Maass waveforms”. In: *Modular Forms (R. A. Rankin ed.)* (1984), pp. 263–269.
- [Str12] F. Strömberg. *Arithmetic Quantum Chaos*. Expository Quantum Lecture Series 5. 2012.
- [Str19] F. Strömberg. “Noncongruence subgroups and Maass waveforms”. In: *Journal of Number Theory* 199 (2019), pp. 436–493. ISSN: 0022-314X. URL: <https://github.com/fredstro/noncongruence>.
- [Str22] P. Strånsky. “Lecture Notes on Quantum Chaos”. Charles University, Prague, June 2022.
- [SU13] A. Strohmaier and V. Uski. “An algorithm for the computation of eigenvalues, spectral zeta functions and zeta-determinants on hyperbolic surfaces”. In: *Comm. Math. Phys.* 317.3 (2013), pp. 827–869.
- [SW00] P. S. Schaller and J. Wolfart. “Semi-arithmetic Fuchsian groups and Modular embeddings”. In: *J. Lon. Math. Soc.* 61.1 (Feb. 2000), pp. 13–24. ISSN: 0024-6107.
- [Tak75] K. Takeuchi. “A characterization of arithmetic Fuchsian group”. In: *J. Math. Soc. Japan* 27.4 (1975).
- [Tao07] T. Tao. *Simons lecture I: Structure and randomness in Fourier analysis and number theory*. Apr. 2007. URL: <http://terrytao.wordpress.com/2007/04/05/%20simons-lecture-i-structure-and-randomness-in-fourier-analysis-and-number-theory/>.
- [Tao08] T. Tao. *Hassell’s proof of scarring for the Bunimovich stadium*. July 2008. URL: <http://terrytao.wordpress.com/2008/07/07/hassells-proof-of-scarring-for-the-bunimovich-stadium/>.
- [The05] H. Then. “Maaß cusp forms for large eigenvalues”. In: *Math. Comput.* 74.249 (2005), pp. 363–381.
- [The18] B. The Pham. “Algorithms Related to Triangle Groups”. PhD thesis in Mathematics. Louisiana State University, July 2018. URL: https://digitalcommons.lsu.edu/cgi/viewcontent.cgi?article=6705&context=gradschool_dissertations.

- [Tur16] M. Turaev. “Quantum Unique Ergodicity and Number Theory”. Lecture notes. 2016. URL: <https://www.diva-portal.org/smash/get/diva2:908119/FULLTEXT01.pdf>.
- [Van51] L. Van Hove. “Sur le probleme des relations entre les transformations unitaires de la mecanique quantique et les transformations canoniques de la mecanique classique”. In: *Bull. Cl. Sci.* 5.37 (1951), pp. 610–620.
- [VC19] J. Voight and P.L. Clark. “Algebraic curves uniformized by congruence subgroups of triangle groups”. In: *Trans. Amer. Math. Soc.* 371.1 (2019), pp. 33–82.
- [Yin02] C. Yingchun. “Prime geodesic Theorem”. In: *Journal de Théorie des Nombres de Bordeaux* 14 (2002), pp. 59–72.
- [Zel87] Steven Zelditch. “Uniform distribution of eigenfunctions on compact hyperbolic surfaces”. In: *Duke Math. J.* 55.4 (1987), pp. 919–941.
- [Zwo12] M. Zworski. *Semiclassical Analysis*. Vol. 138. Graduate Studies in Mathematics. AMS, 2012.